



FGM and Laminated Doubly-Curved and Degenerate Shells Resting on Nonlinear Elastic Foundations: A GDQ Solution for Static Analysis with a Posteriori Stress and Strain Recovery

Francesco Tornabene¹ and J.N. Reddy²

Abstract | This work focuses on the static analysis of functionally graded (FGM) and laminated doubly-curved shells and panels resting on nonlinear and linear elastic foundations using the Generalized Differential Quadrature (GDQ) method. The First-order Shear Deformation Theory (FSDT) for the aforementioned moderately thick structural elements is considered. The solutions are given in terms of generalized displacement components of points lying on the middle surface of the shell. Several types of shell structures such as doubly-curved shells (elliptic and hyperbolic hyperboloids), singly-curved (spherical, cylindrical and conical shells), and degenerate panels (rectangular plates) are considered in this paper. The main contribution of this paper is the application of the differential geometry within GDQ method to solve doubly-curved FGM shells resting on nonlinear elastic foundations. The linear Winkler-Pasternak elastic foundation has been considered as a special case of the nonlinear elastic foundation proposed herein. The discretization of the differential system by means of the GDQ technique leads to a standard nonlinear problem, and the Newton-Raphson scheme is used to obtain the solution. Two different four-parameter power-law distributions are considered for the ceramic volume fraction of each lamina. In order to show the accuracy of this methodology, numerical comparisons between the present formulation and finite element solutions are presented. Very good agreement is observed. Finally, new results are presented to show effects of various parameters of the nonlinear elastic foundation on the behavior of functionally graded and laminated doubly-curved shells and panels.

Keywords: *Static Analysis, Laminated Composite Doubly-Curved Shells and Panels, Nonlinear Elastic and Winkler-Pasternak Foundation, First-order Shear Deformation Theory, Generalized Differential Quadrature Method.*

¹DICAM—Department, School of Engineering and Architecture, University of Bologna, Italy.

francesco.tornabene@unibo.it

²Mechanical Engineering—Department, Texas A&M University, College Station, TX, USA.

jnreddy@tamu.edu

1 Introduction

1.1 Background

Shell theories based on the Kirchhoff-Love assumptions have been developed by various authors.¹⁻¹² The effect of transverse shear deformation has been incorporated into shell theories in the same way as in plates,¹³ and the resulting theories are also termed shear deformation shell theories, where the assumption of the preservation transverse normals to the shell middle surface after the deformation has been abandoned. A comprehensive analysis for elastic isotropic shells was made by Kraus,⁷ Gould,^{14,15} and Qatu.^{16,17} In,^{16,17} the shear correction factor has been eliminated by assuming a parabolic thickness function along the shell lamina thickness and the initial curvature effect has been embedded into the displacement field (also see Reddy and Liu¹⁸ for the third-order shell theory). The curvature effect is not only included in the evaluation of the stress resultants as in Kraus,⁷ Qatu,^{16,17} and Toorani and Lakis,¹⁹ but also in the kinematic analysis of the shell. According to literature, there are three different ways to calculate the thickness-integrated shell stiffness coefficients. The first is the Reissner-Mindlin approach,^{7,20} in which the effect of curvatures is neglected [i.e., $(1 + z/R)^{-1} \gg 1$, where R is the local radius and z is the thickness coordinate]. The resulting elastic stiffnesses are constant and do not depend on curvatures. The second approach, proposed by Kraus⁷ and Toorani and Lakis,¹⁸ is based on the Taylor series expansion of $(1 + z/R)^{-1}$, and the third approach due to Qatu¹⁶ evaluates the shell stiffnesses by exact integration of the elastic constants through the shell thickness. Due to these considerations the stress resultants directly depend on the geometry of the structure in terms of the curvature coefficients and the hypothesis of the symmetry of the in-plane shearing force resultants and the twisting moments is not valid. A further improvement of the previous theories of shells has been proposed by Toorani and Lakis,¹⁹ in which a kinematic model is used in order to include the effect of the curvature from the beginning of the shell formulation. When this hypothesis is considered, the strain-displacement relationships have to change and, as consequence, the equilibrium equations in terms of displacements have to be modified.

1.2 Present study

In this paper, we propose a shell theory, named General Shell Theory (GST) and compare its results with those of the first-order shear deformation shell theory.^{7,20} Furthermore, the GST is employed to analyze doubly-curved shells resting on linear (Winkler-Pasternak) and nonlinear elastic foundation. Due to the increasing importance of the interaction of shells with an elastic medium, a nonlinear elastic foundation including the linear Winkler-Pasternak one is introduced. Unlike the papers in the literature,²¹⁻²⁹ all effects of the foundation, are separately considered.

Over the years, different numerical tools that are used to carry out static and dynamic analyses of every kinds of engineering problem are developed in literature,^{14,15,20,30-36} such as Finite Element Method (FEM) and meshless methods. In this paper the fundamental equations constitute a system of second-order nonlinear partial differential equations. Since the system is written as a function of the displacements of the middle surface, it can be easily solved by using the Generalized Differential Quadrature (GDQ) method. The mathematical fundamentals and recent developments of the GDQ method as well as its major applications in engineering are discussed in detail in the book by Shu.³⁷ The interest in the use of this procedure is increasing due to its great simplicity and versatility. As shown in,³⁸ GDQ technique is a global method, which can yield very accurate numerical results by using a considerably small number of grid points. Therefore, this simple direct procedure has been applied in a large number of cases³⁹⁻¹⁰¹ to circumvent the difficulties of programming complex algorithms in the computer, as well as excessive storage and computing time. In summary, the aim of the present paper is to demonstrate an efficient and accurate application of the GDQ approach by solving the equations governing the static of functionally graded and laminated composite doubly-curved moderately thick shells and panels with the Differential Geometry (DG) tool. Furthermore, due to the fact that a nonlinear algebraic system of equations must be solved, an iterative method has been considered. The Newton-Raphson scheme has been implemented in a MATLAB code in order to solve the nonlinear problem. The use of the GDQ method allows us to obtain, in an easy way, the Jacobian matrix necessary for the Newton-Raphson method. A high rate of convergence has been found and a maximum of three Newton-Raphson iterations has been used for all the results obtained in this paper at each load steps considered. The nonlinear behavior of all the analyzed structures due to the effect of the nonlinear elastic foundation is graphically reported for different load steps. Different lamination schemes are considered to expand the combination of the two functionally graded four-parameter power-law distributions adopted. The treatment is developed

within the theory of linear elasticity, when materials are assumed to be isotropic and inhomogeneous through the lamina thickness direction. A parametric study is performed to illustrate the influence of the parameters on the mechanical behavior of functionally graded shell structures made of a mixture of ceramics and metal.

In summary, the present study is based on four aspects. Firstly, an improvement of the first-order shear deformation shell theory using a different kinematical model is presented and the shear correction factor is included using a parabolic thickness function. Secondly, functionally graded and laminated doubly-curved shells and panels are represented using the differential geometry tools to describe the middle surface of the structure. Thirdly, an investigation has been carried out on the effects of linear and nonlinear elastic foundations on the behavior of shell structures in the static case. In addition, all the effects of the foundation are separately considered. Finally, the GDQ methodology coupled with the Newton-Raphson procedure has been used to solve the system of nonlinear governing equations.

2 Governing Equations

A shell structure can be described by the position vector of an arbitrary point using an orthogonal coordinates α_1 ($\alpha_1^0 \leq \alpha_1 \leq \alpha_1^1$), α_2 ($\alpha_2^0 \leq \alpha_2 \leq \alpha_2^1$) upon the middle surface, or reference surface $\mathbf{r}(\alpha_1, \alpha_2)$, and coordinate ζ directed along the outward normal $\mathbf{n}(\alpha_1, \alpha_2)$, measured from the reference surface ($-h/2 \leq \zeta \leq h/2$). $h(\alpha_1, \alpha_2)$ is the total thickness of the shell. A laminated composite doubly-curved shell, as shown in Figure 1, has l plies and the total shell thickness h is defined as

$$h = \sum_{k=1}^l h_k \quad (1)$$

in which $h_k = \zeta_{k+1} - \zeta_k$ is the thickness of the k -th lamina. Starting from the position vector $\mathbf{r}(\alpha_1, \alpha_2)$ written in the global reference system, $Ox_1x_2x_3$, the shell structure is described using the Differential Geometry (DG) tool^{7,11,12,92,96-102}

$$\mathbf{R}(\alpha_1, \alpha_2, \zeta) = \mathbf{r}(\alpha_1, \alpha_2) + \frac{h(\alpha_1, \alpha_2)}{2} z \mathbf{n}(\alpha_1, \alpha_2) \quad (2)$$

where $z = 2\zeta/h(\alpha_1, \alpha_2)$ and $z \in [-1, 1]$ is the dimensionless shell thickness. From equation (2) the location of each shell point is a function of the position of the corresponding point on the reference surface $\mathbf{r}(\alpha_1, \alpha_2)$ and of the corresponding normal vector $\mathbf{n}(\alpha_1, \alpha_2)$ to the reference surface (Figure 1). Moreover, the position of the generic point of the shell volume is also a function of the shell thickness $h(\alpha_1, \alpha_2)$. The three components of the shell reference surface $\mathbf{r}(\alpha_1, \alpha_2)$ along the three global axes $Ox_1x_2x_3$ can be written as

$$\mathbf{r}(\alpha_1, \alpha_2) = r_1(\alpha_1, \alpha_2) \mathbf{e}_1 + r_2(\alpha_1, \alpha_2) \mathbf{e}_2 + r_3(\alpha_1, \alpha_2) \mathbf{e}_3 \quad (3)$$

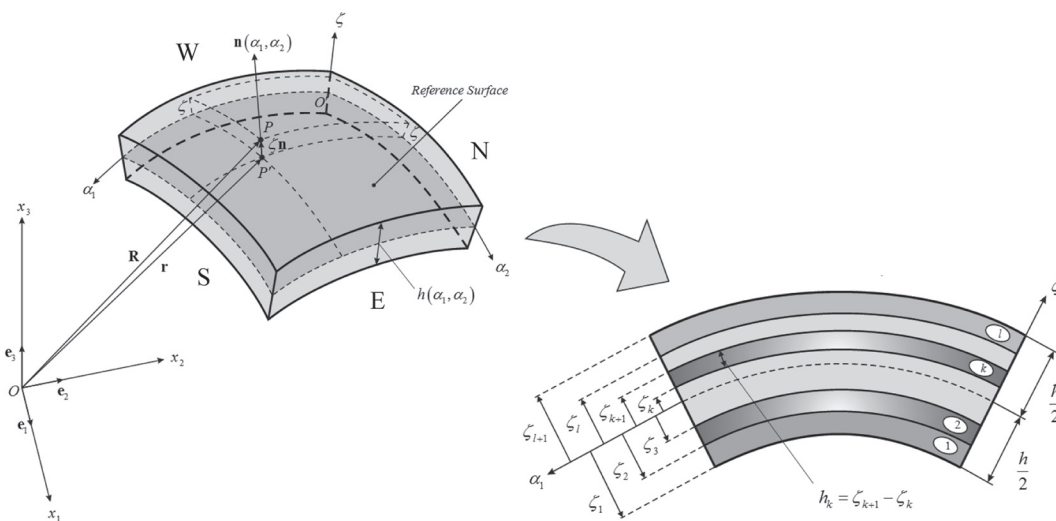


Figure 1: Geometry and coordinate system of a laminated doubly-curved shell.

where $\mathbf{e}_1, \mathbf{e}_2, \mathbf{e}_3$ are the unit vectors of the global reference system $Ox_1x_2x_3$. From the definition of the first fundamental form, the Lamé parameters can be expressed as

$$A_1(\alpha_1, \alpha_2) = \sqrt{\mathbf{r}_{,1} \cdot \mathbf{r}_{,1}}, \quad A_2(\alpha_1, \alpha_2) = \sqrt{\mathbf{r}_{,2} \cdot \mathbf{r}_{,2}} \quad (4)$$

where $\mathbf{r}_{,i}$, for example defines the partial derivative with respect to α_i . Moreover, by considering an orthogonal curvilinear coordinate system $O'\alpha_1\alpha_2\zeta$, from the position vector $\mathbf{r}(\alpha_1, \alpha_2)$ (3) the normal vector $\mathbf{n}(\alpha_1, \alpha_2)$ can be written as

$$\mathbf{n}(\alpha_1, \alpha_2) = \frac{\mathbf{r}_{,1} \times \mathbf{r}_{,2}}{A_1 A_2} \quad (5)$$

Due to the fact that an orthogonal curvilinear coordinate system $O'\alpha_1\alpha_2\zeta$ is considered and following the definition of the second fundamental form, the principal radii of curvature can be evaluated as

$$R_1(\alpha_1, \alpha_2) = -\frac{\mathbf{r}_{,1} \cdot \mathbf{r}_{,11}}{\mathbf{r}_{,11} \cdot \mathbf{n}}, \quad R_2(\alpha_1, \alpha_2) = -\frac{\mathbf{r}_{,2} \cdot \mathbf{r}_{,22}}{\mathbf{r}_{,22} \cdot \mathbf{n}} \quad (6)$$

The displacement field for a moderately thick shell follows the first-order shear deformation theory (FSDT) and can be written as^{13,20}

$$\begin{aligned} U_1(\alpha_1, \alpha_2, \zeta) &= H_1 u_1(\alpha_1, \alpha_2) + \zeta \beta_1(\alpha_1, \alpha_2) \\ U_2(\alpha_1, \alpha_2, \zeta) &= H_2 u_2(\alpha_1, \alpha_2) + \zeta \beta_2(\alpha_1, \alpha_2) \\ U_3(\alpha_1, \alpha_2, \zeta) &= u_3(\alpha_1, \alpha_2) \end{aligned} \quad (7)$$

where

$$H_1 = 1 + \frac{\zeta}{R_1}, \quad H_2 = 1 + \frac{\zeta}{R_2} \quad (8)$$

(u_1, u_2, u_3) are the displacement components on the middle surface ($\zeta = 0$) of the shell, while (β_1, β_2) are the rotations about the α_2 and α_1 axes, respectively. Due to the displacement field (8), the relationships between the generalized strains $\boldsymbol{\eta} = [\varepsilon_1^0 \ \varepsilon_2^0 \ \gamma_1^0 \ \gamma_2^0 \ \chi_1^0 \ \chi_2^0 \ \omega_1^0 \ \omega_2^0 \ \gamma_{1n}^0 \ \gamma_{2n}^0]^T$ and the generalized displacements $\mathbf{u} = [u_1 \ u_2 \ u_3 \ \beta_1 \ \beta_2]^T$ can be written as

$$\boldsymbol{\eta} = \mathbf{D} \mathbf{u} \quad (9)$$

where the definition operator \mathbf{D} is defined as

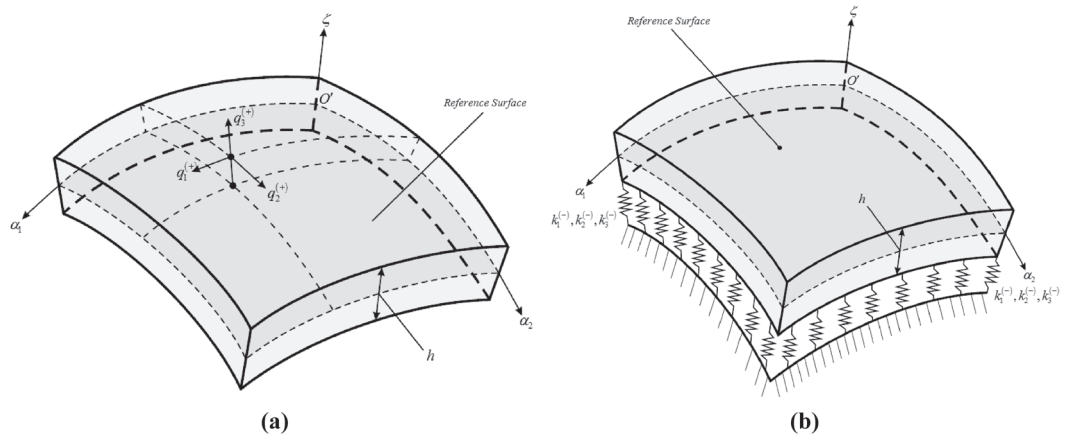


Figure 2: A doubly-curved shell: (a) subjected to external forces at the top surface and (b) resting on an elastic foundation at the bottom surface.

$$\mathbf{D} = \begin{bmatrix}
 \frac{1}{A_1} \frac{\partial}{\partial \alpha_1} & \frac{1}{A_1 A_2} \frac{\partial A_1}{\partial \alpha_2} & \frac{1}{R_1} & 0 & 0 \\
 \frac{1}{A_1 A_2} \frac{\partial A_2}{\partial \alpha_1} & \frac{1}{A_2} \frac{\partial}{\partial \alpha_2} & \frac{1}{R_2} & 0 & 0 \\
 -\frac{1}{A_1 A_2} \frac{\partial A_1}{\partial \alpha_2} & \frac{1}{A_1} \frac{\partial}{\partial \alpha_1} & 0 & 0 & 0 \\
 \frac{1}{A_2} \frac{\partial}{\partial \alpha_2} & -\frac{1}{A_1 A_2} \frac{\partial A_2}{\partial \alpha_1} & 0 & 0 & 0 \\
 \frac{1}{A_1 R_1} \frac{\partial}{\partial \alpha_1} - \frac{1}{A_1 R_1^2} \frac{\partial R_1}{\partial \alpha_1} & \frac{1}{A_1 A_2 R_2} \frac{\partial A_1}{\partial \alpha_2} & 0 & \frac{1}{A_1} \frac{\partial}{\partial \alpha_1} & \frac{1}{A_1 A_2} \frac{\partial A_1}{\partial \alpha_2} \\
 \frac{1}{A_1 A_2 R_1} \frac{\partial A_2}{\partial \alpha_1} & \frac{1}{A_2 R_2} \frac{\partial}{\partial \alpha_2} - \frac{1}{A_2 R_2^2} \frac{\partial R_2}{\partial \alpha_2} & 0 & \frac{1}{A_1 A_2} \frac{\partial A_2}{\partial \alpha_1} & \frac{1}{A_2} \frac{\partial}{\partial \alpha_2} \\
 -\frac{1}{A_1 A_2 R_1} \frac{\partial A_1}{\partial \alpha_2} & \frac{1}{A_1 R_2} \frac{\partial}{\partial \alpha_1} - \frac{1}{A_1 R_2^2} \frac{\partial R_2}{\partial \alpha_1} & 0 & -\frac{1}{A_1 A_2} \frac{\partial A_1}{\partial \alpha_2} & \frac{1}{A_1} \frac{\partial}{\partial \alpha_1} \\
 \frac{1}{A_2 R_1} \frac{\partial}{\partial \alpha_2} - \frac{1}{A_2 R_1^2} \frac{\partial R_1}{\partial \alpha_2} & -\frac{1}{A_1 A_2 R_2} \frac{\partial A_2}{\partial \alpha_1} & 0 & \frac{1}{A_2} \frac{\partial}{\partial \alpha_2} & -\frac{1}{A_1 A_2} \frac{\partial A_2}{\partial \alpha_1} \\
 0 & 0 & \frac{1}{A_1} \frac{\partial}{\partial \alpha_1} & 1 & 0 \\
 0 & 0 & \frac{1}{A_2} \frac{\partial}{\partial \alpha_2} & 0 & 1
 \end{bmatrix} \quad (10)$$

According to the generalized Hooke's laws,²⁰ the internal stress resultants and the internal couples $\mathbf{S} = [N_1 \ N_2 \ N_{12} \ N_{21} \ M_1 \ M_2 \ M_{12} \ M_{21} \ T_1 \ T_2]^T$ can be obtained as a function of the generalized strain components (9)

$$\mathbf{S} = \mathbf{A} \boldsymbol{\eta} \quad (11)$$

where the constitutive matrix \mathbf{A} is defined as

$$\mathbf{A} = \begin{bmatrix}
 A_{11(20)}^{(0)} & A_{12(11)}^{(0)} & A_{16(20)}^{(0)} & A_{16(11)}^{(0)} & A_{11(20)}^{(1)} & A_{12(11)}^{(1)} & A_{16(20)}^{(1)} & A_{16(11)}^{(1)} & 0 & 0 \\
 A_{12(11)}^{(0)} & A_{22(02)}^{(0)} & A_{26(11)}^{(0)} & A_{26(02)}^{(0)} & A_{12(11)}^{(1)} & A_{22(02)}^{(1)} & A_{26(11)}^{(1)} & A_{26(02)}^{(1)} & 0 & 0 \\
 A_{16(20)}^{(0)} & A_{26(11)}^{(0)} & A_{66(20)}^{(0)} & A_{66(11)}^{(0)} & A_{16(20)}^{(1)} & A_{26(11)}^{(1)} & A_{66(20)}^{(1)} & A_{66(11)}^{(1)} & 0 & 0 \\
 A_{16(11)}^{(0)} & A_{26(02)}^{(0)} & A_{66(11)}^{(0)} & A_{66(02)}^{(0)} & A_{16(11)}^{(1)} & A_{26(02)}^{(1)} & A_{66(11)}^{(1)} & A_{66(02)}^{(1)} & 0 & 0 \\
 A_{11(20)}^{(1)} & A_{12(11)}^{(1)} & A_{16(20)}^{(1)} & A_{16(11)}^{(1)} & A_{11(20)}^{(2)} & A_{12(11)}^{(2)} & A_{16(20)}^{(2)} & A_{16(11)}^{(2)} & 0 & 0 \\
 A_{12(11)}^{(1)} & A_{22(02)}^{(1)} & A_{26(11)}^{(1)} & A_{26(02)}^{(1)} & A_{12(11)}^{(2)} & A_{22(02)}^{(2)} & A_{26(11)}^{(2)} & A_{26(02)}^{(2)} & 0 & 0 \\
 A_{16(20)}^{(1)} & A_{26(11)}^{(1)} & A_{66(20)}^{(1)} & A_{66(11)}^{(1)} & A_{16(20)}^{(2)} & A_{26(11)}^{(2)} & A_{66(20)}^{(2)} & A_{66(11)}^{(2)} & 0 & 0 \\
 A_{16(11)}^{(1)} & A_{26(02)}^{(1)} & A_{66(11)}^{(1)} & A_{66(02)}^{(1)} & A_{16(11)}^{(2)} & A_{26(02)}^{(2)} & A_{66(11)}^{(2)} & A_{66(02)}^{(2)} & 0 & 0 \\
 0 & 0 & 0 & 0 & 0 & 0 & 0 & 0 & A_{44(20)}^{(0)} & A_{45(11)}^{(0)} \\
 0 & 0 & 0 & 0 & 0 & 0 & 0 & 0 & A_{45(11)}^{(0)} & A_{55(02)}^{(0)}
 \end{bmatrix} \quad (12)$$

The elastic stiffnesses $A_{nm}^{(\tau)}$ are expressed in the following form

$$\begin{aligned}
 A_{nm}^{(\tau)} &= \sum_{k=1}^l \int_{\zeta_k}^{\zeta_{k+1}} \bar{Q}_{nm}^{(k)} \zeta^\tau \frac{H_1 H_2}{H_1^p H_2^q} d\zeta & \text{for } \tau, p, q = 0, 1, 2 \text{ for } n, m = 1, 2, 3, 6 \\
 A_{nm}^{(\tau)} &= \sum_{k=1}^l \int_{\zeta_k}^{\zeta_{k+1}} g(\zeta) \bar{Q}_{nm}^{(k)} \zeta^\tau \frac{H_1 H_2}{H_1^p H_2^q} d\zeta & \text{for } \tau, p, q = 0, 1, 2 \text{ for } n, m = 4, 5
 \end{aligned} \tag{13}$$

where the shear function $g(\zeta)$ is defined as

$$g(\zeta) = \frac{5}{4} \left(1 - \frac{4\zeta^2}{h^2} \right) \tag{14}$$

Recently, different approaches have been presented to evaluate the engineering elastic constants $A_{nm}^{(\tau)}$. In the present paper, the relations of the elastic stiffness $A_{nm}^{(\tau)}$ are numerically evaluated using the Generalized Integral Quadrature (GIQ) in order to avoid numerical instabilities. For more details about the GIQ rule, the reader can refer to the book by Shu.³⁷ Since the elastic constants $A_{nm}^{(\tau)}$ depend on the shell curvature (11), the corresponding derivatives evaluated along the coordinates α_1 and α_2 directions of the reference surface have to be evaluated. In order to perform this operation, the GDQ rule³⁷ is used. Thus, the derivatives of the elastic constants $A_{ij}^{(\tau)}$ are numerically evaluated. The corresponding elastic constants $\bar{Q}_{nm}^{(k)}$ can be found in literature (see, for example),^{20,85,87,92,93} in which $\bar{Q}_{nm}^{(k)}$ and $Q_{nm}^{(k)}$ are explicitly defined for a laminated composite and functionally graded shells and panels. For the sake of clarity, they are reported in the following for the k -th orthotropic lamina (see Reddy):²⁰

$$\begin{aligned}
 \bar{Q}_{11}^{(k)} &= Q_{11}^{(k)} \cos^4 \theta^{(k)} + 2 \left(Q_{12}^{(k)} + 2Q_{66}^{(k)} \right) \sin^2 \theta^{(k)} \cos^2 \theta^{(k)} + Q_{22}^{(k)} \cos^4 \theta^{(k)} \\
 \bar{Q}_{12}^{(k)} &= \left(Q_{11}^{(k)} + Q_{22}^{(k)} - 4Q_{66}^{(k)} \right) \sin^2 \theta^{(k)} \cos^2 \theta^{(k)} + Q_{12}^{(k)} \left(\sin^4 \theta^{(k)} + \cos^4 \theta^{(k)} \right) \\
 \bar{Q}_{22}^{(k)} &= Q_{11}^{(k)} \sin^4 \theta^{(k)} + 2 \left(Q_{12}^{(k)} + 2Q_{66}^{(k)} \right) \sin^2 \theta^{(k)} \cos^2 \theta^{(k)} + Q_{22}^{(k)} \cos^4 \theta^{(k)} \\
 \bar{Q}_{16}^{(k)} &= \left(Q_{11}^{(k)} - Q_{12}^{(k)} - 2Q_{66}^{(k)} \right) \sin \theta^{(k)} \cos^3 \theta^{(k)} + \left(Q_{12}^{(k)} - Q_{22}^{(k)} + 2Q_{66}^{(k)} \right) \sin^3 \theta^{(k)} \cos \theta^{(k)} \\
 \bar{Q}_{26}^{(k)} &= \left(Q_{11}^{(k)} - Q_{12}^{(k)} - 2Q_{66}^{(k)} \right) \sin^3 \theta^{(k)} \cos \theta^{(k)} + \left(Q_{12}^{(k)} - Q_{22}^{(k)} + 2Q_{66}^{(k)} \right) \sin \theta^{(k)} \cos^3 \theta^{(k)} \\
 \bar{Q}_{66}^{(k)} &= \left(Q_{11}^{(k)} + Q_{22}^{(k)} - 2Q_{12}^{(k)} - 2Q_{66}^{(k)} \right) \sin^2 \theta^{(k)} \cos^2 \theta^{(k)} + Q_{66}^{(k)} \left(\sin^4 \theta^{(k)} + \cos^4 \theta^{(k)} \right) \\
 \bar{Q}_{44}^{(k)} &= Q_{44}^{(k)} \cos^2 \theta^{(k)} + Q_{55}^{(k)} \sin^2 \theta^{(k)} \\
 \bar{Q}_{45}^{(k)} &= \left(Q_{44}^{(k)} - Q_{55}^{(k)} \right) \cos \theta^{(k)} \sin \theta^{(k)} \\
 \bar{Q}_{55}^{(k)} &= Q_{55}^{(k)} \cos^2 \theta^{(k)} + Q_{44}^{(k)} \sin^2 \theta^{(k)}
 \end{aligned} \tag{15}$$

where $\theta^{(k)}$ is the orientation angle of the principal material coordinate system $O'\hat{\alpha}_1\hat{\alpha}_2\hat{\zeta}$ of the k -th orthotropic ply with respect to the laminate coordinate system $O'\alpha_1\alpha_2\zeta$. The elastic constants $Q_{nm}^{(k)}$ in the material co-ordinate system $O'\hat{\alpha}_1\hat{\alpha}_2\hat{\zeta}$ are expressed as follows:

$$\begin{aligned}
 Q_{11}^{(k)} &= \frac{E_1^{(k)}}{1 - \nu_{12}^{(k)} \nu_{21}^{(k)}}, & Q_{22}^{(k)} &= \frac{E_2^{(k)}}{1 - \nu_{12}^{(k)} \nu_{21}^{(k)}}, & Q_{12}^{(k)} &= \frac{\nu_{12}^{(k)} E_2^{(k)}}{1 - \nu_{12}^{(k)} \nu_{21}^{(k)}} \\
 Q_{66}^{(k)} &= G_{12}^{(k)}, & Q_{44}^{(k)} &= G_{13}^{(k)}, & Q_{55}^{(k)} &= G_{23}^{(k)}
 \end{aligned} \tag{16}$$

where $E_1, E_2, G_{13}, G_{23}, G_{12}, \nu_{12}$ are the engineering parameters of the k -th lamina. It should be noted that for a complete characterization of an orthotropic material, parameters E_3, ν_{13}, ν_{23} have to be taken into account as well.

For the functionally graded material k -th lamina the elastic constants $Q_{nm}^{(k)} = Q_{nm}^{(k)}(\zeta)$ in the material coordinate system $O'\hat{\alpha}_1\hat{\alpha}_2\hat{\zeta}$ are functions of thickness coordinate ζ ($\zeta \in [\zeta_k, \zeta_{k+1}]$) and are defined as:

$$\begin{aligned}
 Q_{11}^{(k)}(\zeta) &= \frac{E_1^{(k)}(\zeta)}{1 - \nu_{12}^{(k)}(\zeta)\nu_{21}^{(k)}(\zeta)}, & Q_{22}^{(k)}(\zeta) &= \frac{E_2^{(k)}(\zeta)}{1 - \nu_{12}^{(k)}(\zeta)\nu_{21}^{(k)}(\zeta)}, & Q_{12}^{(k)}(\zeta) &= \frac{\nu_{12}^{(k)}(\zeta)E_2^{(k)}(\zeta)}{1 - \nu_{12}^{(k)}(\zeta)\nu_{21}^{(k)}(\zeta)} \\
 Q_{66}^{(k)}(\zeta) &= G_{12}^{(k)}(\zeta), & Q_{44}^{(k)}(\zeta) &= G_{13}^{(k)}(\zeta), & Q_{55}^{(k)}(\zeta) &= G_{23}^{(k)}(\zeta)
 \end{aligned} \quad (17)$$

where the following relations have to be introduced:

$$\begin{aligned}
 E_1^{(k)}(\zeta) &= E_2^{(k)}(\zeta) = E_3^{(k)}(\zeta) = E^{(k)}(\zeta), \\
 \nu_{12}^{(k)}(\zeta) &= \nu_{21}^{(k)}(\zeta) = \nu_{13}^{(k)}(\zeta) = \nu_{23}^{(k)}(\zeta) = \nu^{(k)}(\zeta), \\
 G_{12}^{(k)}(\zeta) &= G_{13}^{(k)}(\zeta) = G_{23}^{(k)}(\zeta) = G^{(k)}(\zeta)
 \end{aligned} \quad (18)$$

Typically, the functionally graded materials are made of a mixture of two constituents. In the present work, it is assumed that the functionally graded material lamina is made of a mixture of ceramic and metal constituents. The material properties of the functionally graded shell vary continuously and smoothly in the thickness direction ζ of each lamina and are functions of volume fractions of two constituent materials. The Young's modulus $E^{(k)}(\zeta)$, shear modulus $G^{(k)}(\zeta)$, Poisson's ratio $\nu^{(k)}(\zeta)$ and mass density $\rho^{(k)}(\zeta)$ of the functionally graded shell k -th lamina can be expressed as:

$$\begin{aligned}
 \rho^{(k)}(\zeta) &= (\rho_C^{(k)} - \rho_M^{(k)})V_C^{(k)}(\zeta) + \rho_M^{(k)} \\
 E^{(k)}(\zeta) &= (E_C^{(k)} - E_M^{(k)})V_C^{(k)}(\zeta) + E_M^{(k)} \\
 \nu^{(k)}(\zeta) &= (\nu_C^{(k)} - \nu_M^{(k)})V_C^{(k)}(\zeta) + \nu_M^{(k)} \\
 G^{(k)}(\zeta) &= \frac{E^{(k)}(\zeta)}{2(1 + \nu^{(k)}(\zeta))}
 \end{aligned} \quad \text{for } \zeta_k \leq \zeta \leq \zeta_{k+1} \quad (19)$$

where $\rho_C^{(k)}$, $E_C^{(k)}$, $\nu_C^{(k)}$, $V_C^{(k)}$ and $\rho_M^{(k)}$, $E_M^{(k)}$, $\nu_M^{(k)}$, $V_M^{(k)}$ represent mass density, Young's modulus, Poisson's ratio and volume fraction of the ceramic and metal constituent materials, respectively. In this work, the ceramic volume fraction $V_C^{(k)}(\zeta)$ follows two simple four-parameter power-law distributions:⁷¹

$$\begin{aligned}
 FGM_{1(a^{(k)}/b^{(k)}/c^{(k)}/p^{(k)})}: & \quad V_C^{(k)}(\zeta) = \left(1 - a^{(k)} \left(\frac{\zeta}{h_k} - \frac{\zeta_k}{h_k} \right) + b^{(k)} \left(\frac{\zeta}{h_k} - \frac{\zeta_k}{h_k} \right)^{c^{(k)}} \right)^{p^{(k)}} \\
 FGM_{2(a^{(k)}/b^{(k)}/c^{(k)}/p^{(k)})}: & \quad V_C^{(k)}(\zeta) = \left(1 - a^{(k)} \left(\frac{\zeta_{k+1}}{h_k} - \frac{\zeta}{h_k} \right) + b^{(k)} \left(\frac{\zeta_{k+1}}{h_k} - \frac{\zeta}{h_k} \right)^{c^{(k)}} \right)^{p^{(k)}}
 \end{aligned} \quad (20)$$

where the volume fraction index $p^{(k)}$ ($0 \leq p^{(k)} \leq \infty$) and the parameters $a^{(k)}, b^{(k)}, c^{(k)}$ dictate the material variation profile through the functionally graded shell lamina thickness. It is important to remark that the volume fractions of all the constituent materials should add up to unity:

$$V_C^{(k)} + V_M^{(k)} = 1 \quad (21)$$

In order to choose the three parameters $a^{(k)}, b^{(k)}, c^{(k)}$ suitably, the relation (21) must be always satisfied for every volume fraction index $p^{(k)}$ in each lamina. By considering the relations (20), when the power-law exponent is set equal to zero ($p^{(k)} = 0$) or equal to infinity ($p^{(k)} = \infty$), the homogeneous isotropic

material is obtained as a special case of functionally graded material. Some material profiles through the functionally graded shell thickness are illustrated in literature.⁸⁷⁻⁹⁵

Following the principle of virtual works,^{13,20} the five governing equations in terms of internal actions **S** can be written as

$$\mathbf{D}^* \mathbf{S} + \mathbf{q} + \mathbf{q}_f + \mathbf{q}_{mf} = \mathbf{0} \tag{22}$$

The equilibrium operator **D*** is defined as

$$\mathbf{D}^* = \begin{bmatrix} D_1^* & -D_3^* & D_4^* & D_2^* & \frac{D_1^*}{R_1} & -\frac{D_3^*}{R_1} & \frac{D_4^*}{R_1} & \frac{D_2^*}{R_1} & 0 & 0 \\ -D_4^* & D_2^* & D_1^* & D_3^* & -\frac{D_4^*}{R_2} & \frac{D_2^*}{R_2} & \frac{D_1^*}{R_2} & \frac{D_3^*}{R_2} & 0 & 0 \\ -\frac{1}{R_1} & -\frac{1}{R_2} & 0 & 0 & 0 & 0 & 0 & 0 & D_1^* & D_2^* \\ 0 & 0 & 0 & 0 & D_1^* & -D_3^* & D_4^* & D_2^* & -1 & 0 \\ 0 & 0 & 0 & 0 & -D_4^* & D_2^* & D_1^* & D_3^* & 0 & -1 \end{bmatrix} \tag{23}$$

where

$$\begin{aligned} D_1^* &= \frac{1}{A_1} \frac{\partial}{\partial \alpha_1} + \frac{1}{A_1 A_2} \frac{\partial A_2}{\partial \alpha_1}, & D_2^* &= \frac{1}{A_2} \frac{\partial}{\partial \alpha_2} + \frac{1}{A_1 A_2} \frac{\partial A_1}{\partial \alpha_2} \\ D_3^* &= \frac{1}{A_1 A_2} \frac{\partial A_2}{\partial \alpha_1}, & D_4^* &= \frac{1}{A_1 A_2} \frac{\partial A_1}{\partial \alpha_2} \end{aligned} \tag{24}$$

The generalized external forces $\mathbf{q} = [q_1 \ q_2 \ q_3 \ m_1 \ m_2]^T$ due to the external forces $(q_1^{(+)}, q_1^{(-)}, q_2^{(+)}, q_2^{(-)}, q_3^{(+)}, q_3^{(-)})$ acting on the shell top and bottom surfaces are

$$\begin{aligned} q_1 &= q_1^{(+)} (H_1^{(+)})^2 H_2^{(+)} + q_1^{(-)} (H_1^{(-)})^2 H_2^{(-)} \\ q_2 &= q_2^{(+)} H_1^{(+)} (H_2^{(+)})^2 + q_2^{(-)} H_1^{(-)} (H_2^{(-)})^2 \\ q_3 &= q_3^{(+)} H_1^{(+)} H_2^{(+)} + q_3^{(-)} H_1^{(-)} H_2^{(-)} \\ m_1 &= q_1^{(+)} \frac{h}{2} H_1^{(+)} H_2^{(+)} - q_1^{(-)} \frac{h}{2} H_1^{(-)} H_2^{(-)} \\ m_2 &= q_2^{(+)} \frac{h}{2} H_1^{(+)} H_2^{(+)} - q_2^{(-)} \frac{h}{2} H_1^{(-)} H_2^{(-)} \end{aligned} \tag{25}$$

Furthermore, the generalized external forces $\mathbf{q}_f = [q_{1f} \ q_{2f} \ q_{3f} \ m_{1f} \ m_{2f}]^T$ due to the linear Winkler-Pasternak elastic foundation $(k_1^{(+)}, k_1^{(-)}, k_2^{(+)}, k_2^{(-)}, k_3^{(+)}, k_3^{(-)}, G_f^{(+)}, G_f^{(-)})$ acting on the shell bottom and top surfaces can be evaluated using the static equivalence principle as

$$\begin{aligned} q_{1f} &= -\left(k_1^{(+)} (H_1^{(+)})^3 H_2^{(+)} + k_1^{(-)} (H_1^{(-)})^3 H_2^{(-)} \right) u_1 - \frac{h}{2} \left(k_1^{(+)} (H_1^{(+)})^2 H_2^{(+)} - k_1^{(-)} (H_1^{(-)})^2 H_2^{(-)} \right) \beta_1 \\ q_{2f} &= -\left(k_2^{(+)} H_1^{(+)} (H_2^{(+)})^3 + k_2^{(-)} H_1^{(-)} (H_2^{(-)})^3 \right) u_2 - \frac{h}{2} \left(k_2^{(+)} H_1^{(+)} (H_2^{(+)})^2 - k_2^{(-)} H_1^{(-)} (H_2^{(-)})^2 \right) \beta_2 \\ q_{3f} &= -\left(k_3^{(+)} H_1^{(+)} H_2^{(+)} + k_3^{(-)} H_1^{(-)} H_2^{(-)} \right) u_3 + G_f^{(+)} H_1^{(+)} H_2^{(+)} \nabla_{(+)}^2 u_3 + G_f^{(-)} H_1^{(-)} H_2^{(-)} \nabla_{(-)}^2 u_3 \\ m_{1f} &= -\frac{h}{2} \left(k_1^{(+)} (H_1^{(+)})^2 H_2^{(+)} - k_1^{(-)} (H_1^{(-)})^2 H_2^{(-)} \right) u_1 - \frac{h^2}{4} \left(k_1^{(+)} H_1^{(+)} H_2^{(+)} + k_1^{(-)} H_1^{(-)} H_2^{(-)} \right) \beta_1 \\ m_{2f} &= -\frac{h}{2} \left(k_2^{(+)} H_1^{(+)} (H_2^{(+)})^2 - k_2^{(-)} H_1^{(-)} (H_2^{(-)})^2 \right) u_2 - \frac{h^2}{4} \left(k_2^{(+)} H_1^{(+)} H_2^{(+)} + k_2^{(-)} H_1^{(-)} H_2^{(-)} \right) \beta_2 \end{aligned} \tag{26}$$

where the Laplacian $\nabla_{(m)}^2$ operator is defined on the shell bottom and top surfaces as

$$\begin{aligned} \nabla_{(-)}^2 &= \left(\frac{1}{A_1^2 (H_1^{(-)})^2} \frac{\partial^2}{\partial \alpha_1^2} + \frac{1}{A_2^2 (H_2^{(-)})^2} \frac{\partial^2}{\partial \alpha_2^2} \right. \\ &+ \left. \left(\frac{1}{A_1^2 A_2 (H_1^{(-)})^2} \frac{\partial A_2}{\partial \alpha_1} + \frac{h}{2A_1^2 R_2^2 (H_1^{(-)})^2 H_2^{(-)}} \frac{\partial R_2}{\partial \alpha_1} - \frac{1}{A_1^3 (H_1^{(-)})^2} \frac{\partial A_1}{\partial \alpha_1} - \frac{h}{2A_1^2 R_1^2 (H_1^{(-)})^3} \frac{\partial R_1}{\partial \alpha_1} \right) \frac{\partial}{\partial \alpha_1} \right. \\ &+ \left. \left(\frac{1}{A_1 A_2^2 (H_2^{(-)})^2} \frac{\partial A_1}{\partial \alpha_2} + \frac{h}{2A_2^2 R_1^2 (H_2^{(-)})^2 H_1^{(-)}} \frac{\partial R_1}{\partial \alpha_2} - \frac{1}{A_2^3 (H_2^{(-)})^2} \frac{\partial A_2}{\partial \alpha_2} - \frac{h}{2A_2^2 R_2^2 (H_2^{(-)})^3} \frac{\partial R_2}{\partial \alpha_2} \right) \frac{\partial}{\partial \alpha_2} \right) \\ \nabla_{(+)}^2 &= \left(\frac{1}{A_1^2 (H_1^{(+)})^2} \frac{\partial^2}{\partial \alpha_1^2} + \frac{1}{A_2^2 (H_2^{(+)})^2} \frac{\partial^2}{\partial \alpha_2^2} \right. \\ &+ \left. \left(\frac{1}{A_1^2 A_2 (H_1^{(+)})^2} \frac{\partial A_2}{\partial \alpha_1} - \frac{h}{2A_1^2 R_2^2 (H_1^{(+)})^2 H_2^{(+)}} \frac{\partial R_2}{\partial \alpha_1} - \frac{1}{A_1^3 (H_1^{(+)})^2} \frac{\partial A_1}{\partial \alpha_1} + \frac{h}{2A_1^2 R_1^2 (H_1^{(+)})^3} \frac{\partial R_1}{\partial \alpha_1} \right) \frac{\partial}{\partial \alpha_1} \right. \\ &+ \left. \left(\frac{1}{A_1 A_2^2 (H_2^{(+)})^2} \frac{\partial A_1}{\partial \alpha_2} - \frac{h}{2A_2^2 R_1^2 (H_2^{(+)})^2 H_1^{(+)}} \frac{\partial R_1}{\partial \alpha_2} - \frac{1}{A_2^3 (H_2^{(+)})^2} \frac{\partial A_2}{\partial \alpha_2} + \frac{h}{2A_2^2 R_2^2 (H_2^{(+)})^3} \frac{\partial R_2}{\partial \alpha_2} \right) \frac{\partial}{\partial \alpha_2} \right) \end{aligned} \quad (27)$$

On the contrary, the generalized external actions $\mathbf{q}_{nlf} = [q_{1nlf} \ q_{2nlf} \ q_{3nlf} \ m_{1nlf} \ m_{2nlf}]^T$ due to the nonlinear elastic foundation ($k_{1nlin2}^{(+)}, k_{1nlin2}^{(-)}, k_{2nlin2}^{(+)}, k_{2nlin2}^{(-)}, k_{3nlin2}^{(+)}, k_{3nlin2}^{(-)}, k_{1nlin3}^{(+)}, k_{1nlin3}^{(-)}, k_{2nlin3}^{(+)}, k_{2nlin3}^{(-)}, k_{3nlin3}^{(+)}, k_{3nlin3}^{(-)}$) can be expressed on the reference surface of the doubly-curved shell as follows:

$$\begin{aligned} q_{1nlf} &= -k_{1nlin2}^{(+)} \operatorname{sgn} \left(H_1^{(+)} u_1 + \frac{h}{2} \beta_1 \right) \left(\left(H_1^{(+)} \right)^3 u_1^2 + \frac{h^2}{4} H_1^{(+)} \beta_1^2 + h \left(H_1^{(+)} \right)^2 u_1 \beta_1 \right) H_1^{(+)} H_2^{(+)} \\ &\quad - k_{1nlin2}^{(-)} \operatorname{sgn} \left(H_1^{(-)} u_1 - \frac{h}{2} \beta_1 \right) \left(\left(H_1^{(-)} \right)^3 u_1^2 + \frac{h^2}{4} H_1^{(-)} \beta_1^2 - h \left(H_1^{(-)} \right)^2 u_1 \beta_1 \right) H_1^{(-)} H_2^{(-)} \\ &\quad - k_{1nlin3}^{(+)} \left(\left(H_1^{(+)} \right)^4 u_1^3 + \frac{h^3}{8} H_1^{(+)} \beta_1^3 + \frac{3h}{2} \left(H_1^{(+)} \right)^3 u_1^2 \beta_1 + \frac{3h^2}{4} \left(H_1^{(+)} \right)^2 u_1 \beta_1^2 \right) H_1^{(+)} H_2^{(+)} \\ &\quad - k_{1nlin3}^{(-)} \left(\left(H_1^{(-)} \right)^4 u_1^3 - \frac{h^3}{8} H_1^{(-)} \beta_1^3 - \frac{3h}{2} \left(H_1^{(-)} \right)^3 u_1^2 \beta_1 + \frac{3h^2}{4} \left(H_1^{(-)} \right)^2 u_1 \beta_1^2 \right) H_1^{(-)} H_2^{(-)} \\ q_{2nlf} &= -k_{2nlin2}^{(+)} \operatorname{sgn} \left(H_2^{(+)} u_2 + \frac{h}{2} \beta_2 \right) \left(\left(H_2^{(+)} \right)^3 u_2^2 + \frac{h^2}{4} H_2^{(+)} \beta_2^2 + h \left(H_2^{(+)} \right)^2 u_2 \beta_2 \right) H_1^{(+)} H_2^{(+)} + \\ &\quad - k_{2nlin2}^{(-)} \operatorname{sgn} \left(H_2^{(-)} u_2 - \frac{h}{2} \beta_2 \right) \left(\left(H_2^{(-)} \right)^3 u_2^2 + \frac{h^2}{4} H_2^{(-)} \beta_2^2 - h \left(H_2^{(-)} \right)^2 u_2 \beta_2 \right) H_1^{(-)} H_2^{(-)} \\ &\quad - k_{2nlin3}^{(+)} \left(\left(H_2^{(+)} \right)^4 u_2^3 + \frac{h^3}{8} H_2^{(+)} \beta_2^3 + \frac{3h}{2} \left(H_2^{(+)} \right)^3 u_2^2 \beta_2 + \frac{3h^2}{4} \left(H_2^{(+)} \right)^2 u_2 \beta_2^2 \right) H_1^{(+)} H_2^{(+)} \\ &\quad - k_{2nlin3}^{(-)} \left(\left(H_2^{(-)} \right)^4 u_2^3 - \frac{h^3}{8} H_2^{(-)} \beta_2^3 - \frac{3h}{2} \left(H_2^{(-)} \right)^3 u_2^2 \beta_2 + \frac{3h^2}{4} \left(H_2^{(-)} \right)^2 u_2 \beta_2^2 \right) H_1^{(-)} H_2^{(-)} \\ q_{3nlf} &= -k_{3nlin2}^{(+)} \operatorname{sgn} (u_3) u_3^2 H_1^{(+)} H_2^{(+)} - k_{3nlin2}^{(-)} \operatorname{sgn} (u_3) u_3^2 H_1^{(-)} H_2^{(-)} - k_{3nlin3}^{(+)} u_3^3 H_1^{(+)} H_2^{(+)} - k_{3nlin3}^{(-)} u_3^3 H_1^{(-)} H_2^{(-)} \end{aligned} \quad (28)$$

$$\begin{aligned}
 m_{1nlf} = & -k_{1nl2}^{(+)} \operatorname{sgn}\left(H_1^{(+)}u_1 + \frac{h}{2}\beta_1\right) \left(\frac{h}{2}\left(H_1^{(+)}\right)^2 u_1^2 + \frac{h^3}{8}\beta_1^2 + \frac{h^2}{2}H_1^{(+)}u_1\beta_1\right) H_1^{(+)}H_2^{(+)} \\
 & -k_{1nl2}^{(-)} \operatorname{sgn}\left(H_1^{(-)}u_1 - \frac{h}{2}\beta_1\right) \left(-\frac{h}{2}\left(H_1^{(-)}\right)^2 u_1^2 - \frac{h^3}{8}\beta_1^2 + \frac{h^2}{2}H_1^{(-)}u_1\beta_1\right) H_1^{(-)}H_2^{(-)} \\
 & -k_{1nl3}^{(+)} \left(\frac{h}{2}\left(H_1^{(+)}\right)^3 u_1^3 + \frac{h^4}{16}\beta_1^3 + \frac{3h^2}{4}\left(H_1^{(+)}\right)^2 u_1^2\beta_1 + \frac{3h^3}{8}H_1^{(+)}u_1\beta_1^2\right) H_1^{(+)}H_2^{(+)} \\
 & -k_{1nl3}^{(-)} \left(-\frac{h}{2}\left(H_1^{(-)}\right)^3 u_1^3 + \frac{h^4}{16}\beta_1^3 + \frac{3h^2}{4}\left(H_1^{(-)}\right)^2 u_1^2\beta_1 - \frac{3h^3}{8}H_1^{(-)}u_1\beta_1^2\right) H_1^{(-)}H_2^{(-)} \\
 m_{2nlf} = & -k_{2nl2}^{(+)} \operatorname{sgn}\left(H_2^{(+)}u_2 + \frac{h}{2}\beta_2\right) \left(\frac{h}{2}\left(H_2^{(+)}\right)^2 u_2^2 + \frac{h^3}{8}\beta_2^2 + \frac{h^2}{2}H_2^{(+)}u_2\beta_2\right) H_1^{(+)}H_2^{(+)} \\
 & -k_{2nl2}^{(-)} \operatorname{sgn}\left(H_2^{(-)}u_2 - \frac{h}{2}\beta_2\right) \left(-\frac{h}{2}\left(H_2^{(-)}\right)^2 u_2^2 - \frac{h^3}{8}\beta_2^2 + \frac{h^2}{2}H_2^{(-)}u_2\beta_2\right) H_1^{(-)}H_2^{(-)} \\
 & -k_{2nl3}^{(+)} \left(\frac{h}{2}\left(H_2^{(+)}\right)^3 u_2^3 + \frac{h^4}{16}\beta_2^3 + \frac{3h^2}{4}\left(H_2^{(+)}\right)^2 u_2^2\beta_2 + \frac{3h^3}{8}H_2^{(+)}u_2\beta_2^2\right) H_1^{(+)}H_2^{(+)} \\
 & -k_{2nl3}^{(-)} \left(-\frac{h}{2}\left(H_2^{(-)}\right)^3 u_2^3 + \frac{h^4}{16}\beta_2^3 + \frac{3h^2}{4}\left(H_2^{(-)}\right)^2 u_2^2\beta_2 - \frac{3h^3}{8}H_2^{(-)}u_2\beta_2^2\right) H_1^{(-)}H_2^{(-)}
 \end{aligned}$$

The formulation of the linear and nonlinear foundations is based on the first-order approximate assumption that the foundation is made of a homogeneous material of uniform thickness $h_f^{(+)}, h_f^{(-)}$.¹²

By replacing the kinematic equations (9) into the constitutive equations (11) and the result of this substitution into the equilibrium equations (22), the complete nonlinear governing equations in terms of generalized displacements can be written as

$$(\mathbf{L} - \mathbf{L}_f - \mathbf{L}_{nlf}(\mathbf{u}^2, \mathbf{u})) \mathbf{u} + \mathbf{q} = \mathbf{0} \tag{29}$$

where $L_{(ij)}, L_{(ij)f}, L_{(ij)nlf}$, $i, j = 1, \dots, 5$, are the equilibrium, the linear Winkler-Pasternak elastic foundation and the nonlinear elastic foundation operators, respectively. As it can be seen, the nonlinear elastic operators $L_{(ij)nlf}(u_1^2, u_2^2, u_3^2, \beta_1^2, \beta_2^2, u_1, u_2, u_3, \beta_1, \beta_2)$ are linear and nonlinear functions of the generalized displacements themselves.

Three types of boundary conditions are considered, namely the fully clamped edge boundary condition (C), the free edge boundary condition (F) and soft-simply supported boundary condition (S). The following equations describe the boundary conditions introduced previously:

Clamped edge boundary conditions (C)

$$u_1 = u_2 = u_3 = \beta_1 = \beta_2 = 0 \quad \text{at} \quad \alpha_1 = \alpha_1^0 \text{ or } \alpha_1 = \alpha_1^1, \quad \alpha_2^0 \leq \alpha_2 \leq \alpha_2^1 \tag{30}$$

$$u_1 = u_2 = u_3 = \beta_1 = \beta_2 = 0 \quad \text{at} \quad \alpha_2 = \alpha_2^0 \text{ or } \alpha_2 = \alpha_2^1, \quad \alpha_1^0 \leq \alpha_1 \leq \alpha_1^1 \tag{31}$$

Free edge boundary conditions (F)

$$N_1 + \frac{M_1}{R_1} = 0, \quad N_{12} + \frac{M_{12}}{R_2} = 0, \quad T_1 = 0, \quad M_1 = M_{12} = 0 \quad \text{at} \quad \alpha_1 = \alpha_1^0 \text{ or } \alpha_1 = \alpha_1^1, \quad \alpha_2^0 \leq \alpha_2 \leq \alpha_2^1 \tag{32}$$

$$N_2 + \frac{M_2}{R_2} = 0, \quad N_{21} + \frac{M_{21}}{R_1} = 0, \quad T_2 = 0, \quad M_2 = M_{21} = 0 \quad \text{at} \quad \alpha_2 = \alpha_2^0 \text{ or } \alpha_2 = \alpha_2^1, \quad \alpha_1^0 \leq \alpha_1 \leq \alpha_1^1 \tag{33}$$

Soft-simply supported boundary conditions (S)

$$N_1 + \frac{M_1}{R_1} = 0, \quad u_2 = u_3 = 0, \quad M_1 = 0, \quad \beta_2 = 0 \quad \text{at} \quad \alpha_1 = \alpha_1^0 \text{ or } \alpha_1 = \alpha_1^1, \quad \alpha_2^0 \leq \alpha_2 \leq \alpha_2^1 \tag{34}$$

$$u_1 = 0, \quad N_2 + \frac{M_2}{R_2} = 0, \quad u_3 = 0, \quad \beta_1 = 0, \quad M_2 = 0 \quad \text{at} \quad \alpha_2 = \alpha_2^0 \text{ or } \alpha_2 = \alpha_2^1, \quad \alpha_1^0 \leq \alpha_1 \leq \alpha_1^1 \quad (35)$$

To consider complete revolute shells characterized by $\alpha_2^1 = 2\pi$, it is necessary to implement the kinematic and physical compatibility conditions between the two computational meridians with $\alpha_2^0 = 0$ and with $\alpha_2^1 = 2\pi$.

Kinematic compatibility conditions along the closing meridian ($\alpha_2 = 0, 2\pi$)

$$\begin{aligned} u_1(\alpha_1, 0, t) = u_1(\alpha_1, 2\pi, t), \quad u_2(\alpha_1, 0, t) = u_2(\alpha_1, 2\pi, t), \quad u_3(\alpha_1, 0, t) = u_3(\alpha_1, 2\pi, t), \\ \beta_1(\alpha_1, 0, t) = \beta_1(\alpha_1, 2\pi, t), \quad \beta_2(\alpha_1, 0, t) = \beta_2(\alpha_1, 2\pi, t) \end{aligned} \quad \alpha_1^0 \leq \alpha_1 \leq \alpha_1^1 \quad (36)$$

Physical compatibility conditions along the closing meridian ($\alpha_2 = 0, 2\pi$)

$$\begin{aligned} N_2(\alpha_1, 0, t) + \frac{M_2(\alpha_1, 0, t)}{R_2} = N_2(\alpha_1, 2\pi, t) + \frac{M_2(\alpha_1, 2\pi, t)}{R_2}, \\ N_{21}(\alpha_1, 0, t) + \frac{M_{21}(\alpha_1, 0, t)}{R_1} = N_{21}(\alpha_1, 2\pi, t) + \frac{M_{21}(\alpha_1, 2\pi, t)}{R_1}, \\ T_2(\alpha_1, 0, t) = T_2(\alpha_1, 2\pi, t), \quad M_2(\alpha_1, 0, t) = M_2(\alpha_1, 2\pi, t), \quad M_{21}(\alpha_1, 0, t) = M_{21}(\alpha_1, 2\pi, t) \end{aligned} \quad \alpha_1^0 \leq \alpha_1 \leq \alpha_1^1 \quad (37)$$

Analogously, in order to consider toroidal and cylindrical shells it is necessary to implement the kinematic and physical compatibility conditions between the two computational parallels with $\alpha_1^0 = 0$ and with $\alpha_1^1 = 2\pi$.

Kinematic compatibility conditions along the closing parallel ($\alpha_1 = 0, 2\pi$)

$$\begin{aligned} u_1(0, \alpha_2, t) = u_1(2\pi, \alpha_2, t), \quad u_2(0, \alpha_2, t) = u_2(2\pi, \alpha_2, t), \quad u_3(0, \alpha_2, t) = u_3(2\pi, \alpha_2, t), \\ \beta_1(0, \alpha_2, t) = \beta_1(2\pi, \alpha_2, t), \quad \beta_2(0, \alpha_2, t) = \beta_2(2\pi, \alpha_2, t) \end{aligned} \quad \alpha_2^0 \leq \alpha_2 \leq \alpha_2^1 \quad (38)$$

Physical compatibility conditions along the closing parallel ($\alpha_1 = 0, 2\pi$)

$$\begin{aligned} N_1(0, \alpha_2, t) + \frac{M_1(0, \alpha_2, t)}{R_1} = N_1(2\pi, \alpha_2, t) + \frac{M_1(2\pi, \alpha_2, t)}{R_1}, \\ N_{12}(0, \alpha_2, t) + \frac{M_{12}(0, \alpha_2, t)}{R_2} = N_{12}(2\pi, \alpha_2, t) + \frac{M_{12}(2\pi, \alpha_2, t)}{R_2}, \\ T_1(0, \alpha_2, t) = T_1(2\pi, \alpha_2, t), \quad M_1(0, \alpha_2, t) = M_1(2\pi, \alpha_2, t), \quad M_{12}(0, \alpha_2, t) = M_{12}(2\pi, \alpha_2, t) \end{aligned} \quad \alpha_2^0 \leq \alpha_2 \leq \alpha_2^1 \quad (39)$$

3 GDQ Numerical Implementation of Nonlinear Governing Equations

The GDQ method is used to discretize the derivatives in the fundamental system (29), written in terms of generalized displacements, as well as boundary conditions (see Tornabene⁷¹ for a brief review). For all the computations reported in this work, the Chebyshev-Gauss-Lobatto (C-G-L) grid distribution is assumed either along the curvilinear abscissa α_1 and α_2 . For this grid distribution choice the coordinates of grid points $(\alpha_{1i}, \alpha_{2j})$ along the reference surface, in discrete form, are

$$\begin{aligned} \alpha_{1i} = \left(1 - \cos\left(\frac{i-1}{I_N-1}\pi\right) \right) \frac{(\alpha_1^1 - \alpha_1^0)}{2} + \alpha_1^0, \quad i = 1, 2, \dots, I_N, \quad \text{for } \alpha_1 \in [\alpha_1^0, \alpha_1^1] \\ \alpha_{2j} = \left(1 - \cos\left(\frac{j-1}{I_M-1}\pi\right) \right) \frac{(\alpha_2^1 - \alpha_2^0)}{2} + \alpha_2^0, \quad j = 1, 2, \dots, I_M, \quad \text{for } \alpha_2 \in [\alpha_2^0, \alpha_2^1] \end{aligned} \quad (40)$$

where I_N, I_M are the total number of sampling points used to discretize the domain in α_1 and α_2 directions, respectively, of the doubly-curved shell. It has been proven that, for the Lagrange interpolating polynomials, the C-G-L sampling point rule guarantees convergence and efficiency to the GDQ technique.³⁷⁻¹⁰² For the nonlinear static analysis the GDQ procedure enables to write the governing equations (29) and the boundary and compatibility conditions (30)–(39) in discrete form, transforming each space derivative into a weighted sum of node values of independent variables using the GDQ rule³⁷

$$\left. \frac{\partial^n f(x)}{\partial x^n} \right|_{x=x_m} = \sum_{k=1}^T \zeta_{mk}^{(n)} f(x_k), \quad k = 1, 2, \dots, T \quad (41)$$

Each approximate equation is valid in a single sampling point. Thus, the whole system of differential equations has been discretized and the global assembling leads to the following set of nonlinear algebraic equations

$$\mathbf{R}(\boldsymbol{\delta}) = \begin{bmatrix} \mathbf{K}_{bb}(\boldsymbol{\delta}_b, \boldsymbol{\delta}_d) & \mathbf{K}_{bd}(\boldsymbol{\delta}_b, \boldsymbol{\delta}_d) \\ \mathbf{K}_{db}(\boldsymbol{\delta}_b, \boldsymbol{\delta}_d) & \mathbf{K}_{dd}(\boldsymbol{\delta}_b, \boldsymbol{\delta}_d) \end{bmatrix} \begin{bmatrix} \boldsymbol{\delta}_b \\ \boldsymbol{\delta}_d \end{bmatrix} - \begin{bmatrix} \mathbf{f}_b \\ \mathbf{f}_d \end{bmatrix} = \begin{bmatrix} \mathbf{0} \\ \mathbf{0} \end{bmatrix} \quad (42)$$

in which the partitioning is defined following the subscripts b and d , referring to the system degrees of freedom $\boldsymbol{\delta} = [\boldsymbol{\delta}_b \ \boldsymbol{\delta}_d]^T$ associated with boundary $\boldsymbol{\delta}_b$ and domain $\boldsymbol{\delta}_d$, respectively. In other words, b -equations represent the discrete boundary conditions, which are valid only for the points lying on the constrained edges of the shell $\boldsymbol{\delta}_b$ and they are numerically represented by the first matrix line of (42), whereas d -equations are the discretized equilibrium equations, assigned on the interior nodes $\boldsymbol{\delta}_d$.

The nonlinear deflection of the shell structures can be determined by solving the nonlinear algebraic problem (42). In particular, the solution procedure by means of the GDQ technique has been implemented in a MATLAB code and solved using the Newton-Raphson method. The load vector $\mathbf{f} = [\mathbf{f}_b \ \mathbf{f}_d]^T$ is applied incrementally and for each load value \mathbf{f}^r , the Newton-Raphson iterations e are to be continued until the required accuracy is reached. After the evaluation of the Jacobian matrix $\mathbf{J}^{(e)} = \frac{\partial \mathbf{R}}{\partial \boldsymbol{\delta}} \Big|_{\boldsymbol{\delta}^{(e)}}$, the following quantities are evaluated at each e -th iteration

$$\mathbf{J}_r^{(e)} \Delta_r^{(e)} = -\mathbf{R}(\boldsymbol{\delta}_r^{(e)}), \quad \Delta_r^{(e)} = \boldsymbol{\delta}_r^{(e+1)} - \boldsymbol{\delta}_r^{(e)} \quad (43)$$

The residual $\mathbf{R}(\boldsymbol{\delta})$ is gradually reduced to zero if the procedure converge. For this purpose, in the present approach, two different criteria are used and simultaneously satisfied at each e -th iteration

$$\|\Delta_r^{(e)}\| \leq \delta, \quad \|\mathbf{R}(\boldsymbol{\delta}_r^{(e)})\| \leq \rho \quad (44)$$

Here, the convergence tolerances δ, ρ are taken to be equal $\delta = \rho = 10^{-9}$. For each r -th load step \mathbf{f}^r , the generalized displacement field $\boldsymbol{\delta}_r$ can be obtained. For all the results presented in the following a maximum number of three iterations has been used to converge to the solution.

4 A Posteriori Stress and Strain Recovery Procedure

The 3D Elasticity problem represents a starting point for all the engineering problems of mechanics. In fact, the initial problem has been simplified using the well-defined hypotheses of the FSDT. Hence it must be underlined that the approximated solutions found within a 2D Equivalent Single Layer (ESL) theory work only under the limits of the theory. Since the 3D Elasticity equations are always valid for every elastic problem, the approximated solution can be used to evaluate some quantities that had been neglected by the FSDT. For example the in-plane stresses, their derivatives and in addition others quantities of interest can be found solving the 3D equilibrium equations such as shear and normal stresses.^{89,90,92,95,98,100} Thus, starting from the 3D Elasticity in orthogonal curvilinear coordinates for a general doubly-curved shell,¹² the 3D equilibrium equations for a doubly-curved shell can be written as follows

$$\begin{aligned}
 \frac{\partial \tau_{1n}}{\partial \zeta} + \tau_{1n} \left(\frac{2}{R_1 + \zeta} + \frac{1}{R_2 + \zeta} \right) &= -\frac{1}{A_1(1 + \zeta/R_1)} \frac{\partial \sigma_1}{\partial \alpha_1} + \frac{\sigma_2 - \sigma_1}{A_1 A_2 (1 + \zeta/R_2)} \frac{\partial A_2}{\partial \alpha_1} \\
 &\quad - \frac{1}{A_2(1 + \zeta/R_2)} \frac{\partial \tau_{12}}{\partial \alpha_2} - \frac{2\tau_{12}}{A_1 A_2 (1 + \zeta/R_1)} \frac{\partial A_1}{\partial \alpha_2} \\
 \frac{\partial \tau_{2n}}{\partial \zeta} + \tau_{2n} \left(\frac{1}{R_1 + \zeta} + \frac{2}{R_2 + \zeta} \right) &= -\frac{1}{A_2(1 + \zeta/R_2)} \frac{\partial \sigma_2}{\partial \alpha_2} + \frac{\sigma_1 - \sigma_2}{A_1 A_2 (1 + \zeta/R_1)} \frac{\partial A_1}{\partial \alpha_2} \\
 &\quad - \frac{1}{A_1(1 + \zeta/R_1)} \frac{\partial \tau_{12}}{\partial \alpha_1} - \frac{2\tau_{12}}{A_1 A_2 (1 + \zeta/R_2)} \frac{\partial A_1}{\partial \alpha_1} \\
 \frac{\partial \sigma_n}{\partial \zeta} + \sigma_n \left(\frac{1}{R_1 + \zeta} + \frac{1}{R_2 + \zeta} \right) &= -\frac{1}{A_1(1 + \zeta/R_1)} \frac{\partial \tau_{1n}}{\partial \alpha_1} - \frac{\tau_{1n}}{A_1 A_2 (1 + \zeta/R_2)} \frac{\partial A_2}{\partial \alpha_1} \\
 &\quad - \frac{1}{A_2(1 + \zeta/R_2)} \frac{\partial \tau_{2n}}{\partial \alpha_2} - \frac{\tau_{2n}}{A_1 A_2 (1 + \zeta/R_1)} \frac{\partial A_1}{\partial \alpha_2} + \frac{\sigma_1}{R_1 + \zeta} + \frac{\sigma_2}{R_2 + \zeta}
 \end{aligned} \tag{45}$$

It can be seen that if the stresses ($\sigma_1, \sigma_2, \tau_{12}$) and their derivatives ($\sigma_{1,1}, \sigma_{2,2}, \tau_{12,1}, \tau_{12,2}$) are known in all the points of the 3D solid shell, the above three differential equations can be seen as three independent differential equations of the first order that can be solved via the GDQ method along the thickness direction ζ . It is worth noting that the third equation can be evaluated after the numerical computation of the first two unknowns τ_{1n}, τ_{2n} and their derivatives $\tau_{1n,1}, \tau_{2n,2}$.

In order to determine the unknowns present in the right-hand side of the equations (45), it is possible to start from the static solution in terms of the displacements obtained in the previous paragraph. Thus, after solving the static problem, all the displacements in the 3D solid shell can be written in discrete form using the displacement field (7)

$$\begin{aligned}
 U_{1(ijm)} &= \left(1 + \frac{\zeta_m}{R_{1(ij)}} \right) u_{1(ij)} + \zeta_m \beta_{1(ij)} \\
 U_{2(ijm)} &= \left(1 + \frac{\zeta_m}{R_{2(ij)}} \right) u_{2(ij)} + \zeta_m \beta_{2(ij)} \quad \text{for } i = 1, \dots, N, j = 1, \dots, M, m = 1, \dots, T \\
 U_{3(ijm)} &= u_{3(ij)}
 \end{aligned} \tag{46}$$

where T is the total number of sampling points used to discretize the domain in ζ direction. The C-G-L grid distribution is assumed for the coordinates of grid points ζ_m along the shell thickness direction ζ

$$\zeta_m = \left(1 - \cos \left(\frac{m-1}{T-1} \pi \right) \right) \frac{h}{2} - \frac{h}{2}, \quad m = 1, 2, \dots, T, \quad \text{for } \zeta \in \left[-\frac{h}{2}, \frac{h}{2} \right] \tag{47}$$

Furthermore, the discrete external actions ($\bar{q}_{1(ij)}^{(+)}, \bar{q}_{1(ij)}^{(-)}, \bar{q}_{2(ij)}^{(+)}, \bar{q}_{2(ij)}^{(-)}, \bar{q}_{3(ij)}^{(+)}, \bar{q}_{3(ij)}^{(-)}$) acting on the top and bottom surfaces due to the external forces and due to the linear and nonlinear elastic foundations can be evaluated as:

$$\begin{aligned}
 \bar{q}_{1(ij)}^{(+)} &= q_{1(ij)}^{(+)} + q_{1f(ij)}^{(+)} + q_{1nlf(ij)}^{(+)} = q_{1(ij)}^{(+)} + k_{1(ij)}^{(+)} U_{1(ijT)} + k_{1nl2(ij)}^{(+)} \operatorname{sgn} \left(U_{1(ijT)} \right) U_{1(ijT)}^2 + k_{1nl3(ij)}^{(+)} U_{1(ijT)}^3 \\
 \bar{q}_{2(ij)}^{(+)} &= q_{2(ij)}^{(+)} + q_{2f(ij)}^{(+)} + q_{2nlf(ij)}^{(+)} = q_{2(ij)}^{(+)} + k_{2(ij)}^{(+)} U_{2(ijT)} + k_{2nl2(ij)}^{(+)} \operatorname{sgn} \left(U_{2(ijT)} \right) U_{2(ijT)}^2 + k_{2nl3(ij)}^{(+)} U_{2(ijT)}^3 \\
 \bar{q}_{3(ij)}^{(+)} &= q_{3(ij)}^{(+)} + q_{3f(ij)}^{(+)} + q_{3nlf(ij)}^{(+)} = q_{3(ij)}^{(+)} + k_{3(ij)}^{(+)} U_{3(ijT)} + k_{3nl2(ij)}^{(+)} \operatorname{sgn} \left(U_{3(ijT)} \right) U_{3(ijT)}^2 + k_{3nl3(ij)}^{(+)} U_{3(ijT)}^3 \\
 \bar{q}_{1(ij)}^{(-)} &= q_{1(ij)}^{(-)} + q_{1f(ij)}^{(-)} + q_{1nlf(ij)}^{(-)} = q_{1(ij)}^{(-)} + k_{1(ij)}^{(-)} U_{1(ij1)} + k_{1nl2(ij)}^{(-)} \operatorname{sgn} \left(U_{1(ij1)} \right) U_{1(ij1)}^2 + k_{1nl3(ij)}^{(-)} U_{1(ij1)}^3 \\
 \bar{q}_{2(ij)}^{(-)} &= q_{2(ij)}^{(-)} + q_{2f(ij)}^{(-)} + q_{2nlf(ij)}^{(-)} = q_{2(ij)}^{(-)} + k_{2(ij)}^{(-)} U_{2(ij1)} + k_{2nl2(ij)}^{(-)} \operatorname{sgn} \left(U_{2(ij1)} \right) U_{2(ij1)}^2 + k_{2nl3(ij)}^{(-)} U_{2(ij1)}^3 \\
 \bar{q}_{3(ij)}^{(-)} &= q_{3(ij)}^{(-)} + q_{3f(ij)}^{(-)} + q_{3nlf(ij)}^{(-)} = q_{3(ij)}^{(-)} + k_{3(ij)}^{(-)} U_{3(ij1)} + k_{3nl2(ij)}^{(-)} \operatorname{sgn} \left(U_{3(ij1)} \right) U_{3(ij1)}^2 + k_{3nl3(ij)}^{(-)} U_{3(ij1)}^3
 \end{aligned} \tag{48}$$

By using the GDQ rule,³⁷ an approximation of the kinematic relations (9) can be obtained in discrete form

$$\begin{aligned}
 \varepsilon_{1(ij)}^0 &\equiv \frac{1}{A_{1(ij)}} \sum_{k=1}^N \zeta_{ik}^{\alpha_1(1)} u_{1(kj)} + \frac{u_{2(ij)}}{A_{1(ij)} A_{2(ij)}} \frac{\partial A_1}{\partial \alpha_2} \Big|_{(ij)} + \frac{u_{3(ij)}}{R_{1(ij)}} \\
 \varepsilon_{2(ij)}^0 &\equiv \frac{1}{A_{2(ij)}} \sum_{k=1}^M \zeta_{jk}^{\alpha_2(1)} u_{2(ik)} + \frac{u_{1(ij)}}{A_{1(ij)} A_{2(ij)}} \frac{\partial A_2}{\partial \alpha_1} \Big|_{(ij)} + \frac{u_{3(ij)}}{R_{2(ij)}} \\
 \gamma_{1(ij)}^0 &\equiv \frac{1}{A_{1(ij)}} \sum_{k=1}^N \zeta_{ik}^{\alpha_1(1)} u_{2(kj)} - \frac{u_{1(ij)}}{A_{1(ij)} A_{2(ij)}} \frac{\partial A_1}{\partial \alpha_2} \Big|_{(ij)} \\
 \gamma_{2(ij)}^0 &\equiv \frac{1}{A_{2(ij)}} \sum_{k=1}^M \zeta_{jk}^{\alpha_2(1)} u_{1(ik)} - \frac{u_{2(ij)}}{A_{1(ij)} A_{2(ij)}} \frac{\partial A_2}{\partial \alpha_1} \Big|_{(ij)} \\
 \chi_{1(ij)}^0 &\equiv \frac{1}{A_{1(ij)} R_{1(ij)}} \sum_{k=1}^N \zeta_{ik}^{\alpha_1(1)} u_{1(kj)} - \frac{u_{1(ij)}}{A_{1(ij)} R_{1(ij)}^2} \frac{\partial R_1}{\partial \alpha_1} \Big|_{(ij)} + \frac{u_{2(ij)}}{A_{1(ij)} A_{2(ij)} R_{2(ij)}} \frac{\partial A_1}{\partial \alpha_2} \Big|_{(ij)} \\
 &\quad + \frac{1}{A_{1(ij)}} \sum_{k=1}^N \zeta_{ik}^{\alpha_1(1)} \beta_{1(kj)} + \frac{\beta_{2(ij)}}{A_{1(ij)} A_{2(ij)}} \frac{\partial A_1}{\partial \alpha_2} \Big|_{(ij)} \\
 \chi_{2(ij)}^0 &\equiv \frac{u_{1(ij)}}{A_{1(ij)} A_{2(ij)} R_{1(ij)}} \frac{\partial A_2}{\partial \alpha_1} \Big|_{(ij)} + \frac{1}{A_{2(ij)} R_{2(ij)}} \sum_{k=1}^M \zeta_{jk}^{\alpha_2(1)} u_{2(ik)} - \frac{u_{2(ij)}}{A_{2(ij)} R_{2(ij)}^2} \frac{\partial R_2}{\partial \alpha_2} \Big|_{(ij)} \\
 &\quad + \frac{\beta_{1(ij)}}{A_{1(ij)} A_{2(ij)}} \frac{\partial A_2}{\partial \alpha_1} \Big|_{(ij)} + \frac{1}{A_{2(ij)}} \sum_{k=1}^M \zeta_{jk}^{\alpha_2(1)} \beta_{2(ik)} \\
 \omega_{1(ij)}^0 &\equiv -\frac{u_{1(ij)}}{A_{1(ij)} A_{2(ij)} R_{1(ij)}} \frac{\partial A_1}{\partial \alpha_2} \Big|_{(ij)} + \frac{1}{A_{1(ij)} R_{2(ij)}} \sum_{k=1}^N \zeta_{ik}^{\alpha_1(1)} u_{2(kj)} - \frac{u_{2(ij)}}{A_{1(ij)} R_{2(ij)}^2} \frac{\partial R_2}{\partial \alpha_1} \Big|_{(ij)} \\
 &\quad - \frac{\beta_{1(ij)}}{A_{1(ij)} A_{2(ij)}} \frac{\partial A_1}{\partial \alpha_2} \Big|_{(ij)} + \frac{1}{A_{1(ij)}} \sum_{k=1}^N \zeta_{ik}^{\alpha_1(1)} \beta_{2(kj)} \\
 \omega_{2(ij)}^0 &\equiv \frac{1}{A_{2(ij)} R_{1(ij)}} \sum_{k=1}^M \zeta_{jk}^{\alpha_2(1)} u_{1(ik)} - \frac{u_{1(ij)}}{A_{2(ij)} R_{1(ij)}^2} \frac{\partial R_1}{\partial \alpha_2} \Big|_{(ij)} - \frac{u_{2(ij)}}{A_{1(ij)} A_{2(ij)} R_{2(ij)}} \frac{\partial A_2}{\partial \alpha_1} \Big|_{(ij)} \\
 &\quad + \frac{1}{A_{2(ij)}} \sum_{k=1}^M \zeta_{jk}^{\alpha_2(1)} \beta_{1(ik)} - \frac{\beta_{2(ij)}}{A_{1(ij)} A_{2(ij)}} \frac{\partial A_2}{\partial \alpha_1} \Big|_{(ij)}
 \end{aligned} \tag{49}$$

Since the kinematic relation $\varepsilon_1, \varepsilon_2, \varepsilon_{12}$ of the 3D shell medium are the following

$$\begin{aligned}
 \varepsilon_{1(ijm)} &= \frac{1}{1 + \zeta_m / R_{1(ij)}} \left(\varepsilon_{1(ij)}^0 + \zeta_m \chi_{1(ij)}^0 \right) \\
 \varepsilon_{2(ijm)} &= \frac{1}{1 + \zeta_m / R_{2(ij)}} \left(\varepsilon_{2(ij)}^0 + \zeta_m \chi_{2(ij)}^0 \right) \\
 \gamma_{12(ijm)} &= \frac{1}{1 + \zeta_m / R_{1(ij)}} \left(\gamma_{1(ij)}^0 + \zeta_m \omega_{1(ij)}^0 \right) + \frac{1}{1 + \zeta_m / R_{2(ij)}} \left(\gamma_{2(ij)}^0 + \zeta_m \omega_{2(ij)}^0 \right)
 \end{aligned} \tag{50}$$

by using the well-known reduced Hooke's laws²⁰ for elastic composite materials

$$\begin{aligned}
 \sigma_{1(ijm)} &= \bar{Q}_{11}^{(m)} \varepsilon_{1(ijm)} + \bar{Q}_{12}^{(m)} \varepsilon_{2(ijm)} + \bar{Q}_{16}^{(m)} \gamma_{12(ijm)} \\
 \sigma_{2(ijm)} &= \bar{Q}_{12}^{(m)} \varepsilon_{1(ijm)} + \bar{Q}_{22}^{(m)} \varepsilon_{2(ijm)} + \bar{Q}_{26}^{(m)} \gamma_{12(ijm)} \\
 \tau_{12(ijm)} &= \bar{Q}_{16}^{(m)} \varepsilon_{1(ijm)} + \bar{Q}_{26}^{(m)} \varepsilon_{2(ijm)} + \bar{Q}_{66}^{(m)} \gamma_{12(ijm)}
 \end{aligned} \tag{51}$$

and the GDQ rule,³⁷ the derivatives of the stress components $\sigma_{1,1}$, $\sigma_{2,2}$, $\tau_{12,1}$, $\tau_{12,2}$ can be approximated as follows

$$\left. \begin{aligned} \frac{\partial \sigma_1}{\partial \alpha_1} \Big|_{(ijm)} &\equiv \sum_{k=1}^N \zeta_{ik}^{\alpha_1(1)} \sigma_{1(kjm)} \\ \frac{\partial \sigma_2}{\partial \alpha_2} \Big|_{(ijm)} &\equiv \sum_{k=1}^M \zeta_{jk}^{\alpha_2(1)} \sigma_{2(ikm)} \\ \frac{\partial \tau_{12}}{\partial \alpha_1} \Big|_{(ijm)} &\equiv \sum_{k=1}^N \zeta_{ik}^{\alpha_1(1)} \tau_{12(kjm)} \\ \frac{\partial \tau_{12}}{\partial \alpha_2} \Big|_{(ijm)} &\equiv \sum_{k=1}^M \zeta_{jk}^{\alpha_2(1)} \tau_{12(ikm)} \end{aligned} \right\} \quad (52)$$

By considering the boundary conditions at the bottom surface of the shell, the first two 3D equilibrium equations (45) in terms of shear stresses τ_{1n} , τ_{2n} can be directly and independently solved at each reference surface points (α_p, α_j) using the following linear algebraic systems of equations obtained via the GDQ method

$$\left\{ \begin{aligned} \tau_{1n(ij1)} &= \bar{q}_{1(ij)}^{(-)} \text{ (Boundary condition at the bottom surface of the shell)} \\ \sum_{k=1}^T \zeta_{mk}^{\zeta(1)} \tau_{1n(ijk)} + \tau_{1n(ijm)} \left(\frac{2}{R_{1(ij)} + \zeta_m} + \frac{1}{R_{2(ij)} + \zeta_m} \right) &= - \frac{1}{A_{1(ij)} \left(1 + \zeta_m / R_{1(ij)} \right)} \frac{\partial \sigma_1}{\partial \alpha_1} \Big|_{(ijm)} \\ &+ \frac{\sigma_{2(ijm)} - \sigma_{1(ijm)}}{A_{1(ij)} A_{2(ij)} \left(1 + \zeta_m / R_{2(ij)} \right)} \frac{\partial A_2}{\partial \alpha_1} \Big|_{(ij)} + \frac{1}{A_{2(ij)} \left(1 + \zeta_m / R_{2(ij)} \right)} \frac{\partial \tau_{12}}{\partial \alpha_2} \Big|_{(ijm)} \\ &- \frac{2 \tau_{12(ijm)}}{A_{1(ij)} A_{2(ij)} \left(1 + \zeta_m / R_{1(ij)} \right)} \frac{\partial A_1}{\partial \alpha_2} \Big|_{(ij)} \end{aligned} \right\} \quad \text{for } m = 2, \dots, T \quad (53)$$

$$\left\{ \begin{aligned} \tau_{2n(ij1)} &= \bar{q}_{2(ij)}^{(-)} \text{ (Boundary condition at the bottom surface of the shell)} \\ \sum_{k=1}^T \zeta_{mk}^{\zeta(1)} \tau_{2n(ijk)} + \tau_{2n(ijm)} \left(\frac{1}{R_{1(ij)} + \zeta_m} + \frac{2}{R_{2(ij)} + \zeta_m} \right) &= - \frac{1}{A_{2(ij)} \left(1 + \zeta_m / R_{2(ij)} \right)} \frac{\partial \sigma_2}{\partial \alpha_2} \Big|_{(ijm)} \\ &+ \frac{\sigma_{1(ijm)} - \sigma_{2(ijm)}}{A_{1(ij)} A_{2(ij)} \left(1 + \zeta_m / R_{1(ij)} \right)} \frac{\partial A_1}{\partial \alpha_2} \Big|_{(ij)} + \frac{1}{A_{1(ij)} \left(1 + \zeta_m / R_{1(ij)} \right)} \frac{\partial \tau_{12}}{\partial \alpha_1} \Big|_{(ijm)} \\ &- \frac{2 \tau_{12(ijm)}}{A_{1(ij)} A_{2(ij)} \left(1 + \zeta_m / R_{2(ij)} \right)} \frac{\partial A_2}{\partial \alpha_1} \Big|_{(ij)} \end{aligned} \right\} \quad \text{for } m = 2, \dots, T$$

In order to satisfy the second boundary condition at the top surface of the shell, $\tau_{1n(ijT)} = \bar{q}_{1(ij)}^{(+)}$ and $\tau_{2n(ijT)} = \bar{q}_{2(ij)}^{(+)}$, respectively, the shear stress profiles can be linearly corrected in the following manner

$$\left\{ \begin{aligned} \bar{\tau}_{1n(ijm)} &= \tau_{1n(ijm)} + \frac{\bar{q}_{1(ij)}^{(+)} - \tau_{1n(ijT)}}{h} \left(\zeta_m + \frac{h}{2} \right) \\ \bar{\tau}_{2n(ijm)} &= \tau_{2n(ijm)} + \frac{\bar{q}_{2(ij)}^{(+)} - \tau_{2n(ijT)}}{h} \left(\zeta_m + \frac{h}{2} \right) \end{aligned} \right\} \quad \text{for } m = 1, \dots, T \quad (54)$$

Finally, the last 3D equilibrium equation (45) can be written in discrete form and solved via the GDQ method

$$\left\{ \begin{aligned} \sigma_{n(ij1)} &= \bar{q}_{3(ij)}^{(-)} \text{ (Boundary condition at the bottom surface of the shell)} \\ \sum_{k=1}^T \zeta_{mk}^{\alpha_1(1)} \sigma_{n(ijk)} + \sigma_{n(ijm)} \left(\frac{1}{R_{1(ij)} + \zeta_m} + \frac{1}{R_{2(ij)} + \zeta_m} \right) &= \frac{\sigma_{1(ijm)}}{R_{1(ij)} + \zeta_m} + \frac{\sigma_{2(ijm)}}{R_{2(ij)} + \zeta_m} \\ + \frac{1}{A_{1(ij)}(1 + \zeta_m/R_{1(ij)})} \frac{\partial \bar{\tau}_{1n}}{\partial \alpha_1} \Big|_{(ijm)} - \frac{\bar{\tau}_{1n(ijm)}}{A_{1(ij)}A_{2(ij)}(1 + \zeta_m/R_{2(ij)})} \frac{\partial A_2}{\partial \alpha_1} \Big|_{(ij)} & \\ + \frac{1}{A_{2(ij)}(1 + \zeta_m/R_{2(ij)})} \frac{\partial \bar{\tau}_{2n}}{\partial \alpha_2} \Big|_{(ijm)} - \frac{\bar{\tau}_{2n(ijm)}}{A_{1(ij)}A_{2(ij)}(1 + \zeta_m/R_{1(ij)})} \frac{\partial A_1}{\partial \alpha_2} \Big|_{(ij)} & \end{aligned} \right. \quad (55)$$

for $m = 2, \dots, T$

where the derivatives $\bar{\tau}_{1n,1}, \bar{\tau}_{2n,2}$ of the shear stresses $\bar{\tau}_{1n}, \bar{\tau}_{2n}$ can be approximated using the GDQ rule³⁷

$$\left. \begin{aligned} \frac{\partial \bar{\tau}_{1n}}{\partial \alpha_1} \Big|_{(ijm)} &\cong \sum_{k=1}^N \zeta_{ik}^{\alpha_1(1)} \bar{\tau}_{1n(kjm)} \\ \frac{\partial \bar{\tau}_{2n}}{\partial \alpha_2} \Big|_{(ijm)} &\cong \sum_{k=1}^M \zeta_{jk}^{\alpha_2(1)} \bar{\tau}_{2n(ikm)} \end{aligned} \right. \quad (56)$$

In order to satisfy the second boundary condition at the top surface of the shell $\sigma_{n(ijT)} = \bar{q}_{3(ij)}^{(+)}$, the correction profile of the normal stress can be defined as the shear stresses (54) as follows

$$\bar{\sigma}_{n(ijm)} = \sigma_{n(ijm)} + \frac{\bar{q}_{3(ij)}^{(+)} - \sigma_{n(ijT)}}{h} \left(\zeta_m + \frac{h}{2} \right) \quad \text{for } m = 1, \dots, T \quad (57)$$

Furthermore, it is possible to use the generalized Hooke's laws²⁰ in order to evaluate the out-of-plane deformations $\gamma_{1n}, \gamma_{2n}, \epsilon_n$

$$\left. \begin{aligned} \gamma_{1n(ijm)} &= \frac{\bar{C}_{55}^{(m)} \bar{\tau}_{1n(ijm)} - \bar{C}_{45}^{(m)} \bar{\tau}_{2n(ijm)}}{\bar{C}_{55}^{(m)} \bar{C}_{44}^{(m)} - (\bar{C}_{45}^{(m)})^2} \\ \gamma_{2n(ijm)} &= \frac{\bar{C}_{44}^{(m)} \bar{\tau}_{2n(ijm)} - \bar{C}_{45}^{(m)} \bar{\tau}_{1n(ijm)}}{\bar{C}_{55}^{(m)} \bar{C}_{44}^{(m)} - (\bar{C}_{45}^{(m)})^2} \\ \epsilon_{n(ijm)} &= \frac{\bar{\sigma}_{n(ijm)} - \bar{C}_{13}^{(m)} \epsilon_{1(ijm)} - \bar{C}_{23}^{(m)} \epsilon_{2(ijm)} - \bar{C}_{36}^{(m)} \gamma_{12(ijm)}}{\bar{C}_{33}^{(m)}} \end{aligned} \right. \quad (58)$$

It is worth noting that the relations (58) do not guarantee the strain compatibility. In fact, some discontinuities can arise. However, the solution obtained in this way can be used as a good approximation of some quantities that are considered a priori constant or negligible by using the FSDT. In fact, the stresses $\sigma_1, \sigma_2, \tau_{12}$ can be corrected taking into account the contribution of the approximated deformation ϵ_n using the following generalized constitutive relations

$$\left. \begin{aligned} \bar{\sigma}_{1(ijm)} &= \bar{C}_{11}^{(m)} \epsilon_{1(ijm)} + \bar{C}_{12}^{(m)} \epsilon_{2(ijm)} + \bar{C}_{16}^{(m)} \gamma_{12(ijm)} + \bar{C}_{13}^{(m)} \epsilon_{n(ijm)} \\ \bar{\sigma}_{2(ijm)} &= \bar{C}_{12}^{(m)} \epsilon_{1(ijm)} + \bar{C}_{22}^{(m)} \epsilon_{2(ijm)} + \bar{C}_{26}^{(m)} \gamma_{12(ijm)} + \bar{C}_{23}^{(m)} \epsilon_{n(ijm)} \\ \bar{\tau}_{12(ijm)} &= \bar{C}_{16}^{(m)} \epsilon_{1(ijm)} + \bar{C}_{26}^{(m)} \epsilon_{2(ijm)} + \bar{C}_{66}^{(m)} \gamma_{12(ijm)} + \bar{C}_{36}^{(m)} \epsilon_{n(ijm)} \end{aligned} \right. \quad (59)$$

Thus, after the above considerations all the stress components ($\bar{\sigma}_1, \bar{\sigma}_2, \bar{\tau}_{12}, \bar{\tau}_{1n}, \bar{\tau}_{2n}, \bar{\sigma}_n$) of the 3D shell medium are numerically computed using the relations (54), (57), and (59). Finally, the simple efficient method for accurate evaluation of the through-the-thickness distribution of shear and normal stresses in composite laminated shells presented above can be easily applied to different generalized displacement field solutions obtained with other numerical methods and with more sophisticated kinematical models. In fact, since no restriction has been assumed about the methodology used to perform the pre-processing static analysis, the post-processing procedure proposed can yield stress distributions starting from the knowledge of the displacement field previously evaluated with an alternative methodology different from the FSDT solution presented in this work.

5 Numerical Results

In the present section, some results and considerations about the static problem of functionally graded and laminated composite doubly-curved, singly-curved and degenerate shells and panels resting on nonlinear elastic foundations are presented. The geometrical boundary conditions for a panel are identified by the following convention. Considering the Figure 1, the West edge (W) is defined by the relations $\alpha_2 = \alpha_2^0, \alpha_1^0 \leq \alpha_1 \leq \alpha_1^1$, whereas its opposite, the East edge (E), is characterized by the relations $\alpha_2 = \alpha_2^1, \alpha_1^0 \leq \alpha_1 \leq \alpha_1^1$. Likewise, the North edge (N) is defined by the relations $\alpha_1 = \alpha_1^0, \alpha_2^0 \leq \alpha_2 \leq \alpha_2^1$, whereas its opposite, the South edge (S), is characterized by the relations $\alpha_1 = \alpha_1^1, \alpha_2^0 \leq \alpha_2 \leq \alpha_2^1$. Thus, the boundary condition sequence for a panel structure can be represented with the following symbology WSEN. In this way, the first side is the West edge, the second one is the South edge, the third one is the East edge and finally, the last one is the North edge. For example, the symbolism CFCF shows that the West and East edges are clamped, whereas the South and North edges are free. Differently, the CF symbol denotes that the South and North edges are clamped and free for a revolution shell, whereas the West and East edges are clamped and free for a toroidal shell. The missing boundary conditions are the kinematical and physical compatibility conditions that are applied at the same closing meridians, the West and East edges, for a revolution shell and at the same closing parallels, the South and North edges, for a toroidal shell, respectively.

In order to verify the theoretical formulation proposed in the second section, the solution procedure has been implemented in a MATLAB code.¹⁰² In this study the geometric parameters are calculated by using the differential geometry, as it is shown in.⁹²⁻¹⁰² Since a 2D Equivalent Single Layer (ESL) theory²⁰ has been considered, it is important to specify in which surface the foundation is applied; it can be on the bottom $k^{(-)}$ or on the top surface $k^{(+)}$, depending on whether the foundation is considered to support the structure. With the same symbology the top and bottom nonlinear elastic normal and in-plane stiffnesses have been applied.

Figure 3 shows the six investigated shell structures: a rectangular plate, a cylindrical shell, a conical shell, a spherical shell, an elliptic paraboloid and a hyperbolic paraboloid. For these structure, the local coordinate system and the reference surface vector $\mathbf{r}(\alpha_1, \alpha_2)$ are shown in Figure 3.

For the present GDQ results coupled with the Newton-Raphson method, a Chebyshev-Gauss-Lobatto grid distribution (40) with $I_N = I_M = 31$ is considered for all the shell structures depicted in Figure 3. Moreover, a C-G-L grid of 31 points for each lamina is considered through the thickness of the shell. The external load has applied on the top and bottom surfaces of the shell and the numerical value of the nonlinear foundation varies from case to case and it is indicated in the corresponding figures and tables.

Figure 4 shows the lamination schemes for the six structures analysed varying the value of the exponent of the four-parameter power-law distribution adopted. Tables 1–6 present numerical results in terms of the static center deflection of the six considered structures. The material properties used and the lamination schemes adopted as well as the geometric parameters and the boundary conditions considered for each structure are indicated in Tables 1–6.

Figure 5 graphically shows some of the results of Tables 1–6 and presents the effects of various parameters of the nonlinear elastic foundation introduced. Finally, Figures 6–23 report the through-the-thickness displacement, stress and strain profiles for all the structures under consideration obtained using the stress recovery procedure.

Table 1 presents results for a square plates (Figure 3a) with a (30/65/45) lamination scheme as shown in Figure 4a. Two different composite material has been considered: Graphite-Epoxy and Glass-Epoxy. The orthotropic materials and the lamina thicknesses, as well as the boundary conditions and lamination scheme are also reported in Table 1. The external laminae are made of different orthotropic materials

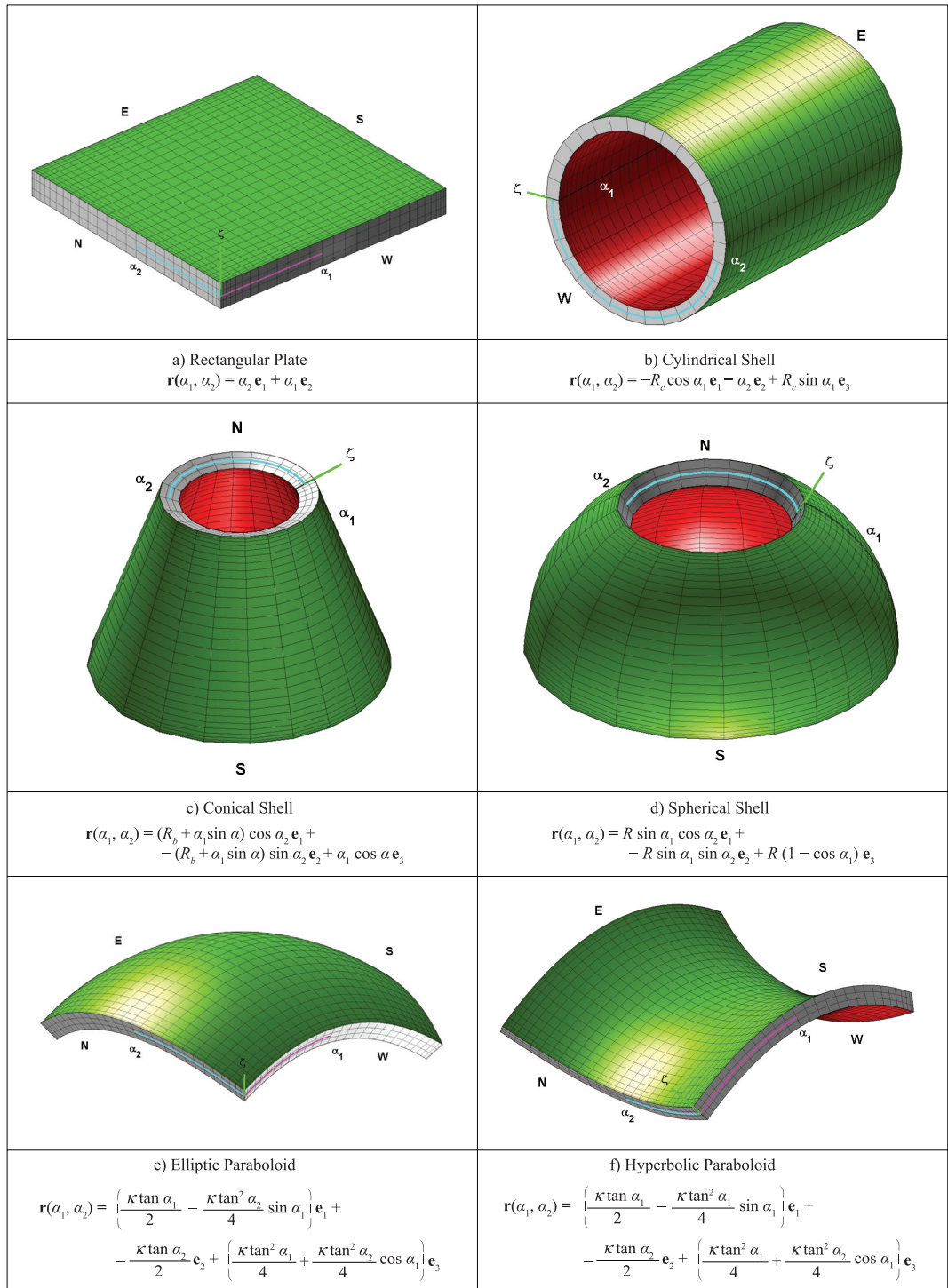


Figure 3: Different shell and panel structures and relative reference position vectors $\mathbf{r}(\alpha_1, \alpha_2)$.

with respect to the middle lamina (see Table 1 and Figure 4). The thickness of the first and third laminae are equal to $h_1 = h_3 = 0.03$ m, whereas the second lamina has a thickness equal to $h_2 = 0.04$ m. Figure 5a shows the response of the structure surrounded by different kinds of linear and nonlinear foundations. The static center deflections are compared for seven different cases: the first has no foundation, the second is a Winkler elastic foundation with $k_3^{(-)}$, the third is a Winkler-Pasternak elastic foundation with $k_3^{(-)}, G_f^{(-)}$, the fourth is characterized by $k_3^{(-)}, k_{3nl2}^{(-)}$, the fifth considers $k_3^{(-)}, k_{3nl2}^{(-)}, G_f^{(-)}$ and finally the sixth

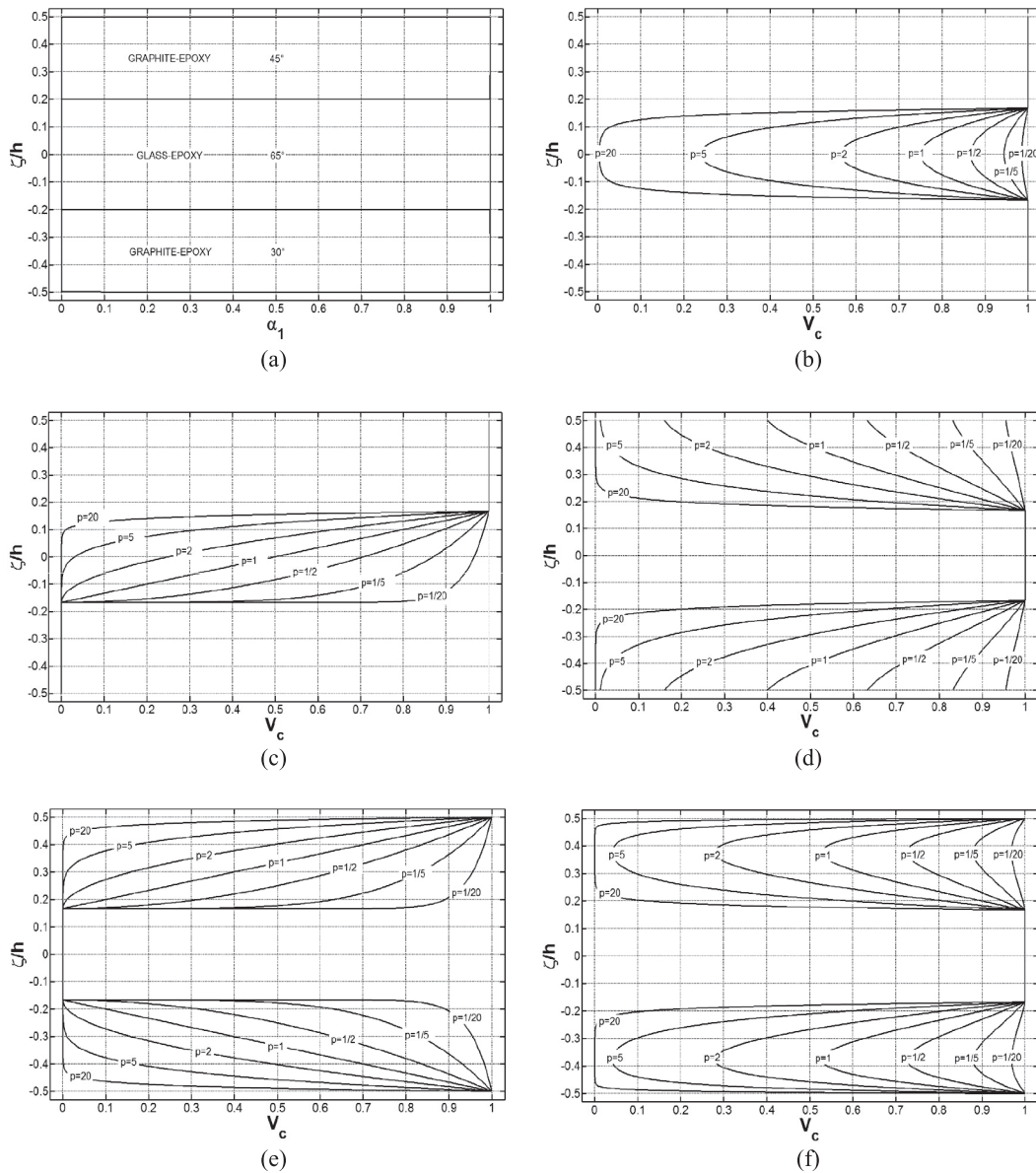


Figure 4: Lamination schemes and volume fraction distributions V_c for the six structures of Figure 1: (a) rectangular plate of Table 1, (b) cylindrical shell of Table 2, (c) conical shell of Table 3, (d) spherical shell of Table 4, (e) elliptic paraboloid of Table 5, (f) hyperbolic paraboloid of Table 6.

and the seventh are characterized by the following parameters $k_3^{(-)}$, $k_{3nl2}^{(-)}$, $k_{3nl3}^{(-)}$ and $k_3^{(-)}$, $k_{3nl2}^{(-)}$, $k_{3nl3}^{(-)}$, $G_f^{(-)}$, respectively. In analogous way, Figure 5 shows similar results for the others five structures considered.

In order to validate the procedure in Figures 6–8 the GDQ results in terms of displacements, strains and stresses are compared with 3D FEM solution obtained using Straus code. 16000 bricks with 20 nodes are used to obtain 3D FEM solutions for the square plate with and without Winkler foundation. The reference 3D FEM mesh is taken as $40 \times 40 \times 10$, where 10 represents the number of elements along the thickness direction. Very good agreement is observed with the FEM solutions as it can be seen from the Figures 6–8, even though a 2D FSDT is considered.

In Figures 9–11 a cylindrical shell (Figure 3b and Table 2) is considered. The material properties are reported in Table 2. The lamination scheme is reported in Figure 3b. Figure 5b reports the results by varying the nonlinear elastic foundation parameters, whereas Figures 9–11 show the response of the structure by varying the exponent of the four-parameter power-law distribution.

The results in terms of displacements, strains and stresses for the conical (Figure 3c and Table 3) and the spherical (Figure 3d and Table 4) shells, which have the lamination schemes reported in Figure 4c and 4d, respectively, are shown in Figures 12–14 and 15–17. Also for these two cases Figures 5c and 5d present the structural response by varying elastic foundation parameters, whereas Figures 12–14 and 15–17 show the response of the structures by varying the exponent of the four-parameter power-law distribution.

In conclusion, Figures 18–20 and 21–23 present results for two doubly-curved panels: an elliptic paraboloid of Figure 3e (Table 5) and a hyperbolic paraboloid of Figure 3f (Table 6). The lamination schemes adopted are shown in Figure 4e and 4f, respectively. Also for these two last cases Figures 5e and 5f present the structural response by varying elastic foundation parameters, whereas Figures 18–20 and 21–23 show the response of the structures by varying the exponent of the four-parameter power-law distribution.

As expected, from the parameter investigation the structural response of the last five structures does not present any discontinuities in terms of stresses, strains and displacements, as it can be seen for the

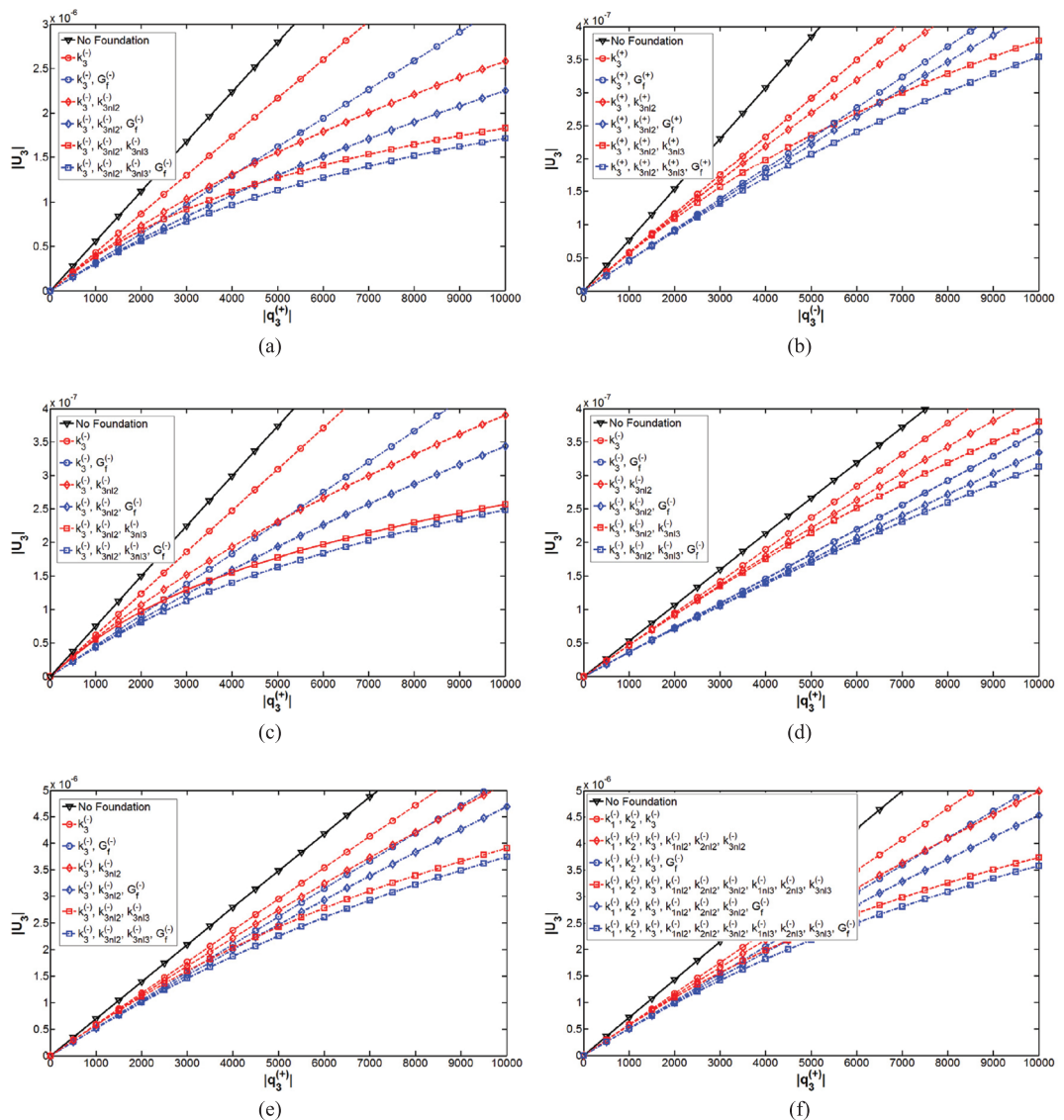


Figure 5: Static center deflection u_3 [m], at the point $B = (0.5(\alpha_1^+ - \alpha_1^-), 0.5(\alpha_2^+ - \alpha_2^-))$ for different load steps, of six different structures resting on elastic foundations, using a 31×31 Chebyshev-Gauss-Lobatto (C-G-L) grid distribution: (a) rectangular plate of Table 1, (b) cylindrical shell of Table 2, (c) conical shell of Table 3, (d) spherical shell of Table 4, (e) elliptic paraboloid of Table 5, (f) hyperbolic paraboloid of Table 6.

Table 1: Static center deflection u_3 [m] of a (30/65/45) C-C-C square plate resting on elastic foundations at the point $B = (0.5(\alpha_1^+ - \alpha_1^-), 0.5(\alpha_2^+ - \alpha_2^-))$ for different load step $q_{3(i)}^{(+)}$ using a 31×31 Chebyshev-Gauss-Lobatto (C-G-L) grid distribution.

Geometric characteristics: $\alpha_1 = [0, 1]$ m, $\alpha_2 = [0, 1]$ m, $h = 0.1$ m
 Properties of the laminae 1 and 3: $E_1 = 137.9$ GPa, $E_2 = E_3 = 8.96$ GPa, $G_{12} = G_{13} = 7.1$ GPa, $G_{23} = 6.21$ GPa, $V_{12} = V_{13} = 0.3$, $V_{23} = 0.49$, $\rho = 1450$ kg/m³, $h_1 = h_3 = 0.03$ m
 Properties of the lamina 2: $E_1 = 53.78$ GPa, $E_2 = E_3 = 17.93$ GPa, $G_{12} = G_{13} = 8.96$ GPa, $G_{23} = 3.45$ GPa, $V_{12} = V_{13} = 0.25$, $V_{23} = 0.34$, $\rho = 1900$ kg/m³, $h_2 = 0.04$ m
 Foundation properties: $k_3^{(-)} = 7.5 \cdot 10^8$ N/m³, $G_f^{(-)} = 5 \cdot 10^7$ N/m, $k_{3nl2}^{(-)} = 1 \cdot 10^{15}$ N/m⁴, $k_{3nl3}^{(-)} = 1 \cdot 10^{21}$ N/m⁵

Load step $q_{3(i)}^{(+)}$	No foundation	$k_3^{(-)}$	$k_3^{(-)}, G_f^{(-)}$	$k_3^{(-)}, k_{3nl2}^{(-)}$	$k_3^{(-)}, G_f^{(-)}, k_{3nl2}^{(-)}$	$k_3^{(-)}, k_{3nl2}^{(-)}, k_{3nl3}^{(-)}$	$k_3^{(-)}, G_f^{(-)}, k_{3nl2}^{(-)}, k_{3nl3}^{(-)}$
$q_{3(1)}^{(+)} = -1$ kPa	-5.5918E-07	-4.3325E-07	-3.2338E-07	-3.9549E-07	-3.0623E-07	-3.8560E-07	-3.0238E-07
$q_{3(2)}^{(+)} = -2$ kPa	-1.1184E-06	-8.6650E-07	-6.4676E-07	-7.3452E-07	-5.8386E-07	-6.8377E-07	-5.6072E-07
$q_{3(3)}^{(+)} = -3$ kPa	-1.6775E-06	-1.2998E-06	-9.7014E-07	-1.0348E-06	-8.3920E-07	-9.1868E-07	-7.7968E-07
$q_{3(4)}^{(+)} = -4$ kPa	-2.2367E-06	-1.7330E-06	-1.2935E-06	-1.3064E-06	-1.0765E-06	-1.1103E-06	-9.6694E-07
$q_{3(5)}^{(+)} = -5$ kPa	-2.7959E-06	-2.1663E-06	-1.6169E-06	-1.5557E-06	-1.2989E-06	-1.2714E-06	-1.1293E-06
$q_{3(6)}^{(+)} = -6$ kPa	-3.3551E-06	-2.5995E-06	-1.9403E-06	-1.7870E-06	-1.5086E-06	-1.4104E-06	-1.2722E-06
$q_{3(7)}^{(+)} = -7$ kPa	-3.9142E-06	-3.0328E-06	-2.2637E-06	-2.0035E-06	-1.7075E-06	-1.5324E-06	-1.3994E-06
$q_{3(8)}^{(+)} = -8$ kPa	-4.4734E-06	-3.4660E-06	-2.5870E-06	-2.2074E-06	-1.8969E-06	-1.6414E-06	-1.5140E-06
$q_{3(9)}^{(+)} = -9$ kPa	-5.0326E-06	-3.8993E-06	-2.9104E-06	-2.4006E-06	-2.0779E-06	-1.7398E-06	-1.6182E-06
$q_{3(10)}^{(+)} = -10$ kPa	-5.5918E-06	-4.3325E-06	-3.2338E-06	-2.5844E-06	-2.2515E-06	-1.8297E-06	-1.7138E-06

Table 2: Static center deflection u_s [m] of a (Zirconia/FGM/Zirconia) C-C cylindrical shell resting on elastic foundations at the point $B = (0.5(\alpha_1^2 - \alpha_2^2), 0.5(\alpha_2^2 - \alpha_1^2))$ for different load step $q_{3(r)}^{(-)}$ and different values of the exponent $p = p^{(2)}$, using a 31×31 Chebyshev-Gauss-Lobatto (C-G-L) grid distribution.

Geometric characteristics: $R_c = 2$ m, $\alpha_1 = [0, 360^\circ]$, $\alpha_2 = [0, 6$ m], $h = 0.3$ m
 Properties of the lamina 1: $E = 168$ GPa, $\nu = 0.3$, $\rho = 5700$ kg/m³ (Zirconia), $h = 0.1$ m
 Properties of the lamina 2: $FGM_{1(a^{(2)}=1/b^{(2)}=1/c^{(2)}=2/p^{(2)})}$ (mixture of Aluminum and Zirconia), $h = 0.1$ m
 Properties of the lamina 3: $E = 168$ GPa, $\nu = 0.3$, $\rho = 5700$ kg/m³ (Zirconia), $h = 0.1$ m
 Foundation properties: $k_3^{(+)} = 3.5 \cdot 10^9$ N/m³, $G_f^{(+)} = 2.5 \cdot 10^{10}$ N/m, $k_{3nl2}^{(+)} = 5 \cdot 10^{15}$ N/m⁴, $k_{3nl3}^{(+)} = 5 \cdot 10^{22}$ N/m⁵

		$p = 5$					
Load step $q_{3(r)}^{(-)}$	No foundation	$k_3^{(+)}$	$k_3^{(+)}, G_f^{(+)}$	$k_3^{(+)}, k_{3nl2}^{(+)}$	$k_3^{(+)}, G_f^{(+)}, k_{3nl2}^{(+)}$	$k_3^{(+)}, k_{3nl2}^{(+)}, k_{3nl3}^{(+)}$	$k_3^{(+)}, G_f^{(+)}, k_{3nl2}^{(+)}, k_{3nl3}^{(+)}$
$q_{3(1)}^{(-)} = 1$ kPa	7.6942E-08	5.8289E-08	4.6234E-08	5.7301E-08	4.5833E-08	5.6764E-08	4.5665E-08
$q_{3(2)}^{(-)} = 2$ kPa	1.5388E-07	1.1658E-07	9.2468E-08	1.1276E-07	9.0889E-08	1.0907E-07	8.9635E-08
$q_{3(3)}^{(-)} = 3$ kPa	2.3083E-07	1.7487E-07	1.3870E-07	1.6653E-07	1.3520E-07	1.5608E-07	1.3131E-07
$q_{3(4)}^{(-)} = 4$ kPa	3.0777E-07	2.3316E-07	1.8494E-07	2.1878E-07	1.7881E-07	1.9803E-07	1.7038E-07
$q_{3(5)}^{(-)} = 5$ kPa	3.8471E-07	2.9145E-07	2.3117E-07	2.6962E-07	2.2175E-07	2.3560E-07	2.0679E-07
$q_{3(6)}^{(-)} = 6$ kPa	4.6165E-07	3.4974E-07	2.7740E-07	3.1917E-07	2.6403E-07	2.6948E-07	2.4063E-07
$q_{3(7)}^{(-)} = 7$ kPa	5.3860E-07	4.0802E-07	3.2364E-07	3.6752E-07	3.0570E-07	3.0030E-07	2.7210E-07
$q_{3(8)}^{(-)} = 8$ kPa	6.1554E-07	4.6631E-07	3.6987E-07	4.1476E-07	3.4677E-07	3.2855E-07	3.0139E-07
$q_{3(9)}^{(-)} = 9$ kPa	6.9248E-07	5.2460E-07	4.1611E-07	4.6095E-07	3.8727E-07	3.5463E-07	3.2872E-07
$q_{3(10)}^{(-)} = 10$ kPa	7.6942E-07	5.8289E-07	4.6234E-07	5.0617E-07	4.2722E-07	3.7887E-07	3.5431E-07

Load step $q_{3(r)}^{(-)}$	$k_3^{(+)}, G_f^{(+)}, k_{3m/2}^{(+)}, k_{3m/3}^{(+)}$						
	$p = 1/20$	$p = 1/5$	$p = 1/2$	$p = 1$	$p = 2$	$p = 5$	$p = 20$
$q_{3(1)}^{(-)} = 1 \text{ kPa}$	4.2888E-08	4.3016E-08	4.3262E-08	4.3642E-08	4.4302E-08	4.5665E-08	4.7476E-08
$q_{3(2)}^{(-)} = 2 \text{ kPa}$	8.4396E-08	8.4639E-08	8.5105E-08	8.5824E-08	8.7069E-08	8.9635E-08	9.3028E-08
$q_{3(3)}^{(-)} = 3 \text{ kPa}$	1.2402E-07	1.2436E-07	1.2501E-07	1.2601E-07	1.2774E-07	1.3131E-07	1.3599E-07
$q_{3(4)}^{(-)} = 4 \text{ kPa}$	1.6146E-07	1.6188E-07	1.6268E-07	1.6391E-07	1.6603E-07	1.7038E-07	1.7605E-07
$q_{3(5)}^{(-)} = 5 \text{ kPa}$	1.9662E-07	1.9710E-07	1.9802E-07	1.9942E-07	2.0185E-07	2.0679E-07	2.1320E-07
$q_{3(6)}^{(-)} = 6 \text{ kPa}$	2.2954E-07	2.3007E-07	2.3107E-07	2.3261E-07	2.3526E-07	2.4063E-07	2.4757E-07
$q_{3(7)}^{(-)} = 7 \text{ kPa}$	2.6033E-07	2.6089E-07	2.6196E-07	2.6360E-07	2.6641E-07	2.7210E-07	2.7940E-07
$q_{3(8)}^{(-)} = 8 \text{ kPa}$	2.8915E-07	2.8973E-07	2.9084E-07	2.9255E-07	2.9548E-07	3.0139E-07	3.0895E-07
$q_{3(9)}^{(-)} = 9 \text{ kPa}$	3.1616E-07	3.1676E-07	3.1790E-07	3.1966E-07	3.2267E-07	3.2872E-07	3.3644E-07
$q_{3(10)}^{(-)} = 10 \text{ kPa}$	3.4153E-07	3.4214E-07	3.4331E-07	3.4510E-07	3.4816E-07	3.5431E-07	3.6213E-07

Table 3: Static center deflection u_3 [m] of a (Aluminum/FGM_z/Zirconia) C-F conical shell resting on elastic foundations at the point $B = (0.5(\alpha_1^1 - \alpha_1^0), 0.5(\alpha_2^1 - \alpha_2^0))$ for different load step $q_{3(i)}^{(+)}$ and different values of the exponent $p = p^{(2)}$, using a 31×31 Chebyshev-Gauss-Lobatto (C-G-L) grid distribution.

Geometric characteristics: $R_0 = 1$ m, $\alpha = 20^\circ$, $\alpha_1 = [0, 3]$ m, $\alpha_2 = [0, 360^\circ]$, $h = 0.3$ m
 Properties of the lamina 1: $E = 70$ GPa, $\nu = 0.3$, $\rho = 2707$ kg/m³ (Aluminum), $h_1 = 0.1$ m
 Properties of the lamina 2: $FGM_{2(d^{(2)}=1/b^{(2)}=0/r^{(2)}=0/\rho^{(2)})}$ (mixture of Aluminum and Zirconia), $h_2 = 0.1$ m
 Properties of the lamina 3: $E = 168$ GPa, $\nu = 0.3$, $\rho = 5700$ kg/m³ (Zirconia), $h_3 = 0.1$ m
 Foundation properties: $k_3^{(-)} = 3.5 \cdot 10^9$ N/m³, $G_f^{(-)} = 1 \cdot 10^{10}$ N/m, $k_{3n/2}^{(-)} = 3 \cdot 10^{16}$ N/m⁴, $k_{3n/3}^{(-)} = 3 \cdot 10^{23}$ N/m⁵

$p = 1/5$

Load step $q_{3(i)}^{(+)}$	No foundation	$k_3^{(-)}$	$k_3^{(-)}$, $G_f^{(-)}$	$k_3^{(-)}$, $k_3^{(-)}$, $k_{3n/2}^{(-)}$	$k_3^{(-)}$, $G_f^{(-)}$, $k_{3n/2}^{(-)}$	$k_3^{(-)}$, $k_3^{(-)}$, $k_{3n/3}^{(-)}$	$k_3^{(-)}$, $G_f^{(-)}$, $k_{3n/2}^{(-)}$, $k_{3n/3}^{(-)}$
$q_{3(1)}^{(+)} = -1$ kPa	-7.4764E-08	-6.1865E-08	-4.5798E-08	-5.7128E-08	-4.3976E-08	-5.5064E-08	-4.3307E-08
$q_{3(2)}^{(+)} = -2$ kPa	-1.4953E-07	-1.2373E-07	-9.1596E-08	-1.0701E-07	-8.4796E-08	-9.6756E-08	-8.0687E-08
$q_{3(3)}^{(+)} = -3$ kPa	-2.2429E-07	-1.8560E-07	-1.3739E-07	-1.5179E-07	-1.2303E-07	-1.2906E-07	-1.1238E-07
$q_{3(4)}^{(+)} = -4$ kPa	-2.9905E-07	-2.4746E-07	-1.8319E-07	-1.9273E-07	-1.5910E-07	-1.5532E-07	-1.3946E-07
$q_{3(5)}^{(+)} = -5$ kPa	-3.7382E-07	-3.0933E-07	-2.2899E-07	-2.3066E-07	-1.9331E-07	-1.7751E-07	-1.6295E-07
$q_{3(6)}^{(+)} = -6$ kPa	-4.4858E-07	-3.7119E-07	-2.7479E-07	-2.6613E-07	-2.2592E-07	-1.9682E-07	-1.8365E-07
$q_{3(7)}^{(+)} = -7$ kPa	-5.2335E-07	-4.3306E-07	-3.2059E-07	-2.9957E-07	-2.5713E-07	-2.1398E-07	-2.0215E-07
$q_{3(8)}^{(+)} = -8$ kPa	-5.9811E-07	-4.9492E-07	-3.6639E-07	-3.3128E-07	-2.8709E-07	-2.2949E-07	-2.1889E-07
$q_{3(9)}^{(+)} = -9$ kPa	-6.7287E-07	-5.5679E-07	-4.1218E-07	-3.6150E-07	-3.1594E-07	-2.4367E-07	-2.3419E-07
$q_{3(10)}^{(+)} = -10$ kPa	-7.4764E-07	-6.1865E-07	-4.5798E-07	-3.9042E-07	-3.4379E-07	-2.5677E-07	-2.4829E-07

Load step $q_{3(i)}^{(+)}$	$k_3^{(-)}, G_f^{(-)}, k_{3m/2}^{(-)}, k_{3m/3}^{(-)}$						
	$p = 1/20$	$p = 1/5$	$p = 1/2$	$p = 1$	$p = 2$	$p = 5$	$p = 20$
$q_{3(1)}^{(+)} = -1$ kPa	-4.2570E-08	-4.3307E-08	-4.4386E-08	-4.5516E-08	-4.6695E-08	-4.7923E-08	-4.8828E-08
$q_{3(2)}^{(+)} = -2$ kPa	-7.9515E-08	-8.0687E-08	-8.2383E-08	-8.4137E-08	-8.5943E-08	-8.7795E-08	-8.9144E-08
$q_{3(3)}^{(+)} = -3$ kPa	-1.1100E-07	-1.1238E-07	-1.1438E-07	-1.1642E-07	-1.1850E-07	-1.2062E-07	-1.2214E-07
$q_{3(4)}^{(+)} = -4$ kPa	-1.3798E-07	-1.3946E-07	-1.4158E-07	-1.4374E-07	-1.4593E-07	-1.4813E-07	-1.4971E-07
$q_{3(5)}^{(+)} = -5$ kPa	-1.6143E-07	-1.6295E-07	-1.6511E-07	-1.6730E-07	-1.6951E-07	-1.7172E-07	-1.7331E-07
$q_{3(6)}^{(+)} = -6$ kPa	-1.8213E-07	-1.8365E-07	-1.8581E-07	-1.8799E-07	-1.9018E-07	-1.9237E-07	-1.9393E-07
$q_{3(7)}^{(+)} = -7$ kPa	-2.0065E-07	-2.0215E-07	-2.0428E-07	-2.0643E-07	-2.0859E-07	-2.1074E-07	-2.1227E-07
$q_{3(8)}^{(+)} = -8$ kPa	-2.1741E-07	-2.1889E-07	-2.2099E-07	-2.2309E-07	-2.2521E-07	-2.2731E-07	-2.2881E-07
$q_{3(9)}^{(+)} = -9$ kPa	-2.3273E-07	-2.3419E-07	-2.3624E-07	-2.3831E-07	-2.4037E-07	-2.4244E-07	-2.4390E-07
$q_{3(10)}^{(+)} = -10$ kPa	-2.4686E-07	-2.4829E-07	-2.5030E-07	-2.5232E-07	-2.5435E-07	-2.5636E-07	-2.5779E-07

Table 4: Static center deflection u_3 [m] of a (FGM₂/Zirconia/FGM₁) C-F spherical shell resting on elastic foundations at the point $B = (0.5(\alpha_1^+ - \alpha_1^0), 0.5(\alpha_2^+ - \alpha_2^0))$ for different load step $q_{3(r)}^{(+)}$ and different values of the exponent $p = p^{(0)} = p^{(3)}$, using a 31 x 31 Chebyshev-Gauss-Lobatto (C-G-L) grid distribution.

Geometric characteristics: $R = 2$ m, $\alpha_1 = [30^\circ, 90^\circ]$, $\alpha_2 = [0, 360^\circ]$, $h = 0.3$ m
 Properties of the lamina 1: $FGM_{2(a^{(0)}=0.8/b^{(0)}=0.2/c^{(0)}=3/p^{(0)})}$ (mixture of Aluminum and Zirconia), $h_1 = 0.1$ m
 Properties of the lamina 2: $E = 168$ GPa, $\nu = 0.3$, $\rho = 5700$ kg/m³ (Zirconia), $h_2 = 0.1$ m
 Properties of the lamina 3: $FGM_{1(a^{(3)}=0.8/b^{(3)}=0.2/c^{(3)}=3/p^{(3)})}$ (mixture of Aluminum and Zirconia), $h_3 = 0.1$ m
 Foundation properties: $k_3^{(-)} = 3.5 \cdot 10^9$ N/m³, $G_f^{(-)} = 7.5 \cdot 10^9$ N/m, $k_{3n2}^{(-)} = 1 \cdot 10^{16}$ N/m⁴, $k_{3n3}^{(-)} = 3 \cdot 10^{22}$ N/m⁵

$p = 1$						
Load step $q_{3(r)}^{(+)}$	No foundation	$k_3^{(-)}$	$k_3^{(-)}, G_f^{(-)}$	$k_3^{(-)}, k_{3n2}^{(-)}$	$k_3^{(-)}, G_f^{(-)}, k_{3n2}^{(-)}$	$k_3^{(-)}, k_{3n2}^{(-)}, k_{3n3}^{(-)}$
$q_{3(1)}^{(+)} = -1$ kPa	-5.3174E-08	-4.7315E-08	-3.6529E-08	-4.6660E-08	-3.6158E-08	-4.6574E-08
$q_{3(2)}^{(+)} = -2$ kPa	-1.0635E-07	-9.4629E-08	-7.3059E-08	-9.2078E-08	-7.1609E-08	-9.1440E-08
$q_{3(3)}^{(+)} = -3$ kPa	-1.5952E-07	-1.4194E-07	-1.0959E-07	-1.3634E-07	-1.0640E-07	-1.3437E-07
$q_{3(4)}^{(+)} = -4$ kPa	-2.1270E-07	-1.8926E-07	-1.4612E-07	-1.7954E-07	-1.4057E-07	-1.7524E-07
$q_{3(5)}^{(+)} = -5$ kPa	-2.6587E-07	-2.3657E-07	-1.8265E-07	-2.2173E-07	-1.7417E-07	-2.1406E-07
$q_{3(6)}^{(+)} = -6$ kPa	-3.1905E-07	-2.8389E-07	-2.1918E-07	-2.6299E-07	-2.0721E-07	-2.5088E-07
$q_{3(7)}^{(+)} = -7$ kPa	-3.7222E-07	-3.3120E-07	-2.5570E-07	-3.0337E-07	-2.3974E-07	-2.8579E-07
$q_{3(8)}^{(+)} = -8$ kPa	-4.2539E-07	-3.7852E-07	-2.9223E-07	-3.4293E-07	-2.7177E-07	-3.1891E-07
$q_{3(9)}^{(+)} = -9$ kPa	-4.7857E-07	-4.2583E-07	-3.2876E-07	-3.8170E-07	-3.0334E-07	-3.5036E-07
$q_{3(10)}^{(+)} = -10$ kPa	-5.3174E-07	-4.7315E-07	-3.6529E-07	-4.1974E-07	-3.3447E-07	-3.8027E-07

$K_{31}^{(-)}, G_1^{(-)}, K_{3n/2}^{(-)}, K_{3n/3}^{(-)}$							
Load step $q_{3(r)}^{(+)}$	$p = 1/20$	$p = 1/5$	$p = 1/2$	$p = 1$	$p = 2$	$p = 5$	$p = 20$
$q_{3(1)}^{(+)} = -1$ kPa	-3.2617E-08	-3.3260E-08	-3.4440E-08	-3.6116E-08	-3.8568E-08	-4.1968E-08	-4.4572E-08
$q_{3(2)}^{(+)} = -2$ kPa	-6.4558E-08	-6.5800E-08	-6.8074E-08	-7.1292E-08	-7.5977E-08	-8.2413E-08	-8.7289E-08
$q_{3(3)}^{(+)} = -3$ kPa	-9.5731E-08	-9.7523E-08	-1.0080E-07	-1.0541E-07	-1.1209E-07	-1.2117E-07	-1.2798E-07
$q_{3(4)}^{(+)} = -4$ kPa	-1.2608E-07	-1.2837E-07	-1.3254E-07	-1.3841E-07	-1.4684E-07	-1.5821E-07	-1.6663E-07
$q_{3(5)}^{(+)} = -5$ kPa	-1.5556E-07	-1.5830E-07	-1.6329E-07	-1.7026E-07	-1.8023E-07	-1.9355E-07	-2.0331E-07
$q_{3(6)}^{(+)} = -6$ kPa	-1.8418E-07	-1.8732E-07	-1.9303E-07	-2.0098E-07	-2.1228E-07	-2.2725E-07	-2.3813E-07
$q_{3(7)}^{(+)} = -7$ kPa	-2.1193E-07	-2.1544E-07	-2.2178E-07	-2.3059E-07	-2.4305E-07	-2.5942E-07	-2.7122E-07
$q_{3(8)}^{(+)} = -8$ kPa	-2.3884E-07	-2.4266E-07	-2.4957E-07	-2.5913E-07	-2.7259E-07	-2.9016E-07	-3.0272E-07
$q_{3(9)}^{(+)} = -9$ kPa	-2.6492E-07	-2.6903E-07	-2.7644E-07	-2.8666E-07	-3.0098E-07	-3.1956E-07	-3.3275E-07
$q_{3(10)}^{(+)} = -10$ kPa	-2.9021E-07	-2.9457E-07	-3.0242E-07	-3.1322E-07	-3.2828E-07	-3.4771E-07	-3.6143E-07

Table 5: Static center deflection u_3 [m] of a (FGM/Aluminum/FGM)₂ C-C-C-C elliptic paraboloid resting on elastic foundations at the point $B = (0.5(\alpha_1^+ - \alpha_1^0), 0.5(\alpha_2^+ - \alpha_2^0))$ for different load step $q_{3(r)}^{(+)}$ and different values of the exponent $p = p^{(1)} = p^{(2)} = p^{(3)}$, using a 31×31 Chebyshev-Gauss-Lobatto (C-G-L) grid distribution.

Geometric characteristics of the two parabolas: $\alpha_1 = \alpha_2 = [-33.69^\circ, 33.69^\circ]$, $\kappa = 18$ m, $h = 0.9$ m
 Properties of the lamina 1: FGM₁($\rho^{(1)}=1/b^{(1)}=0/c^{(1)}=0/\rho^{(1)}$) (mixture of Aluminum and Zirconia), $h_1 = 0.3$ m
 Properties of the lamina 2: $E = 70$ GPa, $\nu = 0.3$, $\rho = 2707$ kg/m³ (Aluminum), $h_2 = 0.3$ m
 Properties of the lamina 3: FGM₂($\rho^{(3)}=1/b^{(3)}=0/c^{(3)}=0/\rho^{(3)}$) (mixture of Aluminum and Zirconia), $h_3 = 0.3$ m
 Foundation properties: $k_3^{(-)} = 3.5 \cdot 10^8$ N/m³, $G_f^{(-)} = 2.5 \cdot 10^9$ N/m, $k_{3n2}^{(-)} = 5 \cdot 10^{12}$ N/m⁴, $k_{3n3}^{(-)} = 5 \cdot 10^{18}$ N/m⁵

		$p = 2$					
Load step $q_{3(r)}^{(+)}$	No foundation	$k_3^{(-)}$	$k_3^{(-)}, G_f^{(-)}$	$k_3^{(-)}, k_{3n2}^{(-)}$	$k_3^{(-)}, G_f^{(-)}, k_{3n2}^{(-)}$	$k_3^{(-)}, k_{3n2}^{(-)}, k_{3n3}^{(-)}$	$k_3^{(-)}, G_f^{(-)}, k_{3n2}^{(-)}, k_{3n3}^{(-)}$
$q_{3(1)}^{(+)} = -1$ kPa	-6.9682E-07	5.9011E-07	-5.2404E-07	-5.8050E-07	-5.1744E-07	-5.7609E-07	-5.1473E-07
$q_{3(2)}^{(+)} = -2$ kPa	-1.3936E-06	1.1802E-06	-1.0481E-06	-1.1429E-06	-1.0223E-06	-1.1118E-06	-1.0026E-06
$q_{3(3)}^{(+)} = -3$ kPa	-2.0905E-06	1.7703E-06	-1.5721E-06	-1.6887E-06	-1.5154E-06	-1.5979E-06	-1.4559E-06
$q_{3(4)}^{(+)} = -4$ kPa	-2.7873E-06	2.3604E-06	-2.0961E-06	-2.2192E-06	-1.9974E-06	-2.0345E-06	-1.8725E-06
$q_{3(5)}^{(+)} = -5$ kPa	-3.4841E-06	2.9506E-06	-2.6202E-06	-2.7355E-06	-2.4691E-06	-2.4262E-06	-2.2536E-06
$q_{3(6)}^{(+)} = -6$ kPa	-4.1809E-06	3.5407E-06	-3.1442E-06	-3.2387E-06	-2.9310E-06	-2.7790E-06	-2.6024E-06
$q_{3(7)}^{(+)} = -7$ kPa	-4.8778E-06	4.1308E-06	-3.6683E-06	-3.7297E-06	-3.3838E-06	-3.0989E-06	-2.9224E-06
$q_{3(8)}^{(+)} = -8$ kPa	-5.5746E-06	4.7209E-06	-4.1923E-06	-4.2092E-06	-3.8278E-06	-3.3911E-06	-3.2173E-06
$q_{3(9)}^{(+)} = -9$ kPa	-6.2714E-06	5.3110E-06	-4.7163E-06	-4.6781E-06	-4.2635E-06	-3.6597E-06	-3.4902E-06
$q_{3(10)}^{(+)} = -10$ kPa	-6.9682E-06	5.9011E-06	-5.2404E-06	-5.1368E-06	-4.6915E-06	-3.9083E-06	-3.7440E-06

Load step $q_{3(r)}^{(+)}$	$k_3^{(-)}, G_f^{(-)}, k_{3n/2}^{(-)}, k_{3n/3}^{(-)}$									
	$p = 1/20$	$p = 1/5$	$p = 1/2$	$p = 1$	$p = 2$	$p = 5$	$p = 20$			
$q_{3(1)}^{(+)} = -1$ kPa	-3.8923E-07	-4.0822E-07	-4.3829E-07	-4.7333E-07	-5.1473E-07	-5.6445E-07	-6.0626E-07			
$q_{3(2)}^{(+)} = -2$ kPa	-7.6807E-07	-8.0426E-07	-8.6109E-07	-9.2655E-07	-1.0026E-06	-1.0918E-06	-1.1645E-06			
$q_{3(3)}^{(+)} = -3$ kPa	-1.1329E-06	-1.1839E-06	-1.2632E-06	-1.3533E-06	-1.4559E-06	-1.5731E-06	-1.6653E-06			
$q_{3(4)}^{(+)} = -4$ kPa	-1.4813E-06	-1.5446E-06	-1.6420E-06	-1.7509E-06	-1.8725E-06	-2.0077E-06	-2.1105E-06			
$q_{3(5)}^{(+)} = -5$ kPa	-1.8122E-06	-1.8853E-06	-1.9966E-06	-2.1192E-06	-2.2536E-06	-2.3994E-06	-2.5069E-06			
$q_{3(6)}^{(+)} = -6$ kPa	-2.1252E-06	-2.2060E-06	-2.3277E-06	-2.4599E-06	-2.6024E-06	-2.7536E-06	-2.8619E-06			
$q_{3(7)}^{(+)} = -7$ kPa	-2.4208E-06	-2.5074E-06	-2.6366E-06	-2.7752E-06	-2.9224E-06	-3.0755E-06	-3.1825E-06			
$q_{3(8)}^{(+)} = -8$ kPa	-2.6998E-06	-2.7907E-06	-2.9252E-06	-3.0678E-06	-3.2173E-06	-3.3701E-06	-3.4744E-06			
$q_{3(9)}^{(+)} = -9$ kPa	-2.9632E-06	-3.0572E-06	-3.1952E-06	-3.3401E-06	-3.4902E-06	-3.6414E-06	-3.7423E-06			
$q_{3(10)}^{(+)} = -10$ kPa	-3.2123E-06	-3.3084E-06	-3.4485E-06	-3.5944E-06	-3.7440E-06	-3.8926E-06	-3.9900E-06			

Table 6: Static center deflection u_g [m] of a (FGM₂/Aluminum/FGM₁) C-C-C hyperbolic paraboloid resting on elastic foundations at the point $B = (0.5(\alpha_1^+ - \alpha_1^-), 0.5(\alpha_2^+ - \alpha_2^-))$ for different load step $(q_{1(r)}^{(+)}, q_{2(r)}^{(+)}, q_{3(r)}^{(+)})$ and different values of the exponent $p = p^{(1)} = p^{(3)}$, using a 31×31 Chebyshev-Gauss-Lobatto (C-G-L) grid distribution.

Geometric characteristics of the two paraboloids: $\alpha_1 = \alpha_2 = [-33.69^\circ, 33.69^\circ]$, $\kappa = 18$ m, $h = 0.9$ m
 Properties of the lamina 1: FGM₂($\rho^{(2)} = 1/B^{(2)} = 1/C^{(2)} = 4/\rho^{(2)}$) (mixture of Aluminum and Zirconia), $h_1 = 0.3$ m
 Properties of the lamina 2: $E = 168$ GPa, $\nu = 0.3$, $\rho = 5700$ kg/m³ (Zirconia), $h_2 = 0.1$ m
 Properties of the lamina 3: FGM₁($\rho^{(1)} = 1/B^{(1)} = 1/C^{(1)} = 4/\rho^{(1)}$) (mixture of Aluminum and Zirconia), $h_3 = 0.3$ m
 Foundation properties: $k_1^{(-)} = k_2^{(-)} = k_3^{(-)} = 3.5 \cdot 10^8$ N/m³, $G_f^{(-)} = 2.5 \cdot 10^9$ N/m, $k_{in/2}^{(-)} = k_{2n/2}^{(-)} = k_{3n/2}^{(-)} = 5 \cdot 10^{12}$ N/m⁴, $k_{in/3}^{(-)} = k_{2n/3}^{(-)} = k_{3n/3}^{(-)} = 5 \cdot 10^{18}$ N/m⁵

$p = 1$							
Load step $(q_{1(r)}^{(+)}, q_{2(r)}^{(+)}, q_{3(r)}^{(+)})$ [kPa]	No foundation	$k_1^{(-)}, k_2^{(-)}, k_3^{(-)}, G_f^{(-)}$	$k_1^{(-)}, k_2^{(-)}, k_3^{(-)}, k_{in/2}^{(-)}, k_{2n/2}^{(-)}, k_{3n/2}^{(-)}$	$k_1^{(-)}, k_2^{(-)}, k_3^{(-)}, k_{in/2}^{(-)}, k_{2n/2}^{(-)}, k_{3n/2}^{(-)}$	$k_1^{(-)}, k_2^{(-)}, k_3^{(-)}, G_f^{(-)}, k_{in/2}^{(-)}, k_{2n/2}^{(-)}, k_{3n/2}^{(-)}$	$k_1^{(-)}, k_2^{(-)}, k_3^{(-)}, k_{in/2}^{(-)}, k_{2n/2}^{(-)}, k_{3n/2}^{(-)}$	$k_1^{(-)}, k_2^{(-)}, k_3^{(-)}, G_f^{(-)}, k_{in/2}^{(-)}, k_{2n/2}^{(-)}, k_{3n/2}^{(-)}$
(-1,0,5,05)	-7.1449E-07	-5.8311E-07	-5.1306E-07	-5.7220E-07	-5.0577E-07	-5.6727E-07	-5.0285E-07
(-2,1,1)	-1.4290E-06	-1.1662E-06	-1.0261E-06	-1.1240E-06	-9.9772E-07	-1.0898E-06	-9.7667E-07
(-3,1,5,1.5)	-2.1435E-06	-1.7493E-06	-1.5392E-06	-1.6574E-06	-1.4768E-06	-1.5591E-06	-1.4140E-06
(-4,2,2)	-2.8580E-06	-2.3324E-06	-2.0522E-06	-2.1740E-06	-1.9440E-06	-1.9767E-06	-1.8133E-06
(-5,2,5,2.5)	-3.5725E-06	-2.9155E-06	-2.5653E-06	-2.6751E-06	-2.4001E-06	-2.3486E-06	-2.1766E-06
(-6,3,3)	-4.2869E-06	-3.4986E-06	-3.0784E-06	-3.1620E-06	-2.8458E-06	-2.6818E-06	-2.5075E-06
(-7,3,5,3.5)	-5.0014E-06	-4.0817E-06	-3.5914E-06	-3.6359E-06	-3.2817E-06	-2.9825E-06	-2.8101E-06
(-8,4,4)	-5.7159E-06	-4.6649E-06	-4.1045E-06	-4.0975E-06	-3.7085E-06	-3.2560E-06	-3.0881E-06
(-8,4,5,4.5)	-6.4304E-06	-5.2480E-06	-4.6175E-06	-4.5479E-06	-4.1266E-06	-3.5067E-06	-3.3447E-06
(-10,5,5)	-7.1449E-06	-5.8311E-06	-5.1306E-06	-4.9876E-06	-4.5364E-06	-3.7381E-06	-3.5829E-06

Load step $(q_{1(r)}^{(+)}, q_{2(r)}^{(+)}, q_{3(r)}^{(+)})$ [kPa]	$k_1^{(-)}, k_2^{(-)}, k_3^{(-)}, G_f^{(-)}, K_{in1}^{(-)}, K_{in2}^{(-)}, K_{in3}^{(-)}, K_{2in1}^{(-)}, K_{2in2}^{(-)}, K_{2in3}^{(-)}, K_{3in1}^{(-)}$						
	$\rho = 1/20$	$\rho = 1/5$	$\rho = 1/2$	$\rho = 1$	$\rho = 2$	$\rho = 5$	$\rho = 20$
(-1,0,5,.05)	-4.3141E-07	-4.3855E-07	-4.5193E-07	-4.7171E-07	-5.0285E-07	-5.5222E-07	-5.9300E-07
(-2,1,1)	-8.4612E-07	-8.5938E-07	-8.8412E-07	-9.2038E-07	-9.7667E-07	-1.0637E-06	-1.1335E-06
(-3,1.5,1.5)	-1.2389E-06	-1.2570E-06	-1.2906E-06	-1.3394E-06	-1.4140E-06	-1.5260E-06	-1.6132E-06
(-4,2,2)	-1.6072E-06	-1.6289E-06	-1.6690E-06	-1.7267E-06	-1.8133E-06	-1.9400E-06	-2.0358E-06
(-5,2.5,2.5)	-1.9505E-06	-1.9748E-06	-2.0194E-06	-2.0828E-06	-2.1766E-06	-2.3105E-06	-2.4095E-06
(-6,3,3)	-2.2699E-06	-2.2959E-06	-2.3433E-06	-2.4101E-06	-2.5075E-06	-2.6438E-06	-2.7425E-06
(-7,3.5,3.5)	-2.5670E-06	-2.5940E-06	-2.6429E-06	-2.7114E-06	-2.8101E-06	-2.9455E-06	-3.0420E-06
(-8,4,4)	-2.8437E-06	-2.8712E-06	-2.9209E-06	-2.9898E-06	-3.0881E-06	-3.2206E-06	-3.3138E-06
(-8,4.5,4.5)	-3.1021E-06	-3.1297E-06	-3.1794E-06	-3.2480E-06	-3.3447E-06	-3.4732E-06	-3.5626E-06
(-10,5,5)	-3.3440E-06	-3.3715E-06	-3.4208E-06	-3.4884E-06	-3.5829E-06	-3.7067E-06	-3.7919E-06

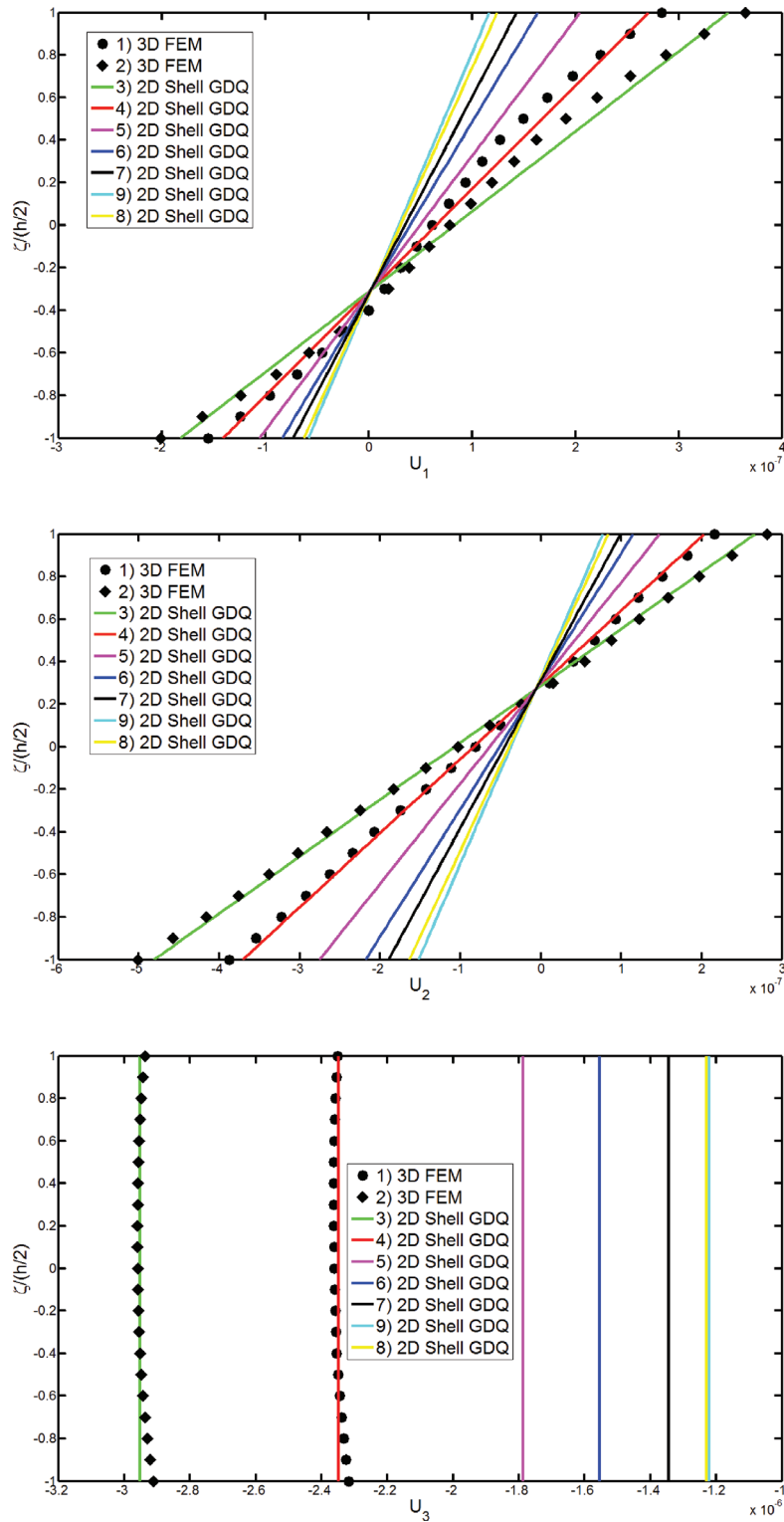


Figure 6: Through-the-thickness variation of the displacement component vector [m] at the point $c = (0.25(a_1^1 - a_1^0), 0.25(a_2^1 - a_2^0))$, for a C-C-C square plate of Table 1 with a (30/65/45) lamination scheme when uniformly distributed load $q_3^{(+)} = -10$ kPa is applied at the top surface: 1) 3D FEM (16000 Bricks with 20 nodes), with no foundation; 2) 3D FEM (16000 Bricks with 20 nodes), with $k_3^{(-)}$; 3) 2D Shell GDQ, with no foundation; 4) 2D Shell GDQ, with $k_3^{(-)}$; 5) 2D Shell GDQ, with $k_3^{(-)}, G_f^{(-)}$; 6) 2D Shell GDQ, with $k_3^{(-)}, k_{3nl2}^{(-)}$; 7) 2D Shell GDQ, with $k_3^{(-)}, k_{3nl2}^{(-)}, G_f^{(-)}$; 8) 2D Shell GDQ, with $k_3^{(-)}, k_{3nl2}^{(-)}, k_{3nl3}^{(-)}$; 9) 2D Shell GDQ, with $k_3^{(-)}, k_{3nl2}^{(-)}, k_{3nl3}^{(-)}, G_f^{(-)}$.

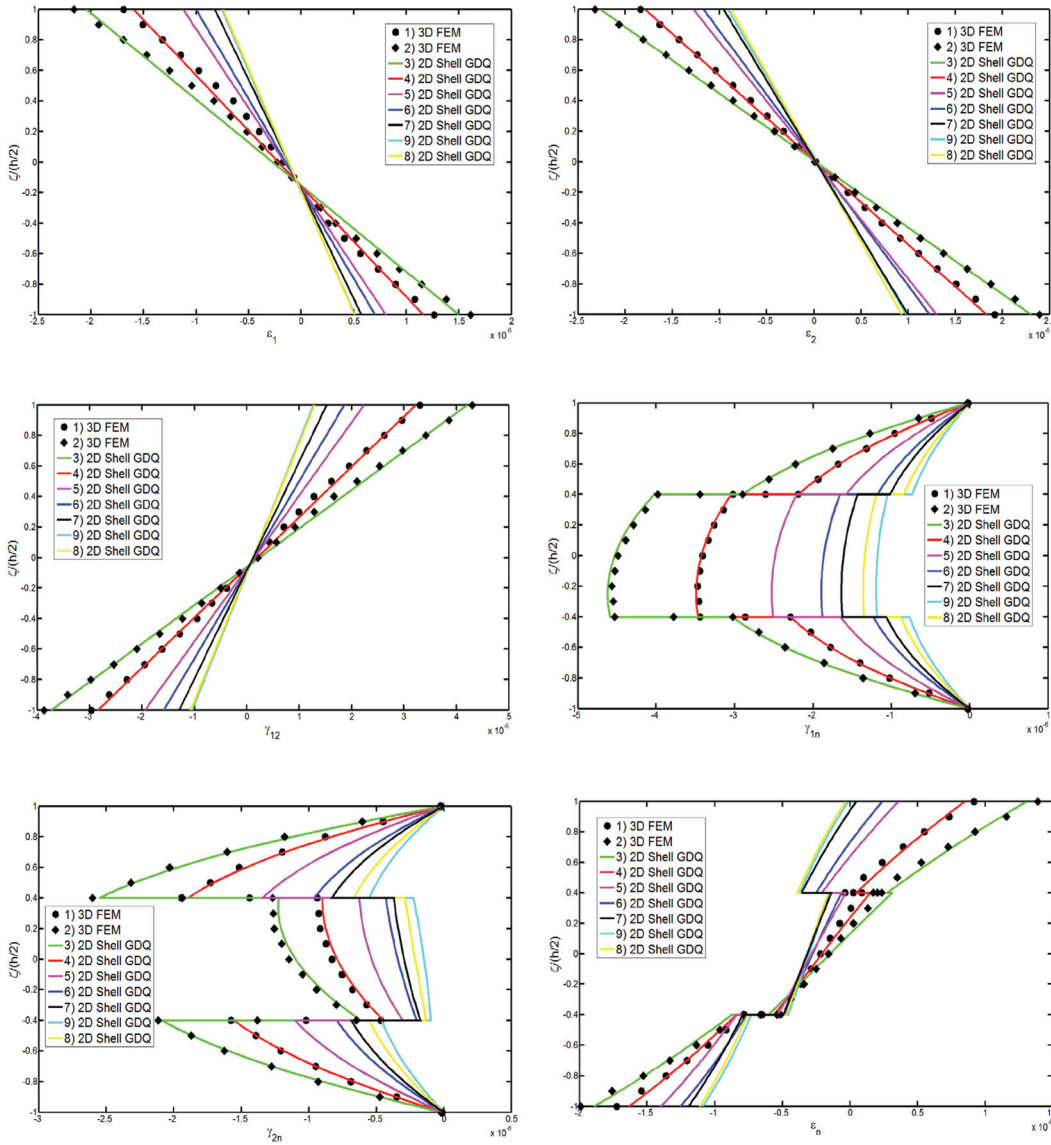


Figure 7: Through-the-thickness variation of all the strain components at the point $c = (0.25(\alpha_1^1 - \alpha_1^0), 0.25(\alpha_2^1 - \alpha_2^0))$, for a C-C-C-C square plate of Table 1 with a (30/65/45) lamination scheme when uniformly distributed load $q_3^{(+)} = -10$ kPa is applied at the top surface: 1) 3D FEM (16000 Bricks with 20 nodes), with no foundation; 2) 3D FEM (16000 Bricks with 20 nodes), with $k_3^{(-)}$; 3) 2D Shell GDQ, with no foundation, 4) 2D Shell GDQ, with $k_3^{(-)}$; 5) 2D Shell GDQ, with $k_3^{(-)}, G_f^{(-)}$; 6) 2D Shell GDQ, with $k_3^{(-)}, k_{3nl2}^{(-)}$; 7) 2D Shell GDQ, with $k_3^{(-)}, k_{3nl2}^{(-)}, G_f^{(-)}$; 8) 2D Shell GDQ, with $k_3^{(-)}, k_{3nl2}^{(-)}, k_{3nl3}^{(-)}$; 9) 2D Shell GDQ, with $k_3^{(-)}, k_{3nl2}^{(-)}, k_{3nl3}^{(-)}, G_f^{(-)}$.

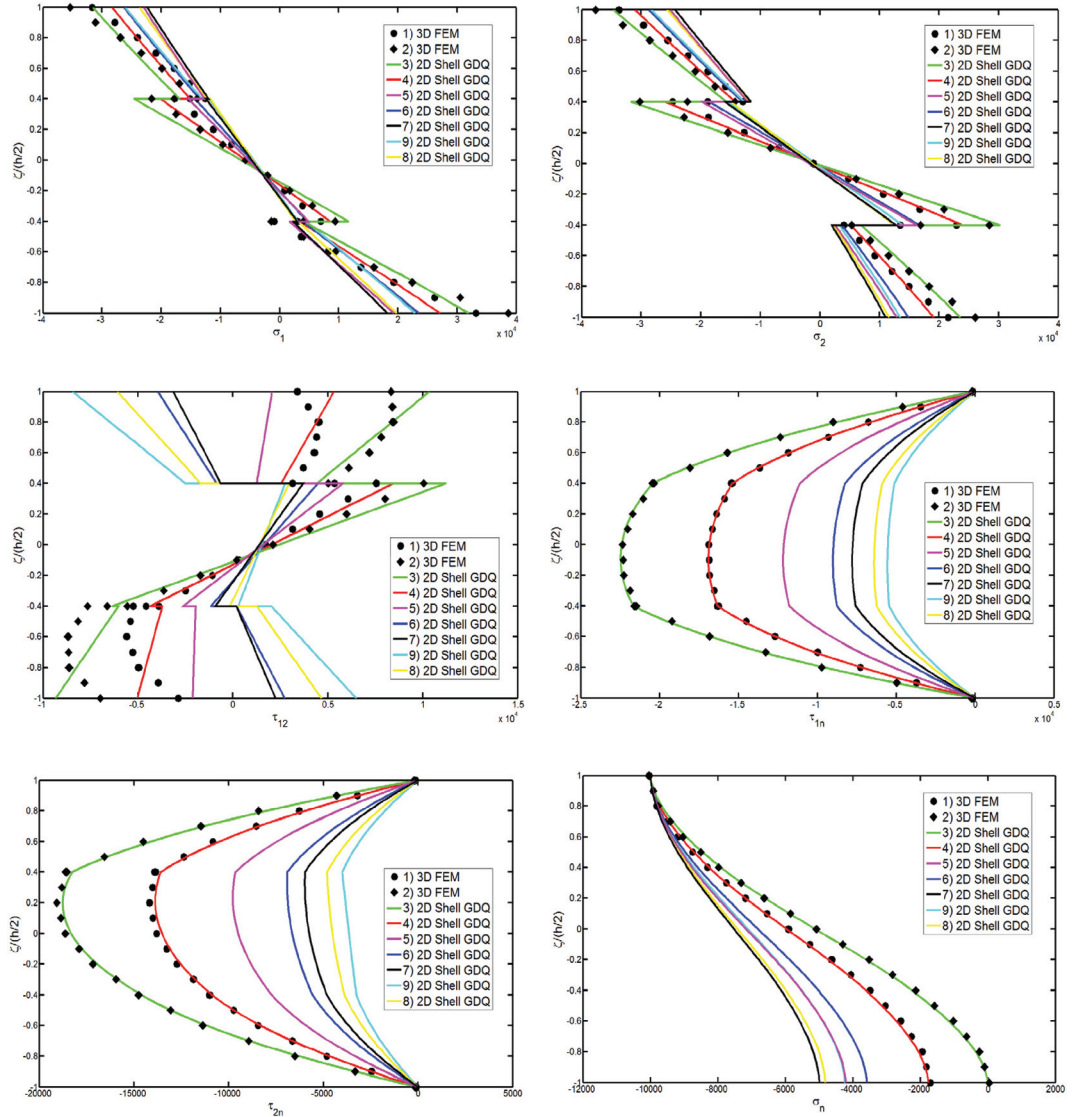


Figure 8: Through-the-thickness variation of all the stress components [Pa] at the point $c = (0.25(\alpha_1^1 - \alpha_1^0), 0.25(\alpha_2^1 - \alpha_2^0))$, for a C-C-C-C square plate of Table 1 with a (30/65/45) lamination scheme when uniformly distributed load $q_3^{(+)} = -10$ kPa is applied at the top surface: 1) 3D FEM (16000 Bricks with 20 nodes), with no foundation; 2) 3D FEM (16000 Bricks with 20 nodes), with $k_3^{(-)}$; 3) 2D Shell GDQ, with no foundation, 4) 2D Shell GDQ, with $k_3^{(-)}$; 5) 2D Shell GDQ, with $k_3^{(-)}, G_f^{(-)}$; 6) 2D Shell GDQ, with $k_3^{(-)}, k_{3nl2}^{(-)}$; 7) 2D Shell GDQ, with $k_3^{(-)}, k_{3nl2}^{(-)}, G_f^{(-)}$; 8) 2D Shell GDQ, with $k_3^{(-)}, k_{3nl2}^{(-)}, k_{3nl3}^{(-)}$; 9) 2D Shell GDQ, with $k_3^{(-)}, k_{3nl2}^{(-)}, k_{3nl3}^{(-)}, G_f^{(-)}$.

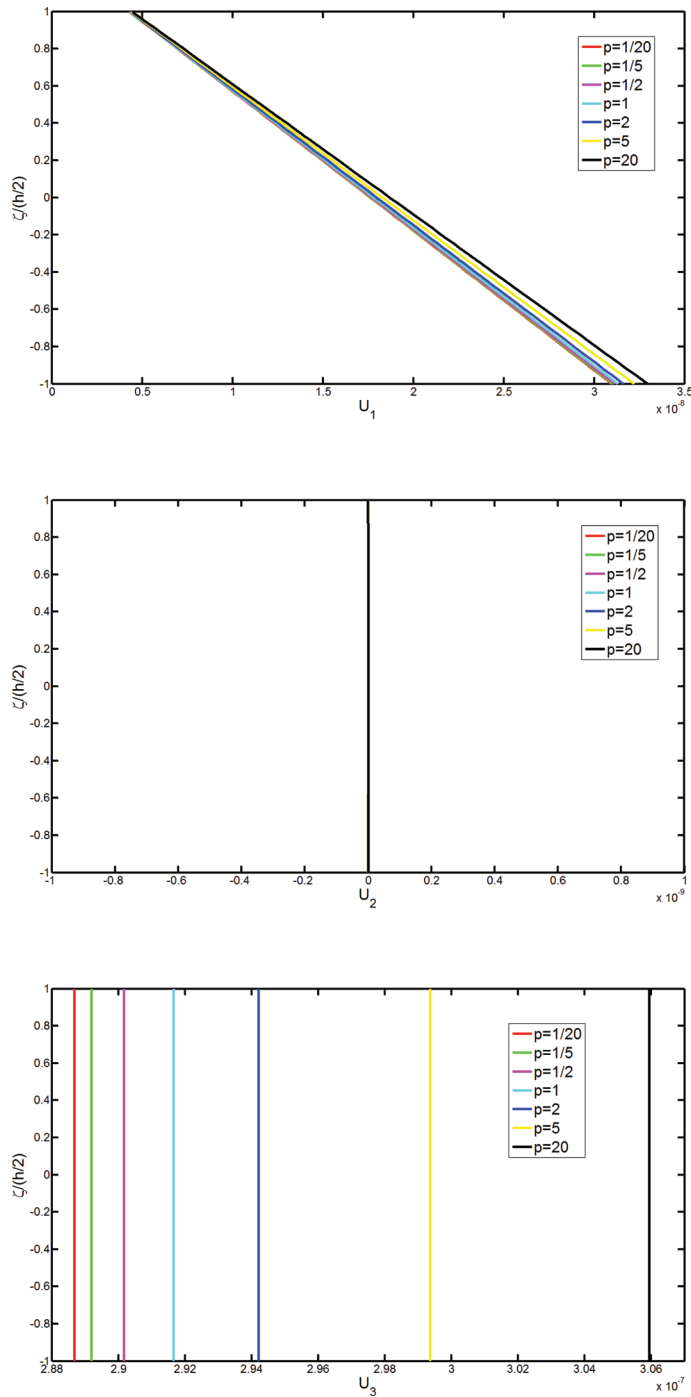


Figure 9: Through-the-thickness variation of the displacement component vector [m] at the point $c = (0.25(\alpha_1^1 - \alpha_1^0), 0.25(\alpha_2^1 - \alpha_2^0))$ for a C-C cylindrical shell of Table 2 with a (Zirconia/FGM_{1(a^{(2)}=1/b^{(2)}=1/c^{(2)}=2/p^{(2)})}/Zirconia) lamination scheme, for different values of the exponent $p = p^{(2)}$, when uniformly distributed load $q_3^{(-)} = 10$ kPa is applied at the bottom surface and a foundation $k_3^{(+)}, G_1^{(+)}, k_{3n/2}^{(+)}, k_{3n/3}^{(+)}$ is applied at the top surface.

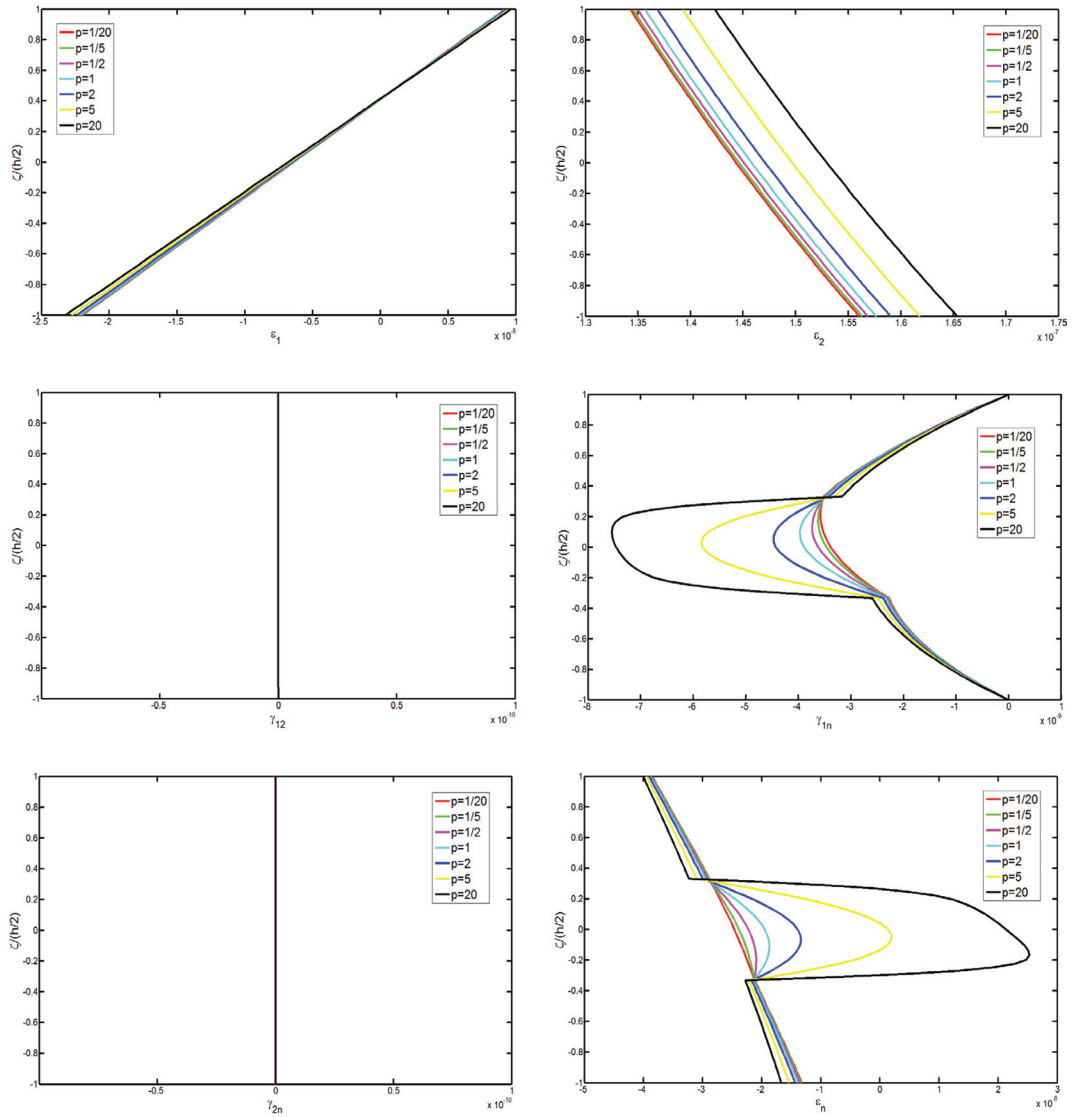


Figure 10: Through-the-thickness variation of all the strain components at the point $c = (0.25(\alpha_1^1 - \alpha_1^0), 0.25(\alpha_2^1 - \alpha_2^0))$, for a C-C cylindrical shell of Table 2 with a $(\text{Zirconia}/FGM_{1(a^{(2)}=1/b^{(2)}=1/c^{(2)}=2/\rho^{(2)})}/\text{Zirconia})$ lamination scheme, for different values of the exponent $p=p^{(2)}$, when uniformly distributed load $q_3^{(-)} = 10$ kPa is applied at the bottom surface and a foundation $k_3^{(+)}, G_f^{(+)}, k_{3n/2}^{(+)}, k_{3n/3}^{(+)}$ is applied at the top surface.

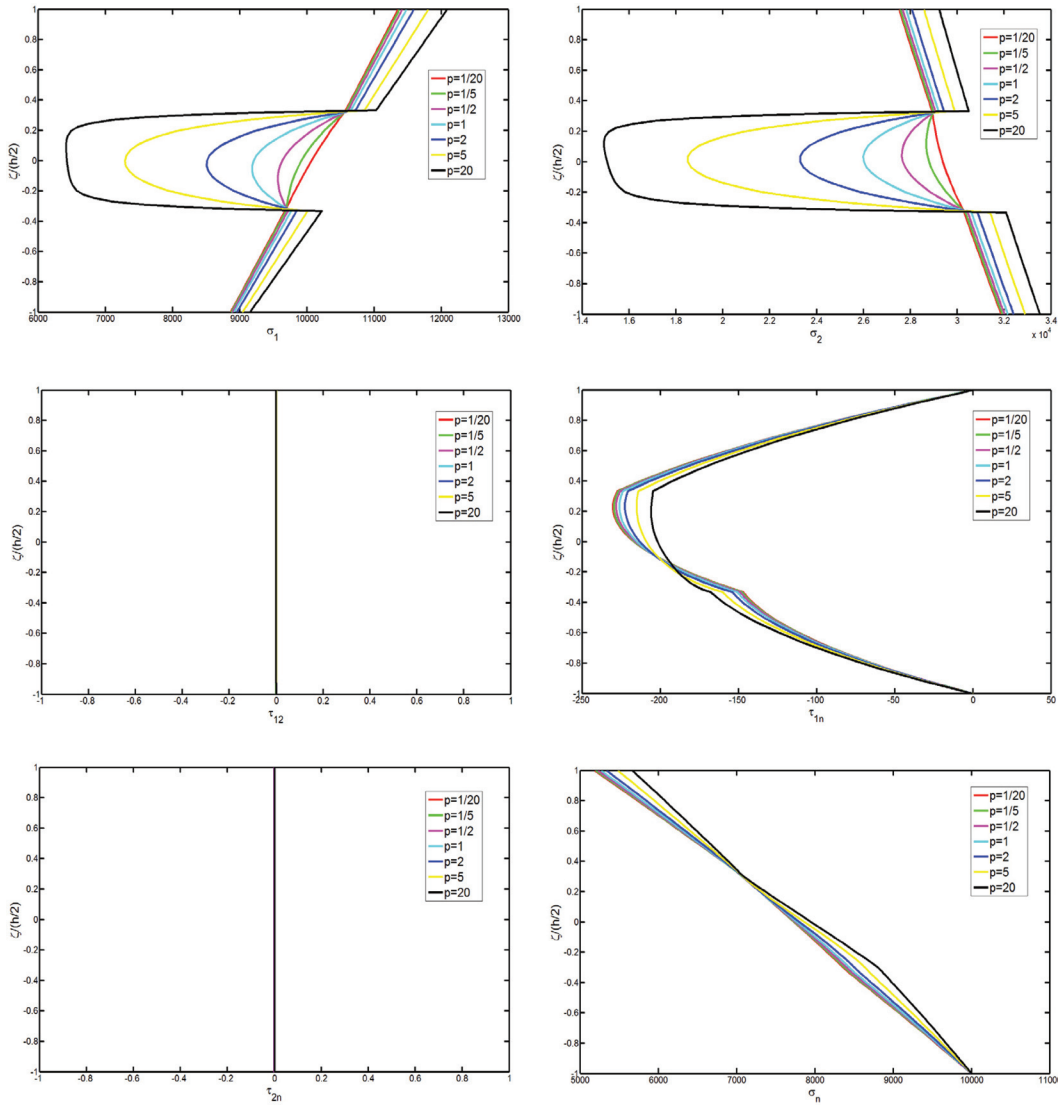


Figure 11: Through-the-thickness variation of all the stress components at the point $c = (0.25(\alpha_1^1 - \alpha_1^0), 0.25(\alpha_2^1 - \alpha_2^0))$, for a C-C cylindrical shell of Table 2 with a (Zirconia/FGM_{1(a^{(2)}=1/b^{(2)}=1/c^{(2)}=2/p^{(2)})}/Zirconia) lamination scheme, for different values of the exponent $p = p^{(2)}$, when uniformly distributed load $q_3^{(-)} = 10$ kPa is applied at the bottom surface and a foundation $k_3^{(+)}, G_f^{(+)}, k_{3n/2}^{(+)}, k_{3n/3}^{(+)}$ is applied at the top surface.

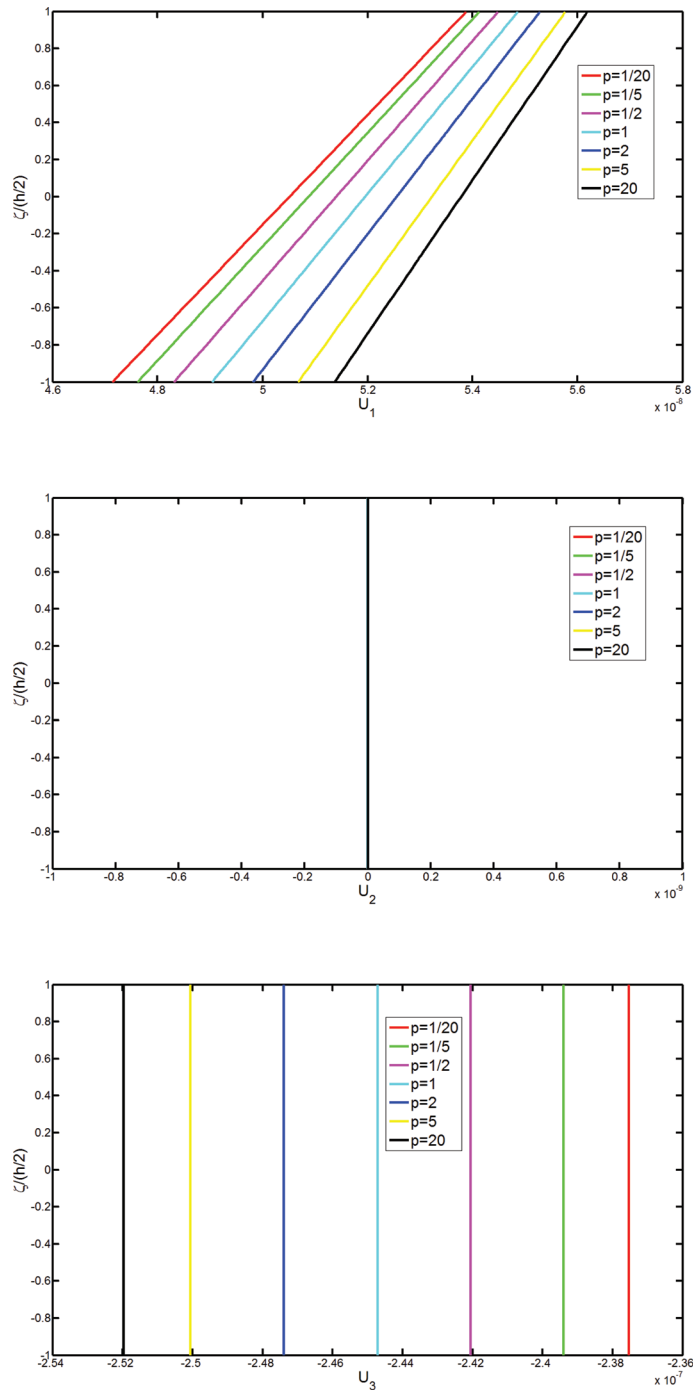


Figure 12: Through-the-thickness variation of the displacement component vector [m] at the point $c = (0.25(\alpha_1^1 - \alpha_1^0), 0.25(\alpha_2^1 - \alpha_2^0))$, for a C-F conical shell of Table 3 with a (Zirconia/FGM_{2(a⁽²⁾=1/b⁽²⁾=0/c⁽²⁾=0/p⁽²⁾)}/Zirconia) lamination scheme, for different values of the exponent $p = p^{(2)}$, when uniformly distributed load $q_3^{(+)} = -10$ kPa is applied at the top surface and a foundation $k_3^{(-)}, G_7^{(-)}, k_{3n/2}^{(-)}, k_{3n/3}^{(-)}$ is applied at the bottom surface.

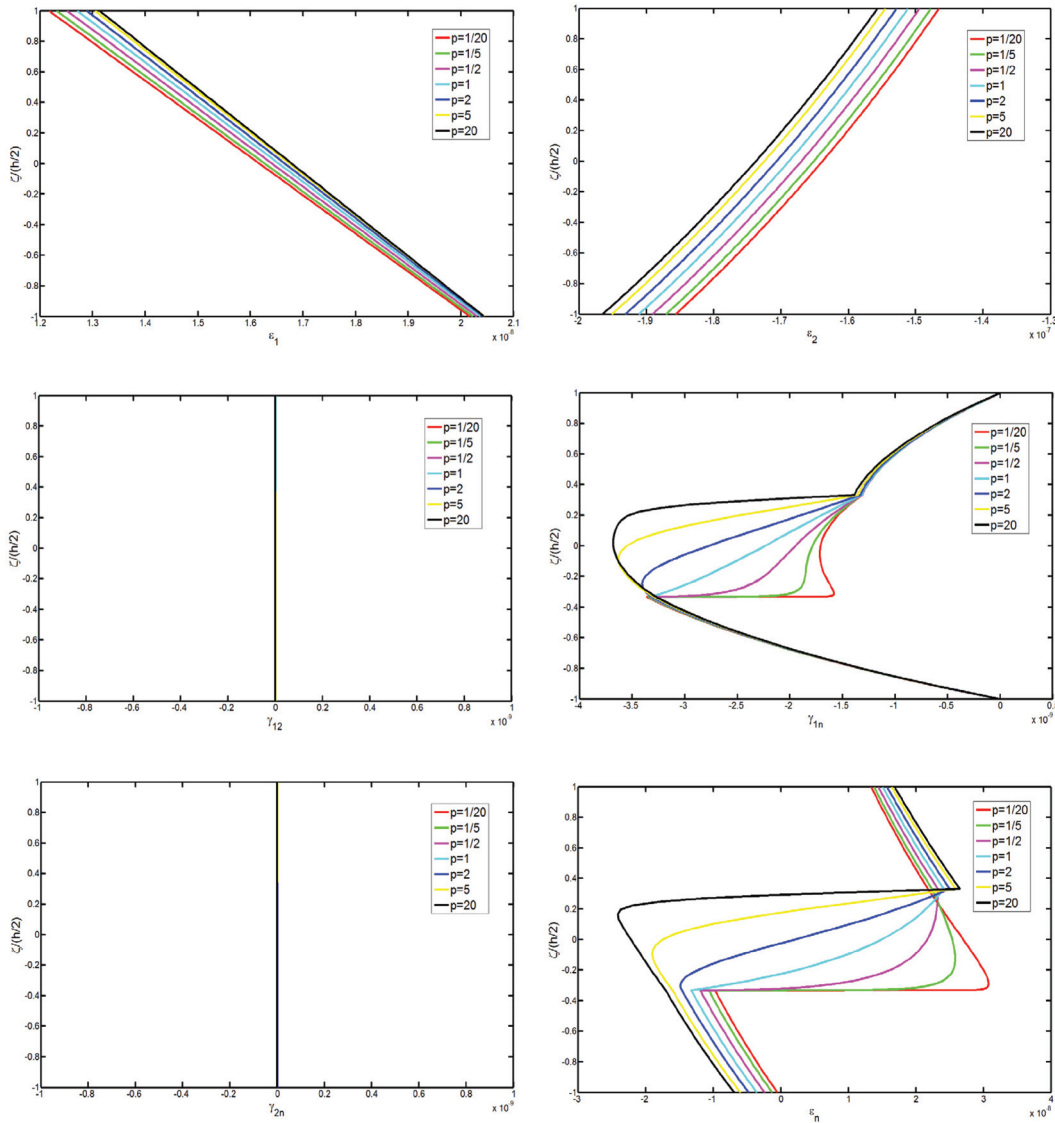


Figure 13: Through-the-thickness variation of all the strain component at the point $c = (0.25(\alpha_1^1 - \alpha_1^0), 0.25(\alpha_2^1 - \alpha_2^0))$, for a C-F conical shell of Table 3 with a (Zirconia/FGM₂ ($a^{(2)}=1/b^{(2)}=0/c^{(2)}=0/\rho^{(2)}$)/Zirconia) lamination scheme, for different values of the exponent $p = p^{(2)}$, when uniformly distributed load $q_3^{(+)} = -10$ kPa is applied at the top surface and a foundation $k_3^{(-)}, G_f^{(-)}, k_{3n/2}^{(-)}, k_{3n/3}^{(-)}$ is applied at the bottom surface.

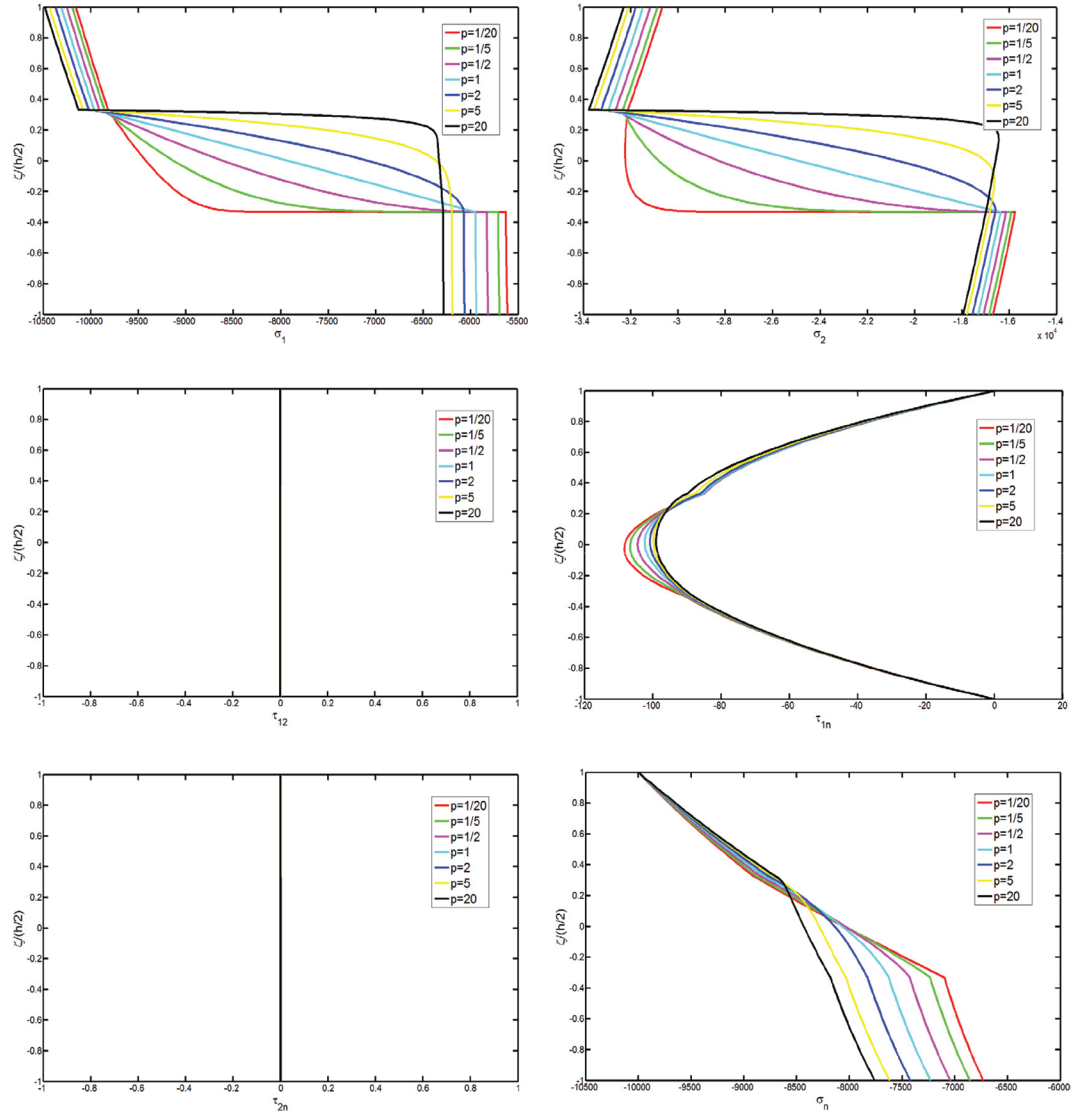


Figure 14: Through-the-thickness variation of all the strain component [Pa] at the point $c = (0.25(\alpha_1^1 - \alpha_1^0), 0.25(\alpha_2^1 - \alpha_2^0))$, for a C-F conical shell of Table 3 with a (Zirconia/FGM₂ ($a^{(2)}=1/b^{(2)}=0/c^{(2)}=0/p^{(2)}$)/Zirconia) lamination scheme, for different values of the exponent $p = p^{(2)}$, when uniformly distributed load $q_3^{(+)} = -10$ kPa is applied at the top surface and a foundation $k_3^{(-)}, G_1^{(-)}, k_{3n/2}^{(-)}, k_{3n/3}^{(-)}$ is applied at the bottom surface.

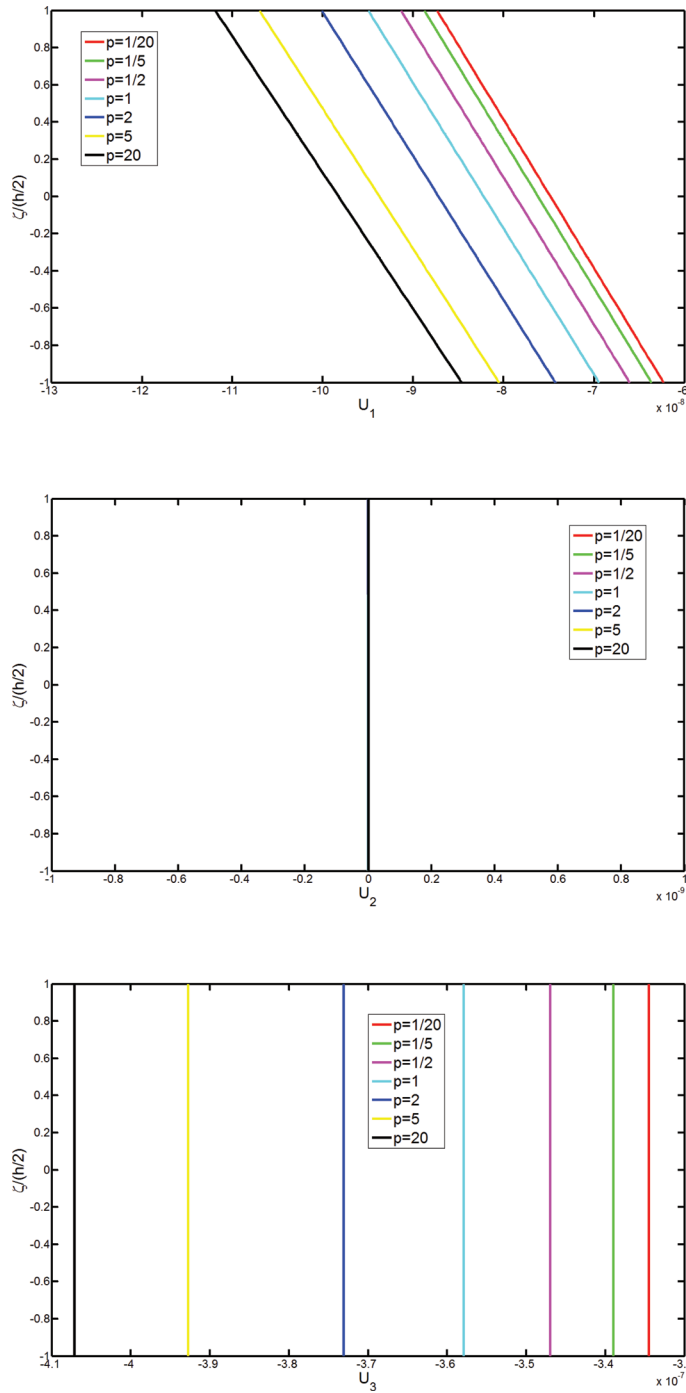


Figure 15: Through-the-thickness variation of the displacement component vector [m] at the point $c = (0.25(\alpha_1^1 - \alpha_1^0), 0.25(\alpha_2^1 - \alpha_2^0))$, for a C-F spherical shell of Table 4 with a $(FGM_{2(a^{(1)}=0.8/b^{(1)}=0.2/c^{(1)}=3/p^{(1)})}/Zirconia/FGM_{1(a^{(3)}=0.8/b^{(3)}=0.2/c^{(3)}=3/p^{(3)})})$ lamination scheme, for different values of the exponent $p = p^{(1)} = p^{(3)}$, when uniformly distributed load $q_3^{(+)} = -10$ kPa is applied at the top surface and a foundation $k_3^{(-)}, G_7^{(-)}, k_{3n/2}^{(-)}, k_{3n/3}^{(-)}$ is applied at the bottom surface.

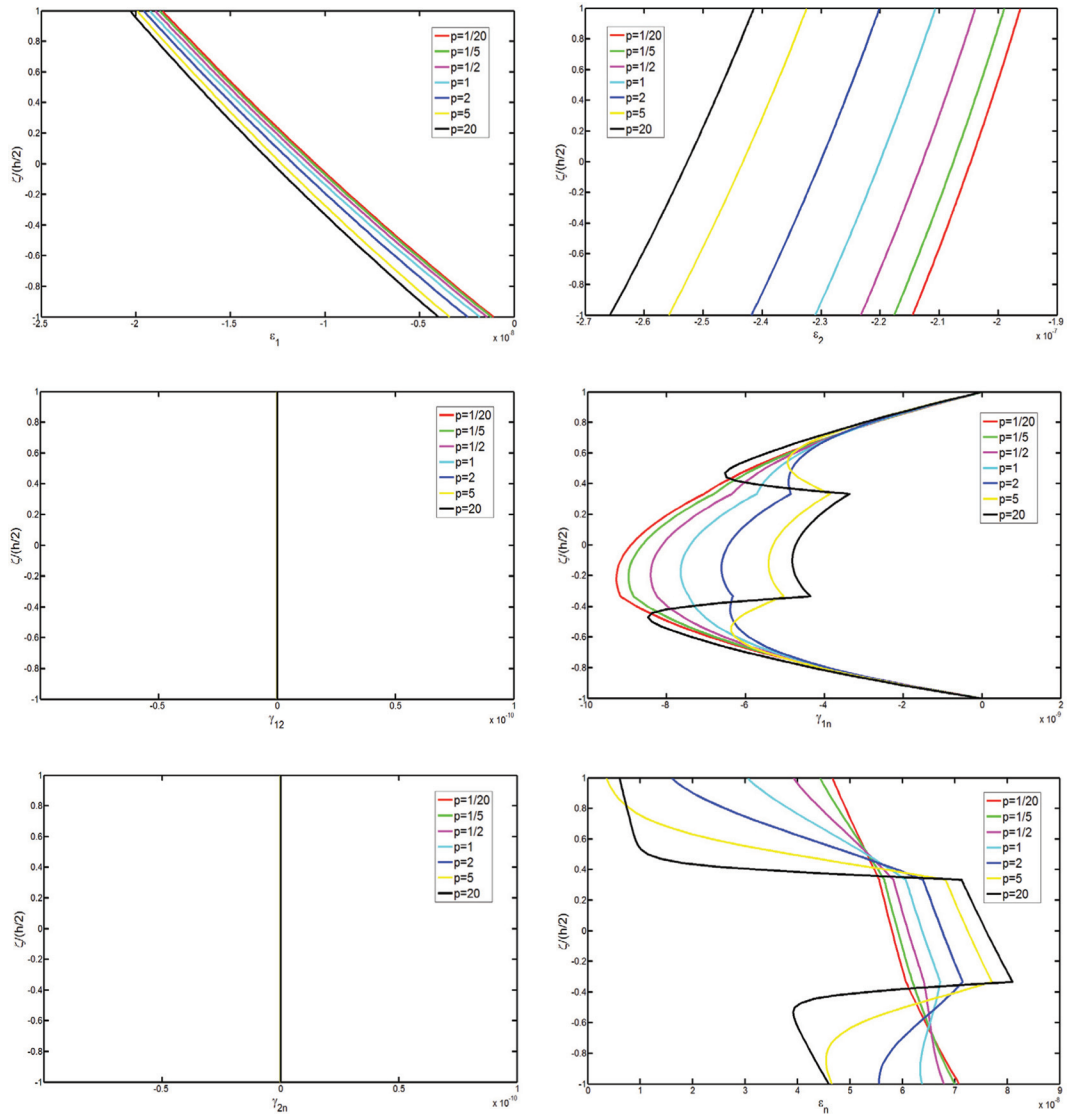


Figure 16: Through-the-thickness variation of all the strain component at the point $c = (0.25(\alpha_1^1 - \alpha_1^0), 0.25(\alpha_2^1 - \alpha_2^0))$, for a C-F spherical shell of Table 4 with a $(FGM_{2(a^{(1)}=0.8/b^{(1)}=0.2/c^{(1)}=3/p^{(1)})} / Zirconia/FGM_{1(a^{(3)}=0.8/b^{(3)}=0.2/c^{(3)}=3/p^{(3)})})$ lamination scheme, for different values of the exponent $p = p^{(1)} = p^{(3)}$, when uniformly distributed load $q_3^{(+)} = -10$ kPa is applied at the top surface and a foundation $k_3^{(-)}, G_f^{(-)}, k_{3n/2}^{(-)}, k_{3n/3}^{(-)}$ is applied at the bottom surface.

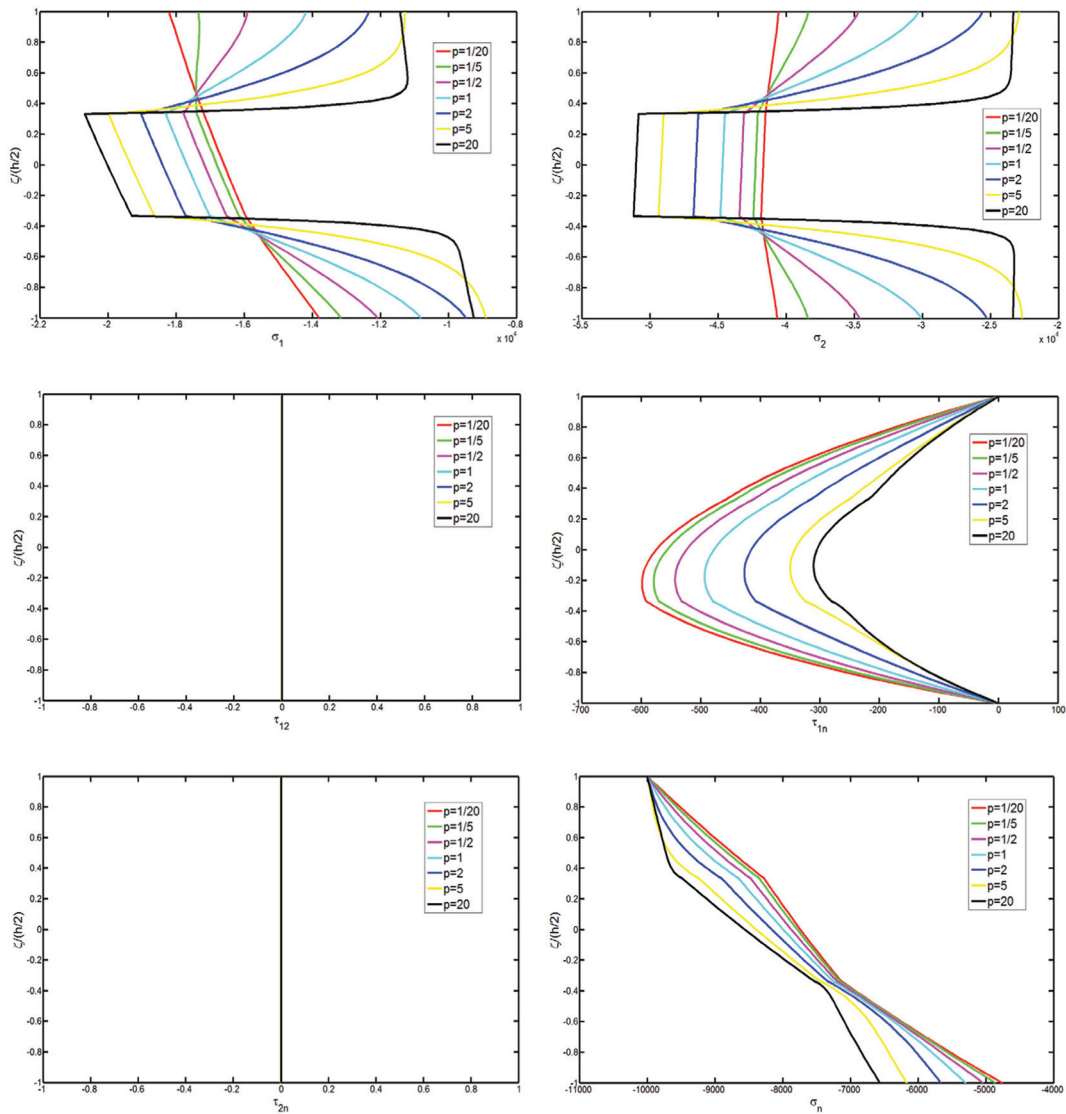


Figure 17: Through-the-thickness variation of all the stress component [Pa] at the point $c = (0.25(\alpha_1^1 - \alpha_1^0), 0.25(\alpha_2^1 - \alpha_2^0))$, for a C-F spherical shell of Table 4 with a $(FGM_{2(a^{(1)}=0.8/b^{(1)}=0.2/c^{(1)}=3/p^{(1)})} / Zirconia/FGM_{1(a^{(3)}=0.8/b^{(3)}=0.2/c^{(3)}=3/p^{(3)})})$ lamination scheme, for different values of the exponent $p = p^{(1)} = p^{(3)}$, when uniformly distributed load $q_3^{(+)} = -10$ kPa is applied at the top surface and a foundation $k_3^{(-)}, G_f^{(-)}, k_{3n/2}^{(-)}, k_{3n/3}^{(-)}$ is applied at the bottom surface.

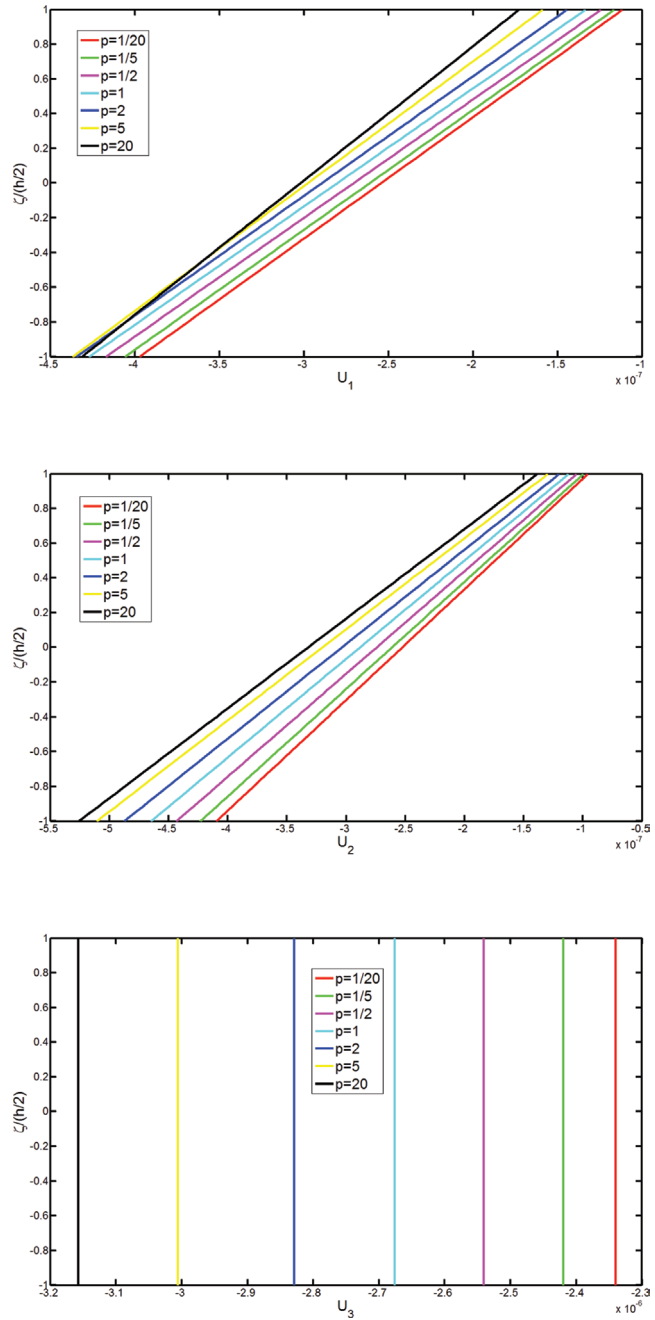


Figure 18: Through-the-thickness variation of the displacement component vector [m] at the point $c = (0.25(\alpha_1^1 - \alpha_1^0), 0.25(\alpha_2^1 - \alpha_2^0))$ for a C-C-C-C elliptic paraboloid of Table 5 with a $(FGM_{1(a^1=1/b^1)=0/c^1=0/p^1})/Zirconia/FGM_{2(a^2=1/b^2)=0/c^2=0/p^2})$ lamination scheme, for different values of the exponent $p = p^{(1)} = p^{(3)}$, when uniformly distributed load $q_3^{(+)} = -10$ kPa is applied at the top surface and a foundation $k_3^{(-)}, G_f^{(-)}, k_{3n/2}^{(-)}, k_{3n/3}^{(-)}$ is applied at the bottom surface.

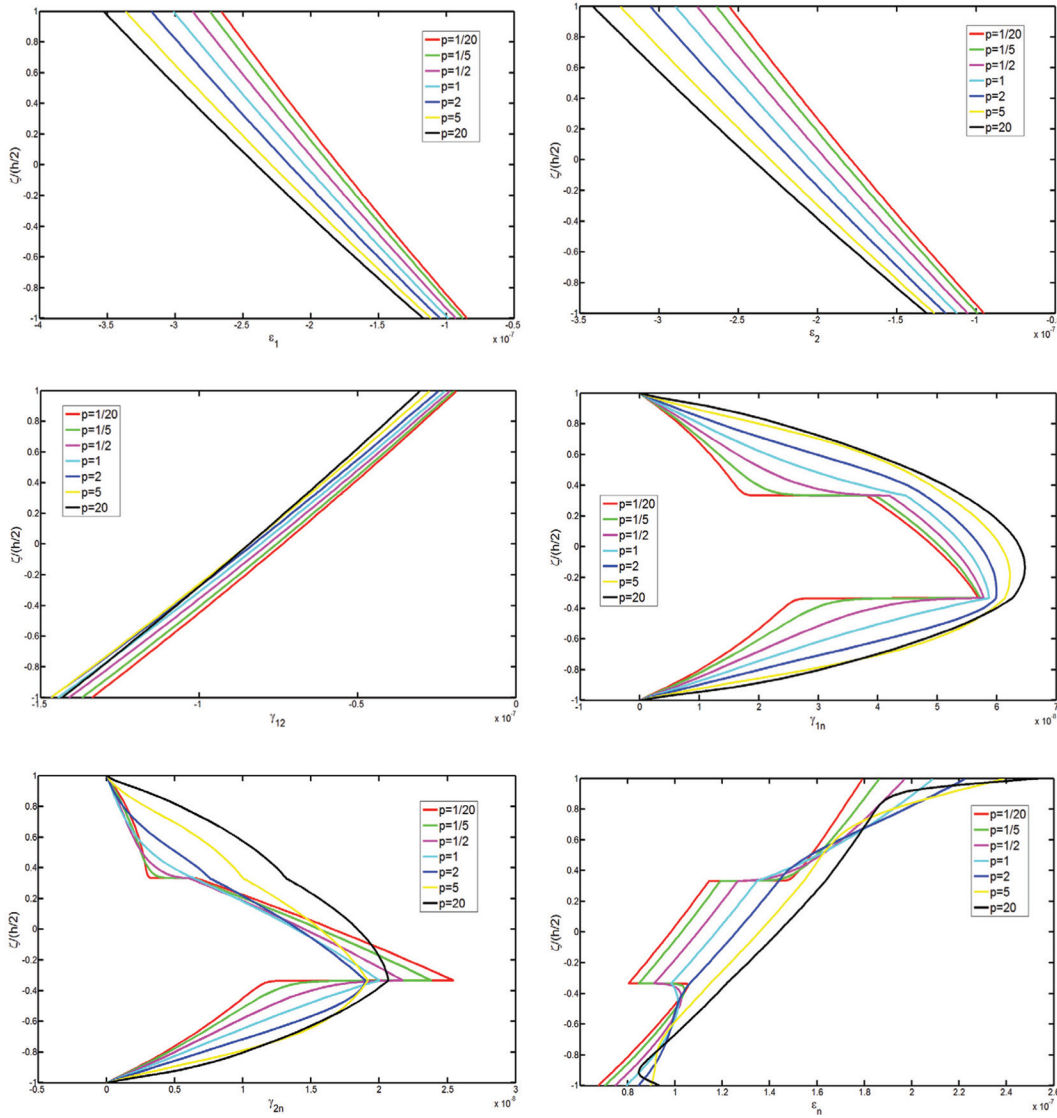


Figure 19: Through-the-thickness variation of all the strain component at the point $c = (0.25(\alpha_1^1 - \alpha_1^0), 0.25(\alpha_2^1 - \alpha_2^0))$ for a C-C-C-C elliptic paraboloid of Table 5 with a $(FGM_{1(a^{(1)}=1/b^{(1)}=0/c^{(1)}=0/p^{(1)})}/Zirconia/FGM_{2(a^{(3)}=1/b^{(3)}=0/c^{(3)}=0/p^{(3)})})$ lamination scheme, for different values of the exponent $p = p^{(1)} = p^{(3)}$, when uniformly distributed load $q_3^{(+)} = -10$ kPa is applied at the top surface and a foundation $k_3^{(-)}, G_f^{(-)}, k_{3n/2}^{(-)}, k_{3n/3}^{(-)}$ is applied at the bottom surface.

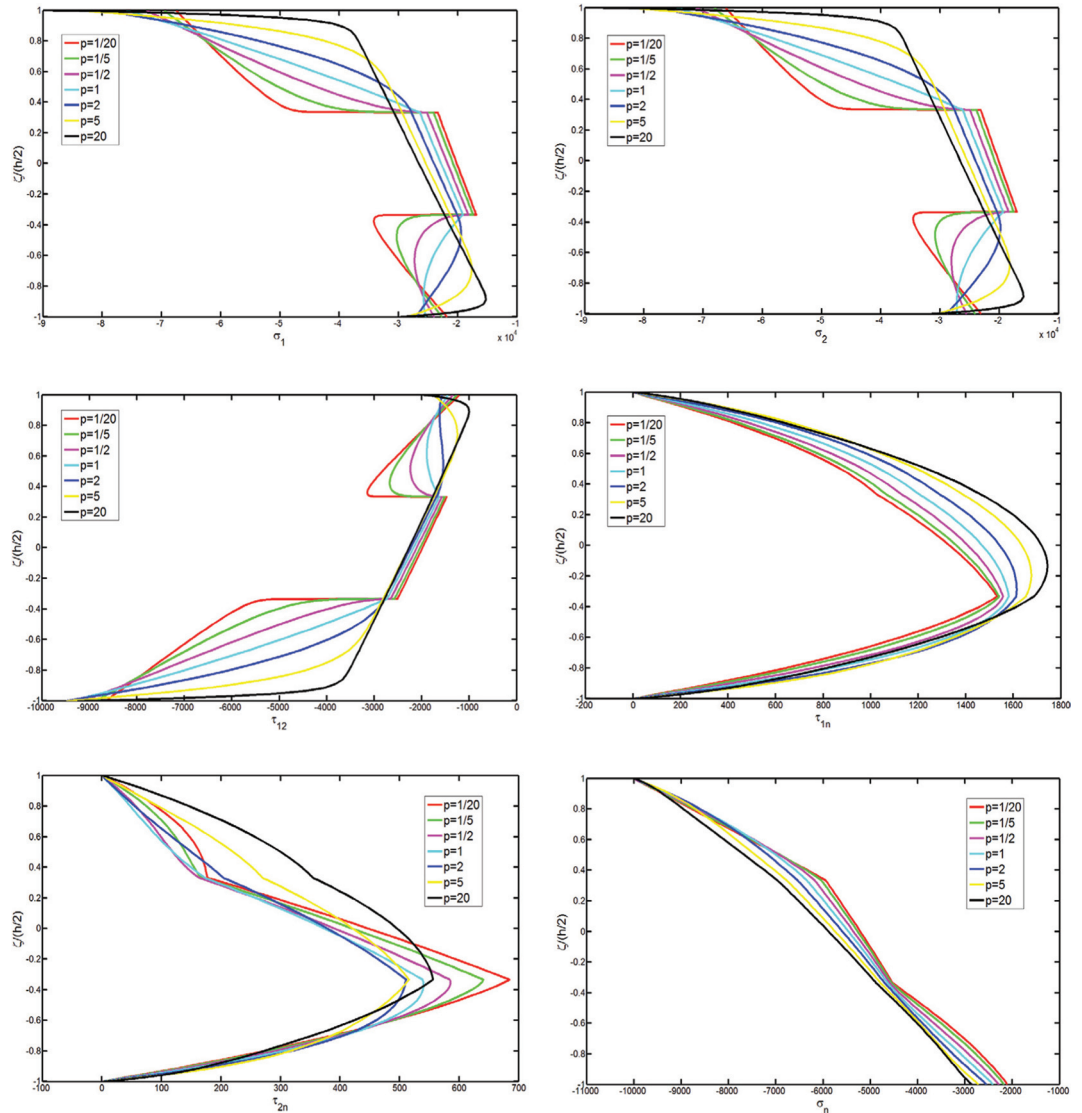


Figure 20: Through-the-thickness variation of all the stress component [Pa] at the point $c = (0.25(\alpha_1^1 - \alpha_1^0), 0.25(\alpha_2^1 - \alpha_2^0))$ for a C-C-C-C elliptic paraboloid of Table 5 with a $(FGM_{1(a^{(1)}=1/b^{(1)}=0/c^{(1)}=0/p^{(1)})}/Zirconia/FGM_{2(a^{(2)}=1/b^{(2)}=0/c^{(2)}=0/p^{(2)})})$ lamination scheme, for different values of the exponent $p = p^{(1)} = p^{(2)} = p^{(3)}$, when uniformly distributed load $q_3^{(+)} = -10$ kPa is applied at the top surface and a foundation $k_3^{(-)}, G_1^{(-)}, k_{3n/2}^{(-)}, k_{3n/3}^{(-)}$ is applied at the bottom surface.

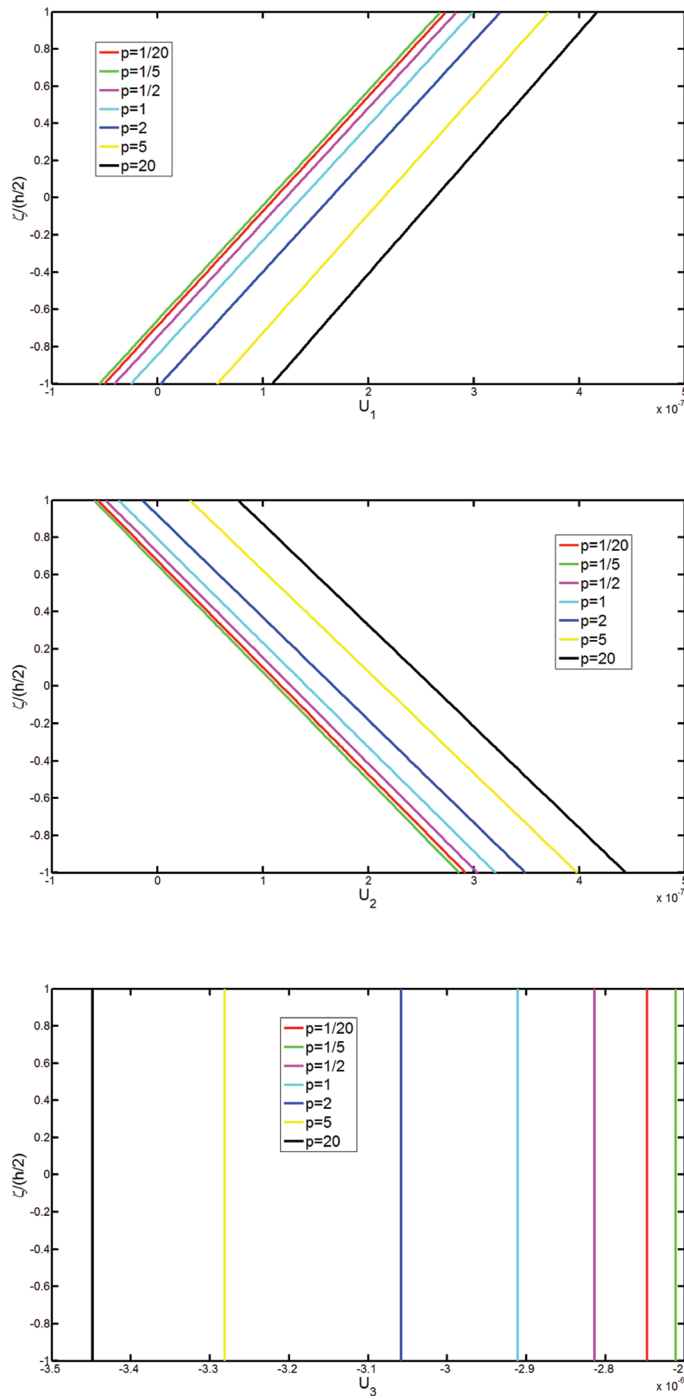


Figure 21: Through-the-thickness variation of the displacement component vector [m] at the point $c = (0.25(\alpha_1^1 - \alpha_1^0), 0.25(\alpha_2^1 - \alpha_2^0))$ for a C-C-C-C hyperbolic paraboloid of Table 6 with a $(FGM_{2(a^{(2)}=1/b^{(2)}=1/c^{(2)}=4/p^{(2)})}/Zirconia/FGM_{1(a^{(2)}=1/b^{(2)}=1/c^{(2)}=4/p^{(2)})})$ lamination scheme, for different values of the exponent $p = p^{(1)} = p^{(3)}$, when uniformly distributed loads $q_3^{(+)} = -10$ kPa, $q_2^{(+)} = q_2^{(+)} = 5$ kPa are applied at the top surface and a foundation $k_1^{(-)} = k_2^{(-)} = k_3^{(-)}, G_i^{(-)}, k_{1n/2}^{(-)} = k_{2n/2}^{(-)} = k_{3n/2}^{(-)}, k_{1n/3}^{(-)} = k_{2n/3}^{(-)} = k_{3n/3}^{(-)}$ is applied at the bottom surface.

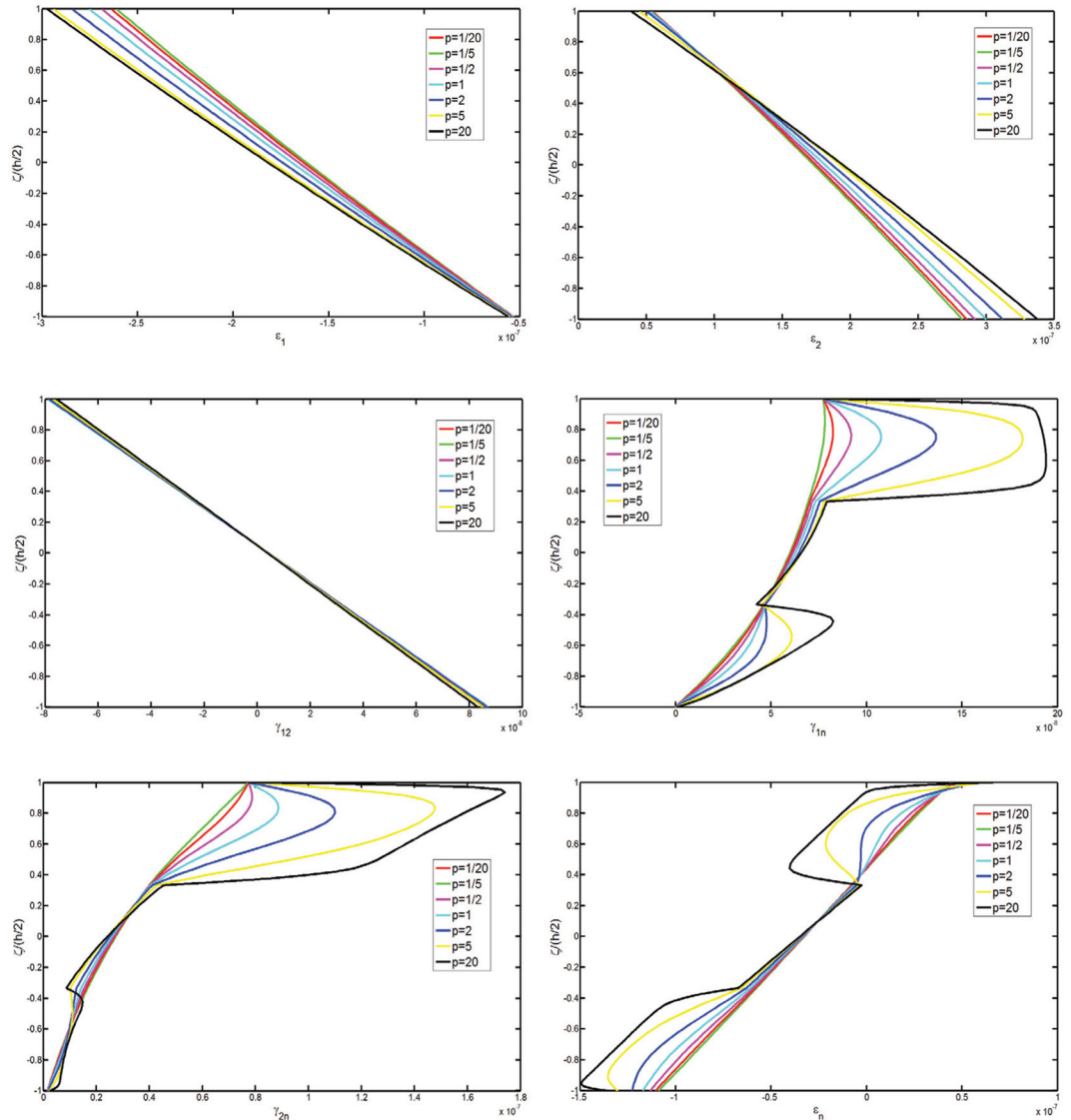


Figure 22: Through-the-thickness variation of all the strain components at the point $c = (0.25(\alpha_1^1 - \alpha_1^0), 0.25(\alpha_2^1 - \alpha_2^0))$ for a C-C-C-C hyperbolic paraboloid of Table 6 with a $(FGM_{2(a^{(2)}=1/b^{(2)}=1/c^{(2)}=4/p^{(2)})}/Zirconia/FGM_{1(a^{(2)}=1/b^{(2)}=1/c^{(2)}=4/p^{(2)})})$ lamination scheme, for different values of the exponent $p = p^{(1)} = p^{(3)}$, when uniformly distributed loads $q_3^{(+)} = -10$ kPa, $q_2^{(+)} = q_2^{(-)} = 5$ kPa are applied at the top surface and a foundation $k_1^{(-)} = k_2^{(-)} = k_3^{(-)}, G_i^{(-)}, k_{1n/2}^{(-)} = k_{2n/2}^{(-)} = k_{3n/2}^{(-)}, k_{1n/3}^{(-)} = k_{2n/3}^{(-)} = k_{3n/3}^{(-)}$ is applied at the bottom surface.

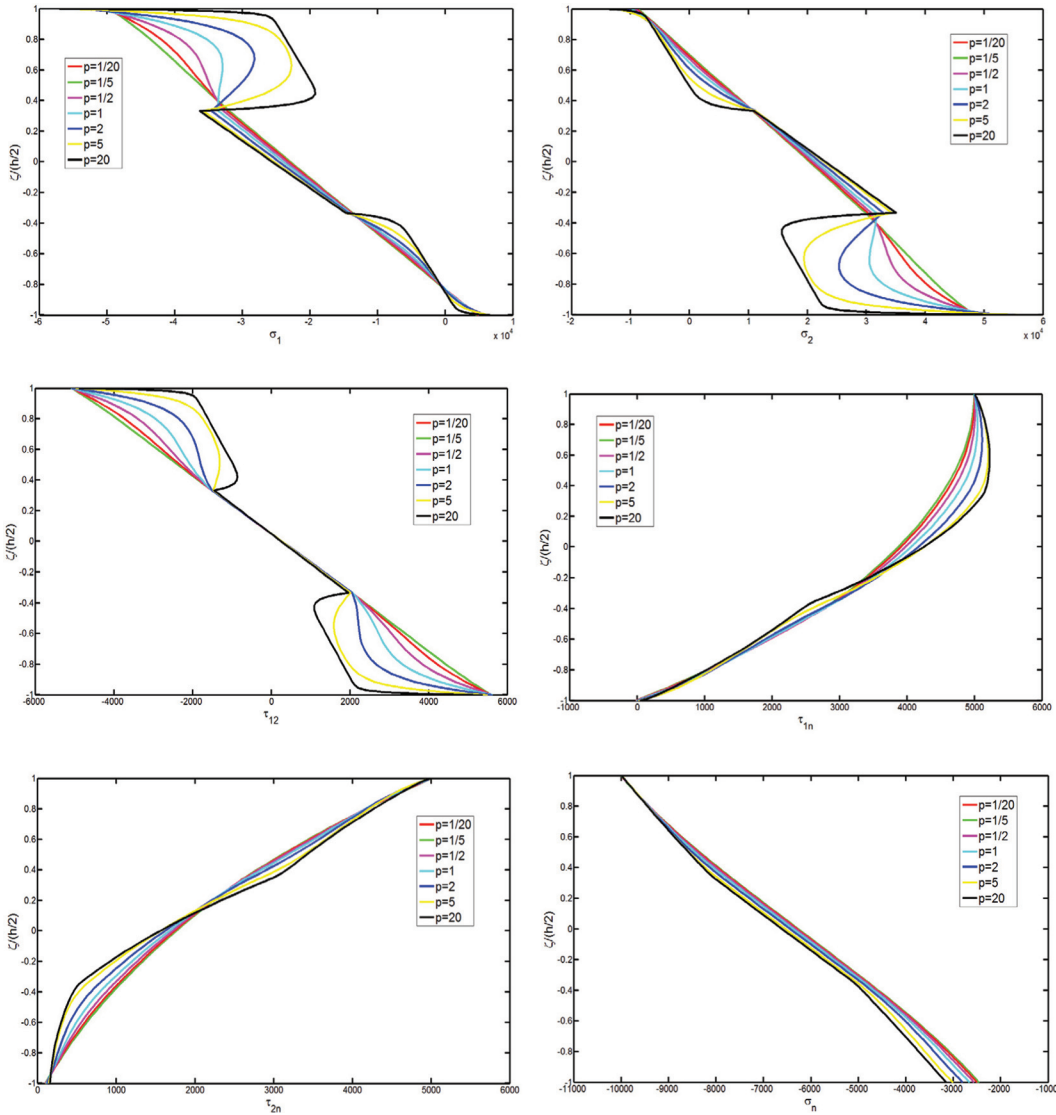


Figure 23: Through-the-thickness variation of all the stress components [Pa] at the point $c = (0.25(a_1^1 - a_1^0), 0.25(a_2^1 - a_2^0))$ for a C-C-C-C hyperbolic paraboloid of Table 6 with a $(FGM_{2(a^{(2)}=1/b^{(2)}=1/c^{(2)}=4/p^{(2)})}/Zirconia/FGM_{1(a^{(2)}=1/b^{(2)}=1/c^{(2)}=4/p^{(2)})})$ lamination scheme, for different values of the exponent $p = p^{(1)} = p^{(3)}$, when uniformly distributed loads $q_3^{(+)} = -10$ kPa, $q_2^{(+)} = q_2^{(-)} = 5$ kPa are applied at the top surface and a foundation $k_1^{(-)} = k_2^{(-)} = k_3^{(-)}$, $G_f^{(-)}$, $k_{1n/2}^{(-)} = k_{2n/2}^{(-)} = k_{3n/2}^{(-)}$, $k_{1n/3}^{(-)} = k_{2n/3}^{(-)} = k_{3n/3}^{(-)}$ is applied at the bottom surface.

laminated square plate, due to the fact that the material properties continuously vary through the thickness of the structure. Furthermore, the behaviour in terms of displacement, strains and stresses is included between the two limit cases of the zirconia and aluminum materials as expected due to the fact that the functionally graded materials considered are mixtures of the two isotropic constituents themselves.

6 Conclusions

The static analysis of functionally graded and laminated doubly-curved shells and panels resting on linear and nonlinear elastic foundations has been investigated using the GDQ method coupled with the Newton-Raphson scheme. All the effects of the nonlinear elastic foundation are separately introduced. New results are presented showing the effects of various parameters of the elastic foundation on the behavior of laminated doubly-curved and degenerate shells. The first-order shear deformation shell theory has been generalized considering the curvature effect in the computation of thickness-integrated shell stiffnesses, and the shear correction factor has been eliminated using a parabolic thickness function. The fundamental equilibrium equations have been discretized with the GDQ method giving a standard nonlinear problem for the static analysis. Numerical solutions are presented and compared with the ones obtained using the finite element method. The comparisons conducted with the FEM codes confirm how the GDQ simple numerical method provides accurate and computationally low cost results for all the structures considered. New results regarding six different structures are presented in this paper that can be used for further verification by numerical analysis performed by others and validated by experimental studies.

Acknowledgments

The first author was supported by the Italian Ministry for University and Scientific, Technological Research MIUR (40% and 60%), while the second author is supported by the Air Force Office of Scientific Research through MURI09 Grant FA9550-09-1-0686. The research topic is one of the subjects of the Centre of Study and Research for the Identification of Materials and Structures (CIMEST)-“M. Capurso” of the University of Bologna (Italy).

Received 1 September 2013.

References

1. S. Timoshenko, S. Woinowsky-Krieger, *Theory of Plates and Shells*, McGraw-Hill, 1959.
2. W. Flügge, *Stresses in Shells*, Springer-Verlag, 1960.
3. A.L. Gol'denveizer, *Theory of Elastic Thin Shells*, Pergamon Press, 1961.
4. V.V. Novozhilov, *Thin Shell Theory*, P. Noordhoff, 1964.
5. V.Z. Vlasov, *General Theory of Shells and its Application in Engineering*, NASA-TT-F-99, 1964.
6. S.A. Ambartsumyan, *Theory of Anisotropic Shells*, NASA-TT-F-118, 1964.
7. H. Kraus, *Thin Elastic Shells*, John Wiley & Sons, 1967.
8. A.W. Leissa, *Vibration of Plates*, NASA-SP-160, 1969.
9. A.W. Leissa, *Vibration of Shells*, NASA-SP-288, 1973.
10. Š. Markuš, *The Mechanics of Vibrations of Cylindrical Shells*, Elsevier, 1988.
11. E. Ventsel, T. Krauthammer, *Thin Plates and Shells*, Marcel Dekker, 2001.
12. W. Soedel, *Vibrations of Shells and Plates*, Marcel Dekker, 2004.
13. J.N. Reddy, *Theory and Analysis of Plates and Shells*, 2nd ed., CRC Press, Boca Raton, FL, 2007.
14. P.L. Gould, *Finite Element Analysis of Shells of Revolution*, Pitman Publishing, 1984.
15. P.L. Gould, *Analysis of Plates and Shells*, Prentice-Hall, 1999.
16. M.S. Qatu, *Accurate Theory for Laminated Composite Deep Thick Shells*, *Int. J. Solids Struct.* 36 (1999) 2917–2941.
17. M.S. Qatu, *Vibration of Laminated Shells and Plates*, Elsevier, 2004.
18. J.N. Reddy and C.F. Liu, “A higher-order shear deformation theory for laminated elastic shells,” *Int. J. Engng. Sci.*, 23 (1985), 319–330.
19. M.H. Toorani, A.A. Lakis, *General equations of anisotropic plates and shells including transverse shear deformations, rotary inertia and initial curvature effects*, *J. Sound Vib.* 237 (2000), 561–615.
20. J.N. Reddy, *Mechanics of Laminated Composites Plates and Shells*, 2nd ed., CRC Press, New York, 2004.
21. D.N. Paliwal, R.K. Pandey, T. Nath, *Free vibration of circular cylindrical shell on Winkler and Pasternak foundations*, *Int. J. Press. Ves. Piping* 69 (1996), 79–89.
22. O. Civalek, *Geometrically nonlinear dynamic analysis of doubly curved isotropic shells resting on elastic foundation by a combination of harmonic differential quadrature-finite difference methods*, *Int. J. Press. Ves. Piping* 82 (2005), 753–761.

23. G.B. Golovko, P.Z. Lugovoi, V.F. Meish, Solution of axisymmetric dynamic problems for cylindrical shells on an elastic foundation, *Int. Appl. Mech.* 43 (2007), 785–793.
24. A.H. Sofiyev, The buckling of FGM truncated conical shells subjected to axial compressive load and resting on Winkler-Pasternak foundations, *Int. J. Press. Ves. Piping* 87 (2010), 753–761.
25. A.H. Sofiyev, Buckling analysis of FGM circular shells under combined loads and resting on Pasternak type elastic foundations, *Mech. Res. Commun.* 37 (2010), 539–544.
26. A.H. Sofiyev, N. Kuruoglu, Natural frequency of laminated orthotropic shells with different boundary conditions and resting on the Pasternak type elastic foundation, *Compos. Part B Eng.* 42 (2011), 1562–1570.
27. H.-T. Thai, D.-H. Choi, A refined shear deformation theory for free vibration of functionally graded plates on elastic foundation, *Compos. Part B Eng.* 43 (2012), 2335–2347.
28. Y. Kiani, M.R. Eslami, An exact solution for thermal buckling of annular FGM plates on an elastic medium, *Compos. Part B Eng.* 45 (2013), 101–110.
29. Ö. Civalek, Nonlinear dynamic response of laminated plates resting on nonlinear elastic foundations by the discrete singular convolution-differential quadrature coupled approaches, *Compos. Part B Eng.* 50 (2013) 171–179.
30. L.F. Qiana, R.C. Batra, L.M. Chen, Static and dynamic deformations of thick functionally graded elastic plates by using higher-order shear and normal deformable plate theory and meshless local Petrov–Galerkin method, *Compos. Part B Eng.* 35 (2004), 685–697.
31. C.M.C. Roque, A.J.M. Ferreira, R.M.N. Jorge, Modelling of composite and sandwich plates by a trigonometric layerwise deformation theory and radial basis functions, *Compos. Part B Eng.* 36 (2005), 559–572.
32. J.R. Xiao, D.F. Gilhooley, R.C. Batra, J.W. Gillespie Jr., M.A. McCarthy, Analysis of thick composite laminates using a higher-order shear and normal deformable plate theory (HOSNDPT) and a meshless method, *Compos. Part B Eng.* 39 (2008), 414–427.
33. E. Carrera, S. Brischetto, M. Cinefra, M. Soave, Effects of thickness stretching in functionally graded plates and shells, *Compos. Part B Eng.* 42 (2011), 123–133.
34. A.J.M. Ferreira, C.M.C. Roque, A.M.A. Neves, R.M.N. Jorge, C.M.M. Soares, K.M. Liew, Buckling and vibration analysis of isotropic and laminated plates by radial basis functions, *Compos. Part B Eng.* 42 (2011), 592–606.
35. G. Giunta, F. Biscani, S. Belouettar, E. Carrera, Hierarchical modelling of doubly curved laminated composite shells under distributed and localised loadings, *Compos. Part B Eng.* 42 (2011), 682–691.
36. A.J.M. Ferreira, E. Carrera, M. Cinefra, C.M.C. Roque, O. Polit, Analysis of laminated shells by a sinusoidal shear deformation theory and radial basis functions collocation, accounting for through-the-thickness deformations, *Compos. Part B Eng.* 42 (2011), 1276–1284.
37. C. Shu, *Differential Quadrature and Its Application in Engineering*, Springer, Berlin, 2000.
38. C. Bert, M. Malik, Differential quadrature method in computational mechanics, *Appl. Mech. Rev.* 49 (1996), 1–27.
39. C. Shu, H. Du, Free vibration analysis of composites cylindrical shells by DQM, *Compos. Part B Eng.* 28B (1997), 267–274.
40. L. Hua, K.Y. Lam, Frequency characteristics of a thin rotating cylindrical shell using the generalized differential quadrature method, *Int. J. Mech. Sci.* 40 (1998), 443–459.
41. K.M. Liew, T.M. Teo, Modeling via differential quadrature method: Three-dimensional solutions for rectangular plates, *Comput. Methods Appl. Mech. Engrg.* 159 (1998), 369–381.
42. J.-B. Han, K.M. Liew, Static analysis of Mindlin plates: The Differential Quadrature Element Method (DQEM), *Comput. Methods Appl. Mech. Engrg.* 177 (1999), 51–75.
43. K.Y. Lam, L. Hua, On free vibration of a rotating truncated circular orthotropic conical shell, *Compos. Part B Eng.* 30 (1999) 135–144.
44. S. Moradi, F. Taheri, Delamination buckling analysis of general laminated composite beams by differential quadrature method, *Compos. Part B Eng.* 30 (1999), 503–511.
45. K.M. Liew, F.-L. Liu, Differential quadrature method for vibration analysis of shear deformable annular sector plates, *J. Sound Vib.* 230 (2000), 335–356.
46. L. Hua, Influence of boundary conditions on the free vibrations of rotating truncated circular multi-layered conical shells, *Compos. Part B Eng.* 31 (2000), 265–275.
47. L. Hua, K.Y. Lam, Orthotropic influence on frequency characteristics of rotating composite laminated conical shell by the generalized differential quadrature method, *Int. J. Solids Struct.* 38 (2001), 3995–4015.
48. G. Karami, P. Malekzadeh, A new differential quadrature methodology for beam analysis and the associated differential quadrature element method, *Comput. Methods Appl. Mech. Engrg.* 191 (2002), 3509–3526.
49. K.M. Liew, T.Y. Ng, J.Z. Zhang, Differential quadrature-layerwise modeling technique for three dimensional analysis of cross-ply laminated plates of various edge supports, *Comput. Methods Appl. Mech. Engrg.* 191 (2002), 3811–3832.
50. K.M. Liew, Y.Q. Huang, Bending and buckling of thick symmetric rectangular laminates using the moving least-squares differential quadrature method, *Int. J. Mech. Sci.* 45 (2003) 95–114.

51. K.M. Liew, Y.Q. Huang, J.N. Reddy, Moving least squares differential quadrature method and its applications to the analysis of shear deformable plates, *Int. J. Numer. Methods Eng.* 56 (2003) 2332–2351.
52. K.M. Liew, Y.Q. Huang, J.N. Reddy, Vibration analysis of symmetrically laminated plates based on FSDT using the moving least squares differential quadrature method, *Comput. Methods Appl. Mech. Engrg.* 192 (2003) 2203–2222.
53. T.Y. Wu, Y.Y. Wang, G.R. Liu, A generalized differential quadrature rule for bending analyses of cylindrical barrel shells, *Comput. Methods Appl. Mech. Engrg.* 192 (2003), 1629–1647.
54. J. Yang, H.-S. Shen, Nonlinear bending analysis of shear deformable functionally graded plates subjected to thermo-mechanical loads under various boundary conditions, *Compos. Part B Eng.* 34 (2003), 103–115.
55. Y.Q. Huang, Q.S. Li, Bending and buckling analysis of antisymmetric laminates using the moving least square differential quadrature method, *Comput. Methods Appl. Mech. Engrg.* 193 (2004), 3471–3492.
56. X. Wang, Y. Wang, Free vibration analyses of thin sector plates by the new version of differential quadrature method, *Comput. Methods Appl. Mech. Engrg.* 193 (2004), 3957–3971.
57. P. Malekzadeh, G. Karami, M. Farid, A semi-analytical DQEM for free vibration analysis of thick plates with two opposite edges simply supported, *Comput. Methods Appl. Mech. Engrg.* 193 (2004), 4781–4796.
58. Ö. Civalek, Geometrically nonlinear dynamic analysis of doubly curved isotropic shells resting on elastic foundation by a combination of HDQ-FD methods, *Int. J. Press. Ves. Piping* 82 (2005), 470–479.
59. E. Viola, F. Tornabene, Vibration analysis of damaged circular arches with varying cross-section, *Struct. Integr. Durab. (SID-SDHM)* 1 (2005), 155–169.
60. Z. Zong, K.Y. Lam, Y.Y. Zhang, A multidomain differential quadrature approach to plane elastic problems with material discontinuity, *Mathematical and Computer Modelling* 41 (2005), 539–553.
61. E. Viola, F. Tornabene, Vibration analysis of conical shell structures using GDQ method, *Far East J. Appl. Math.* 25 (2006), 23–39.
62. Ö. Civalek, Linear vibration analysis of isotropic conical shells by Discrete Singular Convolution (DSC), *Int. J. Struct. Eng. Mech.* 25 (2007), 127–130.
63. F. Tornabene, *Modellazione e Soluzione di Strutture a Guscio in Materiale Anisotropo (Modelling and Solution of Shell Structures made of Anisotropic Materials)*, PhD Thesis, University of Bologna—DISTART Department, 2007.
64. F. Tornabene, E. Viola, Vibration analysis of spherical structural elements using the GDQ method, *Comput. Math. Appl.* 53 (2007), 1538–1560.
65. E. Viola, M. Dilena, F. Tornabene, Analytical and numerical results for vibration analysis of multi-stepped and multi-damaged circular arches, *J. Sound Vib.* 299 (2007), 143–163.
66. X. Wang, Nonlinear stability analysis of thin doubly curved orthotropic shallow shells by the differential quadrature method, *Comput. Methods Appl. Mech. Engrg.* 196 (2007), 2242–2251.
67. X. Wang, X. Wang, X. Shi, Accurate buckling loads of thin rectangular plates under parabolic edge compressions by the differential quadrature method, *Int. J. Mech. Sci.* 49 (2007), 447–453.
68. A. Marzani, F. Tornabene, E. Viola, Nonconservative stability problems via generalized differential quadrature method, *J. Sound Vib.* 315 (2008), 176–196.
69. F. Tornabene, E. Viola, 2-D solution for free vibrations of parabolic shells using generalized differential quadrature method, *Eur. J. Mech. A-Solid* 27 (2008), 1001–1025.
70. A. Alibeigloo, R. Modoliat, Static analysis of cross-ply laminated plates with integrated surface piezoelectric layers using differential quadrature, *Compos. Struct.* 88 (2009), 342–353.
71. F. Tornabene, Free vibration analysis of functionally graded conical, cylindrical and annular shell structures with a four-parameter power-law distribution, *Comput. Methods Appl. Mech. Engrg.* 198 (2009), 2911–2935.
72. F. Tornabene, E. Viola, Free vibrations of four-parameter functionally graded parabolic panels and shell of revolution, *Eur. J. Mech. A-Solid* 28 (2009), 991–1013.
73. F. Tornabene, E. Viola, Free vibration analysis of functionally graded panels and shells of revolution, *Meccanica* 44 (2009), 255–281.
74. F. Tornabene, E. Viola, D.J. Inman, 2-D differential quadrature solution for vibration analysis of functionally graded conical, cylindrical and annular shell structures, *J. Sound Vib.* 328 (2009) 259–290.
75. E. Viola, F. Tornabene, Free vibrations of three parameter functionally graded parabolic panels of revolution, *Mech. Res. Commun.* 36 (2009), 587–594.
76. L. Yang, S. Zhifei, Free vibration of a functionally graded piezoelectric beam via state-space based differential quadrature, *Compos. Struct.* 87 (2009), 257–264.
77. F. Tornabene, A. Marzani, E. Viola, I. Elishakoff, Critical flow speeds of pipes conveying fluid by the generalized differential quadrature method, *Adv. Theor. Appl. Mech.* 3 (2010), 121–138.
78. A. Alibeigloo, V. Nouri, Static analysis of functionally graded cylindrical shell with piezoelectric layers using differential quadrature method, *Compos. Struct.* 92 (2010), 1775–1785.

79. A. Andakhshideh, S. Maleki, M.M. Aghdam, Non-linear bending analysis of laminated sector plates using generalized differential quadrature, *Compos. Struct.* 92 (2010), 2258–2264.
80. Sh. Hosseini-Hashemi, M. Fadaee, M. Es'haighi, A novel approach for in-plane/out-of-plane frequency analysis of functionally graded circular/annular plates, *Int. J. Mech. Sci.* 52 (2010), 1025–1035.
81. P. Malekzadeh, A. Alibeygi Beni, Free vibration of functionally graded arbitrary straight-sided quadrilateral plates in thermal environment, *Compos. Struct.* 92 (2010), 2758–2767.
82. O. Sepahi, M.R. Forouzan, P. Malekzadeh, Large deflection analysis of thermo-mechanical loaded annular FGM plates on nonlinear elastic foundation via DQM, *Compos. Struct.* 92 (2010) 2369–2378.
83. M.H. Yas, B. Sobhani Aragh, Three-dimensional analysis for thermoelastic response of functionally graded fiber reinforced cylindrical panel, *Compos. Struct.* 92 (2010), 2391–2399.
84. F. Tornabene, Free vibrations of laminated composite doubly-curved shells and panels of revolution via the GDQ method, *Comput. Methods Appl. Mech. Engrg.* 200 (2011), 931–952.
85. F. Tornabene, 2-D GDQ solution for free vibrations of anisotropic doubly-curved shells and panels of revolution, *Compos. Struct.* 93 (2011), 1854–1876.
86. F. Tornabene, Free vibrations of anisotropic doubly-curved shells and panels of revolution with a free-form meridian resting on Winkler-Pasternak elastic foundations, *Compos. Struct.* 94 (2011), 186–206.
87. F. Tornabene, A. Liverani, G. Caligiana, FGM and laminated doubly curved shells and panels of revolution with a free-form meridian: A 2-D GDQ solution for free vibrations, *Int. J. Mech. Sci.* 53 (2011), 446–470.
88. X. Zhao, K.M. Liew, Free vibration analysis of functionally graded conical shell panels by a meshless method, *Compos. Struct.* 93 (2011), 649–664.
89. F. Tornabene, A. Liverani, G. Caligiana, Laminated composite rectangular and annular plates: A GDQ solution for static analysis with a posteriori shear and normal stress recovery, *Compos. Part B Eng.* 43 (2012), 1847–1872.
90. F. Tornabene, A. Liverani, G. Caligiana, Static analysis of laminated composite curved shells and panels of revolution with a posteriori shear and normal stress recovery using Generalized Differential Quadrature Method, *Int. J. Mech. Sci.* 61 (2012), 71–87.
91. F. Tornabene, A. Liverani, G. Caligiana, General anisotropic doubly-curved shell theory: A Differential Quadrature Solution for free vibrations of shells and panels of revolution with a free-form meridian, *J. Sound Vib.* 331 (2012), 4848–4869.
92. F. Tornabene, *Meccanica delle Strutture a Guscio in Materiale Composito. Il Metodo Generalizzato di Quadratura Differenziale*, Esculapio, 2012.
93. F. Tornabene, A. Ceruti, Free-form laminated doubly-curved shells and panels of revolution resting on Winkler-Pasternak elastic foundations: a 2-D GDQ solution for static and free vibration analysis, *World J. Mech.* 3 (2013), 1–25.
94. F. Tornabene, A. Ceruti, Mixed Static and Dynamic Optimization of Four-Parameter Functionally Graded Completely Doubly Curved and Degenerate Shells and Panels Using GDQ Method, *Math. Probl. Eng.*, vol. 2013, Article ID 867079, 1–33.
95. F. Tornabene, E. Viola, Static analysis of functionally graded doubly-curved shells and panels of revolution, *Meccanica* 48 (2013), 901–930.
96. F. Tornabene, E. Viola, N. Fantuzzi, General higher-order equivalent single layer theory for free vibrations of doubly-curved laminated composite shells and panels, *Compos. Struct.* 104 (2013), 94–117.
97. F. Tornabene, N. Fantuzzi, E. Viola, A.J.M. Ferreira, Radial basis function method applied to doubly-curved laminated composite shells and panels with a general higher-order equivalent single layer formulation, *Compos. Part B Eng.* (2013), doi: <http://dx.doi.org/10.1016/j.compositesb.2013.07.026>.
98. F. Tornabene, N. Fantuzzi, E. Viola, J.N. Reddy, Winkler-Pasternak foundation effect on the static and dynamic analyses of laminated doubly-curved and degenerate shells and panels, *Compos. Part B Eng.* (2013), doi: <http://dx.doi.org/10.1016/j.compositesb.2013.06.020>.
99. E. Viola, F. Tornabene, N. Fantuzzi, General higher-order shear deformation theories for the free vibration analysis of completely doubly-curved laminated shells and panels, *Compos. Struct.* 95 (2013), 639–666.
100. E. Viola, F. Tornabene, N. Fantuzzi, Static analysis of completely doubly-curved laminated shells and panels using general higher-order shear deformation theories, *Compos. Struct.* 101 (2013), 59–93.
101. E. Viola, F. Tornabene, N. Fantuzzi, Generalized differential quadrature finite element method for cracked composite structures of arbitrary shape, *Compos. Struct.* (2013), doi: <http://dx.doi.org/10.1016/j.compstruct.2013.07.034>.
102. E. Viola, F. Tornabene, N. Fantuzzi, DiQuMASPAB Software, DICAM Department, Alma Mater Studiorum—University of Bologna (<http://software.dicam.unibo.it/diqumaspab-project>).



J.N. Reddy is a Distinguished Professor, Regents Professor, and inaugural holder of the Oscar S. Wyatt Endowed Chair in Mechanical Engineering at Texas A&M University. Dr. Reddy is a prolific researcher in theoretical and computational mechanics with nearly 500 journal papers and 18 books. The shear deformation plate and shell theories that he developed and bear his name are well known and finite element models he developed have been implemented into commercial finite element commercial software like ABAQUS, NISA, and HYPERFORM. Dr. Reddy has been recognized with numerous national and international awards (in addition to many institutional awards), including the Worcester Reed Warner Medal and the Charles Russ Richards Memorial Award of the American Society of Mechanical Engineers, the Nathan M. Newmark Medal from the American Society of Civil Engineers; Award for Excellence in the Field of Composites and Distinguished Research Award from the American Society for Composites; and the Computational Solid Mechanics award from US Association for Computational Mechanics. Recently, he is elected as the Honorary Member of the American Society of Mechanical Engineers and received Honoris Causa (honorary degrees) from Technical University of Lisbon, Portugal and Odlar Yurdu University, Azerbaijan. As a result of his extensive publications of archival journal papers and books in engineering, As a result of Dr. Reddy's extensive publications of archival journal papers and books in wide range of topics in applied sciences and engineering, Dr. Reddy is recognized as one of the selective researchers in engineering around world by ISI Highly Cited Researchers with over 13,000 citations (without self-citations over 12,000) with h-index of over 54 as per Web of Science, 2013; and as per Google Scholar the number of citations is over 29,000 and h-index is 71.



Francesco Tornabene is an Assistant Professor at School of Engineering, Department of Civil, Chemical, Environmental and Materials Engineering, University of Bologna, Bologna, Italy. He obtained a Ph.D. in *Structural Mechanics* from University of Bologna in 2007. He is the winner of the Senior research grant entitled "*Design for Recycling Methodologies Applied to the Nautical Field*" from February 2011 to October 2011 at the University of Bologna and the co-PI of a research grant entitled "*Advanced Numerical Schemes for Anisotropic Materials*" from December 2011 to January 2012. He is the author of more than sixty journal papers and a book (in Italian) entitled *Mechanics of Shell Structures Made of Composite Materials. The Generalized Differential Quadrature Method*, Esculapio, Bologna, 2012. He is also a member of the Editorial Board of *Journal of Computational Engineering* and *ISRN Mechanical Engineering* from 2013 till now.